UNIVERSITEIT VAN PRETORIA
UNIVERSITY OF PRETORIA
YUNIBESITHI YA PRETORIA

In vitro effects of 2-methoxyestradiol, an endogenous estrogen, on MCF-12A and MCF-7 cell cycle progression

by

Magdalena Catherina van Zijl

(98036859)

Submitted in fulfilment of part of the requirements for the degree

Master of Science (Physiology)

in the Faculty of Health Sciences

University of Pretoria

Supervisors: Dr M-L Lottering

Prof AM Joubert

January 2006

Hiermee erken ek met dank die finansiële hulp (beurs) wat ek van die Struwig-Germeshuysen Kankernavorsingstrust ontvang het vir die voltooiing van my studies. Menings wat in die publikasie uitgespreek word of gevolgtrekkings waartoe geraak is, is dié van die navorser alleen en strook nie noodwendig met dié van die SGK-Trust nie.

Summary

2-Methoxyestradiol (2ME) is an endogenous estrogen metabolite with antiproliferative and antiangiogenic properties. 2ME also plays an active role in the induction of apoptosis, especially in cancerous cells. These properties have been confirmed by various *in vitro* and *in vivo* studies and render 2ME a potential antitumor agent. The mechanism of action of 2ME, however, is not yet fully elucidated and it is believed that multiple mechanisms are involved that may be dependent on cell type.

The aim of this study was to investigate the differential effects of 2ME on cell growth, morphology and spindle formation in the non-tumorigenic MCF-12A breast cell line and the tumorigenic MCF-7 breast cell line. In dose-dependent studies, cell growth was determined spectrophotometrically. Light microscopy was used to investigate the morphological changes induced by 2ME and its effect on spindle formation was investigated by means of indirect immunofluorescence. The estrogen receptor status of the MCF-12A cells was confirmed with immunocytochemistry. In order to investigate the effect of 2ME on the length of the cell cycle, cells were blocked in early S-phase with hydroxyurea, then allowed to continue through the cell cycle and mitotic indices determined at regular time intervals. Checkpoint kinase and Cdc2 kinase assays were used to determine the effect of 2ME on relevant cell cycle kinases.

Although 2ME inhibited cell growth in both cell lines, the MCF-7 cells were inhibited from much lower concentrations and growth inhibition was more pronounced than in the MCF-12A cells. Treated MCF-7 cells showed abnormal metaphase cells, membrane blebbing, apoptotic cells and disrupted spindle formation. These observations were either absent, or not as prominent in the MCF-12A cells. Therefore, differential mechanism(s) of growth inhibition are evident between the normal and tumorigenic cells. Although the two cell lines differ in their estrogen receptor status, this could not explain the differential effects, for 2ME has a very low affinity for the estrogen receptor. 2ME had no effect on the length of the cell cycle, but blocked MCF-7 cells in mitosis. There were no significant alterations in the phosphorylation status of Cdc25C after 2ME treatment. However, Cdc2 activity was increased to a

greater extend in the MCF-7 cells than in the MCF-12A cells. Therefore, it is suggested that exposure to 2ME disrupts mitotic spindle formation and enhances Cdc2 kinase activity, leading to persistence of the spindle checkpoint and thus prolonged metaphase arrest, which may result in the induction of apoptosis. The tumorigenic MCF-7 cells are especially sensitive to 2ME treatment compared to the normal MCF-12A cells.

2ME shows potential for the treatment of breast cancer. Selecting the concentration of 2ME that has maximum inhibitory effect on tumorigenic, but minimal effect on normal cells is crucial in its possible application as antitumor agent. Furthermore, research concerning the differential action mechanisms of 2ME is essential to create a better understanding regarding the treatment of cancer and may possibly contribute to the development and/or improvement of novel chemotherapeutic agents.

Keywords: 2-methoxyestradiol, cell cycle regulation, mitotic spindle, Cdc2 kinase, spindle assembly checkpoint

Opsomming

2-Metoksie estradiol (2ME) is ‘n endogene estrogeen metaboliet met antiproliferatiewe en antiangiogenetiese eienskappe. 2ME speel ook ‘n aktiewe rol in die induksie van apoptose, veral in kankeragtige selle. Verskeie *in vitro* en *in vivo* studies het bogenoemde eienskappe van 2ME bevestig, wat dit ‘n potensiële antitumor middel maak. Die aksiemeganismes van 2ME is egter nog nie ten volle bekend nie en daar is aanduidings dat veelvuldige meganismes betrokke is, wat afhanklik is van die seltipe.

Die doel van hierdie studie was om die differensiële effekte van 2ME op selgroei, morfologie en mitotiese spoelvorming in die nie-tumorigeniese MCF-12A en die tumorigeniese MCF-7 borssellyn te ondersoek. Selgroei is spektrofotometries bepaal in dosis-afhanklike studies. Ligmikroskopie is gebruik om die morfologiese veranderinge wat deur 2ME veroorsaak word te ondersoek en die effekte op mitotiese spoelvorming is met behulp van indirekte immunofluoressensie ondersoek. Die estrogeen reseptor status van die MCF-12A selle is bevestig met immunositochemie. Die selle is met hidroksie-urea in vroeë S-fase geblokkeer en daarna weer toegelaat om deur die selsiklus te beweeg, terwyl mitotiese indekse met gereëlde tydsintervalle getel is, om die effek van 2ME op die lengte van die selsiklus te bepaal. Toetse vir die aktiwiteit van Cdc2 kinase en kontrolepunt kinases is gedoen om die effek van 2ME op relevante selsiklus kinases te ondersoek.

Alhoewel 2ME selgroei in beide sellyne geïnhibeer het, was die MCF-7 selle tot ‘n groter mate en vanaf laer konsentrasies geïnhibeer as die MCF-12A selle. Abnormale metafase selle, membraan uitstulpings, apoptotiese selle en versteurde spoelvorming is waargeneem in die blootgestelde MCF-7 selle. Hierdie waarnemings was afwesig of nie so prominent in die blootgestelde MCF-12A selle nie. Vanuit hierdie resultate is dit duidelik dat differensiële meganismes van groei inhibisie bestaan tussen die normale en die kankersellyn. Alhoewel die twee sellyne verskil in estrogeen reseptor status, verklaar dit nie die differensiële effek nie, aangesien 2ME ‘n baie lae affiniteit vir die estrogeen reseptor besit. 2ME het geen effek gehad op die lengte van die selsiklus nie, maar het die MCF-7 selle in mitose geblokkeer. Daar was geen statisties

betekenisvolle verskille in die fosforileringstatus van Cdc25C na 2ME blootstelling nie. Daarteenoor is Cdc2 aktiwiteit na blootstelling tot ‘n groter mate in die MCF-7 sellyn as in die MCF-12A sellyn verhoog. Vanuit die resultate volg dat 2ME mitotiese spoelvorming versteur en Cdc2 kinase aktiwiteit verhoog, wat lei tot ‘n volgehoue spoelsamestellingskontrolepunt en dus verlengde blokkering in metafase, wat die induksie van apoptose tot gevolg kan hê. Die tumorigeniese MCF-7 selle is veral sensitief vir 2ME behandeling in vergelyking met die normale MCF-12A selle.

2ME toon potensiaal in die behandeling van borskanker. Vir die gebruik van 2ME as ‘n antitumor middel is dit belangrik om die konsentrasie te identifiseer wat ‘n maksimum inhibitoriese effek op tumorselle, maar die minimum effekte op normale selle het. Navorsing aangaande die differensiële aksiemeganismes van 2ME is essensiëel om die behandeling van kanker beter te verstaan en in die ontwikkeling en/of verbetering van nuwe chemoterapeutiese middels.

Keywords: 2-metoksie estradiol, selsiklus regulering, mitotiese spoel, Cdc2 kinase, spoelsamestellingskontrolepunt

Acknowledgements

I sincerely thank the following people:

- Doctor Mona-Liza Lottering and professor Annie Joubert, my supervisors, for their interest, continual encouragement and professional guidance

- Professor Dirk van Papendorp, head of the Department of Physiology, for the opportunity to conduct this study in his department

- Professor Neitz and Ms Sandra van Wyngaardt, from the Department of Biochemistry, for their assistance with the use of their ultracentrifuge

- My colleagues at the Department of Physiology and the Department of Urology, for their support and encouragement

- Professor Frans Steffens, for statistical analyses

- The University of Pretoria, for the PUNIV PDP bursary

- The Medical Research Council and the Struwig-Germeshuysen Cancer Research Trust for financial support

- My parents, friends and family, for their continual support and encouragement

- My husband, Stefan, for his unending patience, love, support and for always believing in me

- My Heavenly Father, for the strength, opportunities and for providing all of the above

Table of Contents

List of Figures

List of Tables

List of Abbreviations

µg	Microgram (1 x 10^{-6} g)
µl	Microlitre (1 x 10^{-6} l)
µM	Micromolar (1 x 10^{-6} M)
µm	Micrometre (1 x 10^{-6} m)
ANOVA	Analysis of variance
APC/C	Anaphase-promoting complex/cyclosome
ATP	Adenosine triphosphate
Bcl-2	B-cell leukaemia/lymphoma 2
BMI	Body mass index
BubR1	Budding uninhibited benzimidazole receptor 1
Bub	Budding uninhibited benzimidazole
C	Control well optical density
°C	Degrees centigrade
CAK	Cdk-activating kinase
Cdc	Cell division cycle
Cdh1	Cadherin 1
Cdk	Cyclin-dependent kinase
CENP-E	Centromere protein-E
cm	Centimetre
cm^2	Square centimetre
COMT	Catechol-*O*-methyl transferase
CuZnSOD	Copper/zink-dependent superoxide dismutase
CYP	Cytochrome P450
DAB	3,3' diaminobenzidine
DMEM	Dulbecco's Modified Eagle's Medium
DMSO	Dimethyl sulphoxide
DNA	Deoxyribonucleic acid
DR	Death receptor
DR5	Death receptor 5
E1	Estrone
E2	Estradiol

EDTA	Ethylene diamine tetraacetic acid
EGF	Epidermal growth factor
EGTA	Ethylene glycol-bis-(ß-aminoethyl ether)N,N,N',N'-tetra-acetate
ELISA	Enzyme-linked immunosorbent assay
ER	Estrogen receptor
FCS	Fetal calf serum
FITC	Fluoroisothiocyanate
g	Gram
x g	Gravities (centrifugal force)
G_1-phase	Gap 1 phase
G_2-phase	Gap 2 phase
GI_{50}	50 % growth inhibitory concentration
GSH	Glutathione
GST	Glutathione S-transferase
GTP	Guanosine triphosphate
h	Hours
HEPES	4-(2-hydroxyethyl)-1-piperazine-2-ethanesulfonic acid
HIF-1α	Hypoxia-inducible factor 1α
H_2O_2	Hydrogen peroxide
HRP	Horseradish peroxidase
hsMad	Human homolog of Mad
HU	Hydroxyurea
IgG	Immunoglobulin G (Gamma globulin)
IR	Ionizing radiation
JNK	c-Jun NH_2-terminal kinase
kg	Kilogram (1000 g)
l	Litre
LC_{50}	50 % lethal concentration
M	Molar (mol/litre)
m^2	Square metre
Mad	Mitotic arrest deficiency protein
MAP	Microtubule-associated protein
MARK	Microtubule-affinity-regulating kinases

MCC	Mitotic checkpoint complex
2ME	2-methoxy-17ß-estradiol
MethA sarcoma	3-methylcholanthrene-induced sarcoma
mg	Milligram (1×10^{-3} g)
min	Minutes
ml	Millilitre (1×10^{-3} l)
mm^3	Cubic millimetres
mM	Millimolar (1×10^{-3} M)
MnSOD	Manganese-dependent superoxide dismutase
MPF	M-phase/mitosis promoting factor
M-phase	Mitotic phase
MTOC	Microtubule organising center
MTT	3-[4,5 dimethylthiazol-2-yl]-2,5-diphenyl tetrazolium bromide
n	Sample size
N	Normality (gram equivalent weights of solute per litre of solution)
NADPH	Reduced nicotinamide adenine dinucleotide phosphate
NES	Nuclear export signal
NFκB	Nuclear factor kappa beta
ng	Nanogram (1×10^{-9} g)
nM	Nanomolar (1×10^{-9} M)
nm	Nanometers
NP-40	Nonidet P-40
O_2^-	Superoxide radical
$OH^{\cdot}$	Hydroxyl radical
PBS	Phosphate buffered saline
PCM	Pericentriolar materials
PCNA	Proliferating cell nuclear antigen
pg	Picogram (1×10^{-12} g)
Plk1	Polo-like kinase 1
PMSF	Phenyl methyl sulfonyl fluoride
POD	Peroxidase
pRB	Retinoblastoma protein
psi	Pound per square inch (1 psi = 6895 Pascals)

RA	Retinoic acid
RanBPM	Ran-binding protein
RNA	Ribonucleic acid
ROS	Reactive oxygen species
rpm	Revolutions per minute
SD	Standard deviation
SEAL	Steric and electrostatic alignment
SOD	Superoxide dismutase
S-phase	Synthesis phase
T	Test well optical density after exposure period
T_0	Time zero optical density
TGF-β	Tumor growth factor-beta
TGI	Total growth inhibitory concentration
TMB	Tetra-methylbenzidine
TRAIL	Tumor necrosis factor-related apoptosis-inducing ligand
VEGF	Vascular endothelial growth factor
% (v/v)	Percentage of volume of solute in the volume of solution

Chapter 1

Literature Review

1.1 Breast cancer etiology

Breast cancer is regarded as the most common neoplastic disease in females (1,2). Worldwide, the incidence of breast cancer continues to rise in all age groups (3,4). Breast cancer represents 22 % of cancers in women and there are 999 000 new cases each year and 375 000 deaths (1). The incidence of the 15 most common cancers in women in 2000 is summarized in Figure 1.1 (1). Although various factors may contribute to the development of breast cancer, it may be considered as a hormone-dependent malignancy (2,5,6). The fact that reproductive characteristics affect the risk of breast cancer has been known since 1700, when Ramazzini reported higher incidence among nuns (3). Experimental data strongly suggest that estrogens and their metabolites play a role in the initiation and promotion of breast cancer (2,7,8,9).

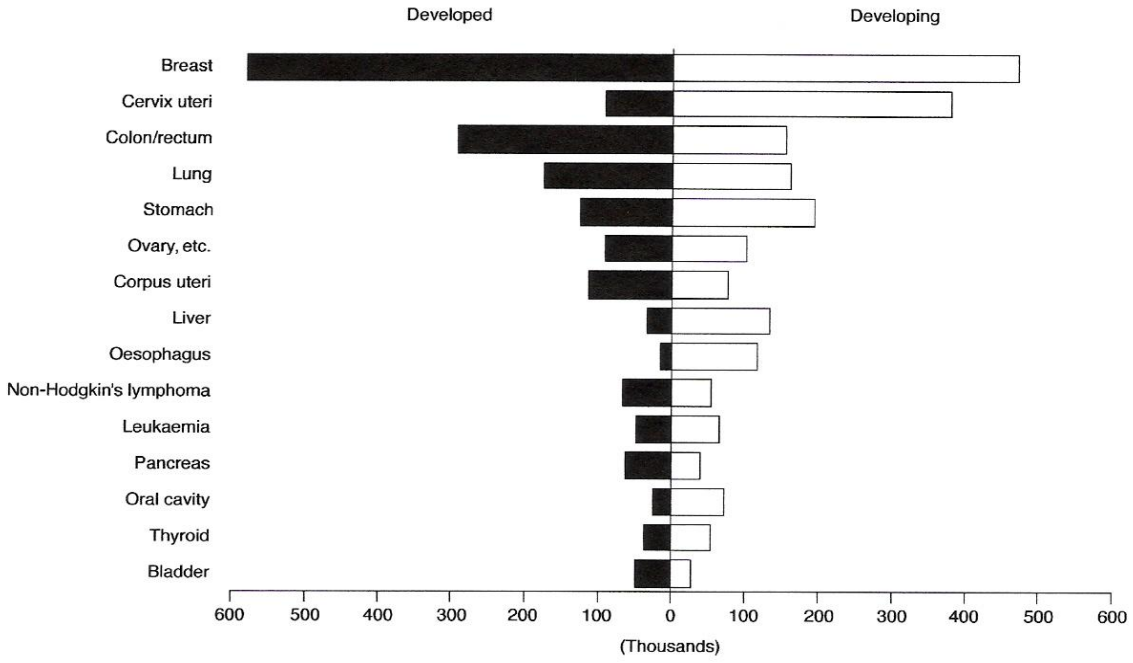

Figure 1.1: Incidence of the 15 most common cancers in women in 2000. Reprinted from the European Journal of Cancer, vol. 37, Parkin DM, Bray FI, Devesa SS, Cancer burden in the year 2000: the global picture, pp. S4-S66, Copyright (2001), with permission from Elsevier (1).

Various mechanisms are considered responsible for the carcinogenicity of estrogens (2). Hormones induce carcinogenesis by inducing cell proliferation through estrogen receptor-mediated signal transduction (2,7,8,10,11). The response of an organ to the proliferative effects of a hormone may be a progression from normal growth to hyperplasia to neoplasia (7). Enhanced cell proliferation increases the probability for mutation to occur during deoxyribonucleic acid (DNA) synthesis and for defective DNA repair (2,8,10). This in turn, leads to mutations, which are subsequently propagated through increased mitotic activity present in proliferating cells and can result in cancer formation (7,10).

Other possible mechanisms of hormone-induced carcinogenesis include the generation of active radicals that can damage DNA (7,8), the induction of enzymes and proteins involved in nucleic acid synthesis and through the activation of oncogenes (7), the inactivation of tumor suppressor genes and cytochrome P450-mediated metabolic activation that elicits direct genotoxic effects by increasing mutation rates (2). Indirect tumor-initiating effects may occur through the stimulation of prolactin secretion and the production of growth factors (*e.g.* transforming growth factor α and epidermal growth factor) and non-growth-factor peptides (*e.g.* plasminogen activators) (7). However, the exact mechanism remains to be fully elucidated (7).

Epidemiological, clinical and genetic studies identified several known risk factors for the development of breast cancer (Table 1). A common thread linking the main risks for developing breast cancer in women is cumulative, excessive exposure to estrogen (7,8,9,12,13). The predictive value of these factors in assessing the risk of breast cancer is increased by combining them (3,7).

Table 1.1: Risk factors for developing breast cancer.

Risk factor	**High risk**	**References**
Sex	Female	3,7,14
Age	70-74 yrs Elderly Mid life	7 2,3,14,15,16 3
Age at menarche	<12 yrs Before 11 yrs	7 16

	Early	1,2,3,8,10,12,14,15,17
Age at natural menopause	≥55 Late After 54	7 2,3,8,10,12,14,15 16
Parity	0 Nulliparity Low	7 2,3,8,10,18 1,10,17
Age at birth of first child	≥30 yrs Late First child early 40's	7 1,2,3,8,10,14,15 16
Age at any birth	Late	10
Breastfeeding (months)	0	2,7,17
Socio-cultural factors	White	3,10,17
Socio-economic status	Higher	1,2,3,8,16
Geographical location	Developed country	1,3,16
Familial history of cancer in the breast, ovary or endometrium	Breast cancer of first degree relative when young Breast cancer genes *BRCA1* and *BRCA2*	1,3,7,8,14,16 1,2,3,16
Individual risk		3
Individual history of breast diseases: Previous benign disease Cancer in other breast	 Atypical hyperplasia 	2 14,16 16
Mammographic screening	No	15
Breast density on mammography (%)	≥75	7
Bone density	Highest quartile	7
	Hyperinsulinemia with insulin resistance (independent of general adiposity or body fat distribution)	5
Diet	High saturated fat	1,16
Consumption of alcohol	Excessive intake	1,2,3,14,16
Body weight: Premenopausal Postmenopausal	 Body Mass Index (BMI) >35 Low BMI >35 BMI >30.7 Higher Obesity	 16 3 16 7 3 1,2,5
Serum estradiol concentration	Highest quartile	7

Taking exogenous hormones: Oral contraceptive Hormone replacement therapy Estrogen therapy Estrogen-progestin therapy Diethylstilbestrol	 Current use Extended use Use for ≥ 10 years Current Prolonged Current Use during pregnancy	 3,7,10,12,16,17 2 10,16 7,14 2,3,8 1,3,7 16
Environmental chemicals	Excessive exposure	3,8
Ionizing radiation exposure	Excessive exposure Abnormal exposure in young females after age 10 Early in life	2,14 16 3
In utero hormonal exposures	Increased estrogen exposure	14

* Although there are some indications of the retroviral etiology of human breast cancer, the results from studies are still inconclusive (19).

1.2 Metabolism of estrogens

Estrogens are produced and secreted mainly by the ovaries and partly by the adrenals in the female body (18,20). 17ß-estradiol causes cell proliferation and has been implicated in spontaneous mutations (8). However, several estradiol metabolites have been shown to be more potent estrogenic compounds than their precursor (11).

Estrogens are catabolized mainly by hydroxylation reactions that takes place principally in the liver by reduced nicotinamide adenine dinucleotide phosphate (NADPH)-dependent cytochrome P450 enzymes (18,21) and result in the formation of 2-hydroxy-estrone and 2-hydroxy-estradiol, 4-hydroxy-estrone and 4-hydroxy-estradiol and 16α-hydroxy-estrone and 16α-hydroxy-estradiol (7,18). 4-hydroxy-estrone and 16α-hydroxy-estradiol are estrogenic and thought to be carcinogenic (7). 2-hydroxy- and 4-hydroxyestradiol have been shown to exhibit estrogenic and genotoxic effects, with 4-hydroxyestradiol being the most potent cell proliferator (8,11). 4-hydroxyestradiol undergoes metabolic oxidation-reduction cycling to generate free radicals such as superoxides. The chemically reactive estrogen semiquinone-quinone intermediates may damage DNA and other cellular components, induce cell transformation, and initiate tumorigenesis (18,22). The quinines-semiquinones can form conjugates with glutathione, catalysed by glutathione

S-transferase, or be reduced to catechol estrogens by quinone reductase (18). DNA adducts can result from these reactive metabolites if the inactivating conjugative pathways are incomplete or absent (18). 4-hydroxyestradiol has been associated with kidney cancer in Syrian male hamsters (18,23).

2- and 4-hydroxy metabolites are converted to 2-methoxyestrone and 2-methoxyestradiol (2ME), 2-hydroxy-estrone and 2-hydroxy-estradiol 3 methyl ether, 4-methoxy-estrone and 4-methoxy-estradiol and 4-hydroxy-estrone and 4-hydroxy-estradiol 3 methyl ether by catechol-*O*-methyltransferase (COMT) (7,18,21,24). COMT is an enzyme present in large amounts in many organs and cells such as liver, kidney, brain, placenta, uterus, mammary gland, blood vessels, lymphocytes, and erythrocytes (7,18,21,24). It has been thought that metabolic *O*-methylation may be a rapid inactivation or detoxification pathway of the catechol estrogens to produce metabolically stable, but inactive, derivatives (24,25,26,27). However, in 1989 Spicer and Hammond noted the potency of 2ME to inhibit cell growth in porcine granulosa cells *in vitro* (24). More recent studies (*in vitro* and *in vivo*) indicated that 2ME may have unique biological activities that are not shared with estradiol or the catechol estrogens (28,29,30,31) and confirmed the anti-carcinogenic properties of 2ME (7,18). Figure 1.2 provides an overview of estrogen metabolism and the role of various metabolites in estrogen-induced carcinogenesis (18).

Yager *et al*. suggested that a balance among the carcinogenic metabolites and metabolites having protective effects are likely required to maintain homeostasis (8).

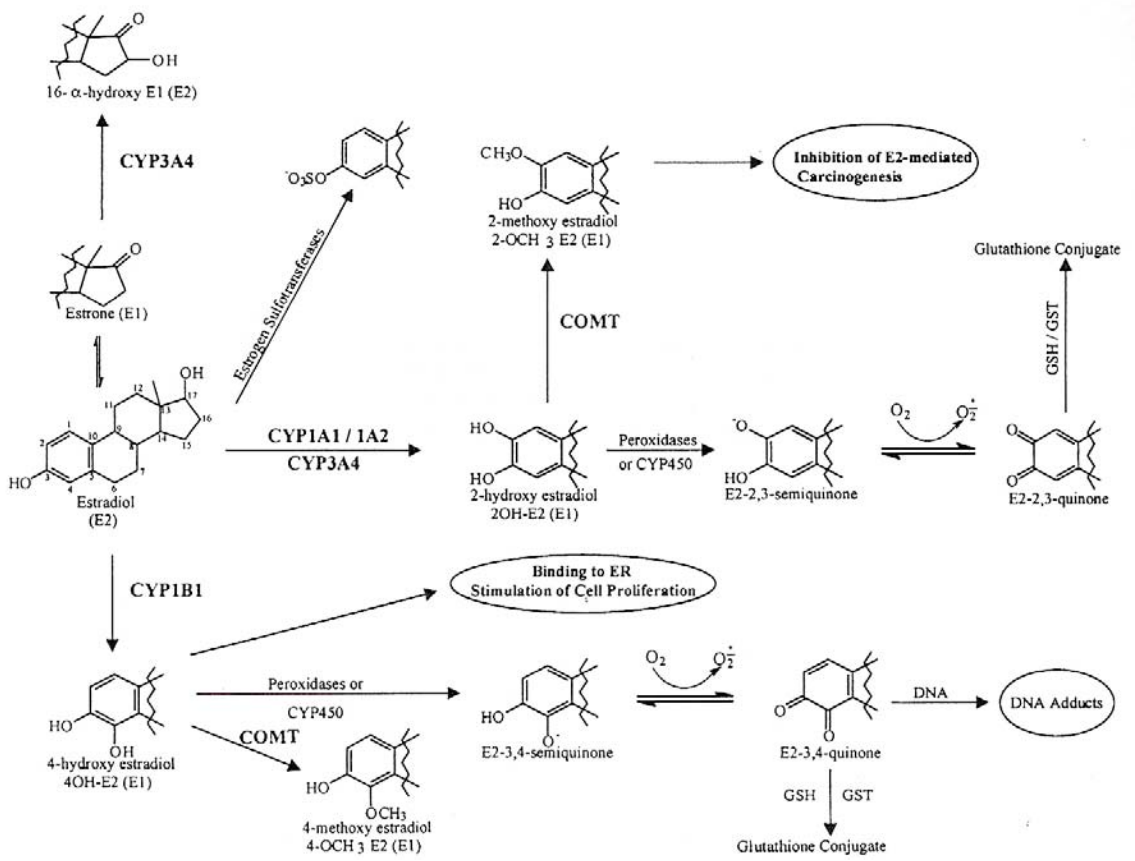

Figure 1.2: Biotransformation scheme for estrogen metabolism and the role of various metabolites in estrogen-induced carcinogenesis. E1 = estrone; E2 = estradiol; CYP = cytochrome P450; COMT = catechol-*O*-methyltransferase; GSH = glutathione; GST = glutathione S-transferase; ER = estrogen receptor. Reproduced from Pharmacotherapy, 2003, vol. 23(2), pp. 165-172 by copyright permission of Pharmacotherapy (18).

1.3 Overview of the cell cycle

The orderly sequence of events by which a cell duplicates its contents and divides into two is known as the cell cycle (32,33,34). Cell proliferation plays a crucial role in cancer development and therefore, it is necessary to understand the cell cycle and how it is regulated before the anti-carcinogenic properties of 2ME can be further explored.

Traditionally, the cell cycle is thought to consist of four phases: G_1 (gap 1), S (synthesis), G_2 (gap 2) and M (mitotic) phase (35,36). DNA replication occurs during S-phase and during M-phase chromosome segregation occurs and the cell physically

separates into two (35,37,38). M-phase can be subdivided into prophase, metaphase, anaphase and telophase (35,38,39). In short, chromosomes condense in prophase, in metaphase chromosomes attach to the mitotic spindle and align on the metaphase plate midway between the two poles, in anaphase sister chromatids move to opposite poles and in telophase the mitotic spindle disappears, chromosomes decondense and the nuclear envelope reassembles (32,40). In somatic cells, S- and M-phases are separated by so-called gap phases, G_1 (cells prepare for DNA synthesis) and G_2 (cells prepare for mitosis) (33,35,39). The period in between two M-phases is called interphase (38). During the transition between mitosis and interphase, breakdown of the spindle apparatus, decondensation of chromosomes, cytokinesis (cell division), reassembly of the nuclear envelope, and formation of prereplication complexes occur (38). Fast-replicating cells from higher vertebrates proceed through an entire cell cycle within 24 hours, with M-phase ≈ 30 min, G_1-phase ≈ 9h, S-phase ≈ 10h, G_2-phase ≈ 4.5h (38). G_0 cells are not actively cycling (35). Although subdivision of the cell cycle into four phases is useful and can serve as an organizing principle, biochemical, genetic and cytological research reveal cell cycle processes as much more intricate (36). A large number of macromolecular components are assembled, activated, or moved, a sequence of events involving one organelle (such as the centrosome) may occur throughout all four stages of the cell cycle and independent sequences are coordinated with one another (36).

The mitotic spindle consists of a dynamic array of microtubules and associated proteins and is responsible for the segregation of chromosomes during mitosis (41). The dynamic nature of microtubules underlies many of the most basic activities of the cell (42). In interphase cells, microtubules radiate outward from the microtubule organizing center (MTOC) and act as relatively static “railroad tracks” for vesicles and protein cargoes (39,42,43). Upon entering mitosis, the cell dismantles and rebuilds this radial array into a bipolar mitotic spindle (39,42,44).

Microtubules have distinct (+) and (-) ends and are composed of heterodimers of individual α- and ß-tubulin subunits, which hydrolyze guanosine triphosphate (GTP) during polymerization (39,42,44). Microtubules grow and shrink from centrosomes (45,46) and alternate between phases of slow growth and rapid shrinkage, a property known as dynamic instability (44,47). A state of rapid shortening is called a

catastrophe, while the transitions from rapid shortening back to growth again is termed a rescue (46). After nuclear envelope breakdown at the onset of prometaphase, microtubules start to grow preferentially toward chromosomes (45,48). Chromosomes attach to the dynamic microtubules from opposite spindle poles and eventually establish bipolar orientation (49).

The kinetochore is defined as a multi-protein, plate-shaped complex, intimately associated with the centromeric DNA and attaches the chromosome to spindle microtubules (48). Kinetochores perform three major functions in mitosis: they attach to the plus ends of spindle microtubules, they generate forces for chromosome movement, and they prevent anaphase onset until chromosomes are properly attached to the mitotic spindle (50).

Growing microtubules associate with the kinetochore to form the kinetochore fibre, the most stable microtubules in the mitotic spindle along which chromosomes move for the separation of the duplicated chromosomes during cell division (39,42,44,45). All the microtubules the centrosomes initiate have the same polarity, *i.e.* all are oriented with their minus ends at centrosomes and their fast-growing or plus ends pointed outward and/or attached to the kinetochores of chromosomes (45,46,50). Microtubules depolymerize at kinetochores when chromosomes move toward poles and polymerize at kinetochores when chromosomes move away from poles (45). The shortening of these microtubules is responsible for the towards-the-pole movement of chromosomes during anaphase (44). In most organisms, a single kinetochore is present on each chromosome and the assembly of only one kinetochore per chromosome is essential for proper chromosome separation (disjunction) at anaphase (44,50). Microtubule motor enzymes move along the microtubule track and are thought to be necessary for both attachments of chromosomes to the spindle microtubules and force generation during mitosis (39,41,46,50).

The decision of the cell to proliferate, to enter into reversible quiescence, or to enter into a postmitotic differentiation state is controlled by the cell cycle clock apparatus, a molecular machinery, operating in the cell nucleus (51). At several transitions, cell cycle progression is subject to controls (32,33). Extracellular growth factors and hormones serve to integrate cell proliferation with cell growth and

differentiation (33), for example, growth factors stimulate the entry of cells into the cell cycle from G_0 (35). On the other hand, checkpoint controls originate from within the cell to coordinate different cell cycle events and to halt cell cycle progression in response to irregularities such as DNA damage or faulty spindle assembly (33). A number of positive and negative feedback loops also contribute to cell cycle progression (52). Negative controls on cell cycle progression are exerted during development, differentiation, senescence, and cell death and may play an important role in preventing tumorigenesis (52).

1.4 Regulators of the cell cycle

1.4.1 Cyclin-dependent protein kinases

Progression through the cell cycle in all eukaryotic cells is regulated by sequential activation and subsequent inactivation of cyclin-dependent protein kinases (Cdks) (33,34,35,39,53,54). There are at least seven Cdks in mammalian cells (35). Cdks are thought to have multiple targets (39) and phosphorylate a variety of target proteins on critical serine and threonine sites (51), thereby catalyzing the process of cell division (35). Phosphorylation reactions catalysed by mitotic Cdk complexes that accumulate during interphase are responsible for condensation of chromosomes (condensin), nuclear-envelope breakdown (nuclear lamins), and assembly of the mitotic spindle apparatus (microtubule-associated proteins) (38). In general, the levels of Cdks are relatively constant throughout the cell cycle (51). The activities of Cdks are regulated positively by cyclins and negatively by Cdk inhibitory proteins in response to a wide variety of anti-proliferative signals (32,35,39,53).

1.4.2 Positive regulators of Cdks: the cyclins

Cyclins are positive regulatory subunits of Cdks (33,35). The cyclins were so named because of their cyclic expression during the cell cycle (35). So far, twelve different cyclins have been described in vertebrates (33).

Cdks need to bind to cyclins to be activated (35,51,52). The cyclin-Cdk complex often contains other proteins as well, but the functions of these proteins are not yet

clear (52). Once physically associated with the Cdks, cyclins are able to guide the Cdks to appropriate substrates and activate their catalytic activity (51). The periodic appearance and disappearance of distinct Cdk/cyclin complexes drive the cell from one stage of the cell cycle to another (33,52). In general, before a cell can enter the next cell cycle phase, the appropriate cyclin of the previous phase is degraded, and the cyclin of the next phase is synthesized (35). Because of this cyclic expression, Cdks can be activated only at specific times during the cell cycle and therefore, the activity of cyclin:cdk complexes is determined in part by the levels of available cyclins (35,51). The programmed synthesis and destruction of individual cyclins assure an appropriate temporal window for the activation of their Cdk partners, and thus maintain an appropriate order of cell cycle events (33). Multiple controls are responsible for the transcription of cyclin genes, the degradation of cyclin proteins, and the modification of the kinase subunits by phosphorylation (52).

D-type cyclins are synthesized as cells emerge from quiescence (51), and are considered to be key regulators of G_1 progression (33). D-type cyclins associate with Cdk4 and Cdk6 in response to growth factors (51,52). Cdk2 is essential for DNA replication (52). In mid/late G_1, cyclin E associates with Cdk2 (51). This is essential for G_1/S transition (51). Cyclin B-associated kinase activity is low during most of the cell cycle and increases dramatically at mitosis, while cyclin A-associated kinase activity increases gradually through S and G_2 but reaches a peak and decreases before cyclin B (55). Cyclin A, in a complex with Cdk2, is essential for progression through S-phase where DNA synthesis occurs (33,38,51). Cyclin A also associates with Cdk1, also referred to as Cdc2 (cell division cycle 2) until the late G_2-phase when B-type cyclins appear (33,35,51,55). Cdk1 kinase is expressed in all cycling mammalian cells (55). Cyclin B is required for entry into mitosis (38) and form complexes with Cdk1 to triggering the complex series of events associated with mitosis (33,35,51,55).

A schematic drawing of the cell cycle and various cdk-cyclin complexes that regulate progression through the cell cycle is represented in Figure 1.3 (35). Undoubtedly, additional vertebrate Cdks and cyclins remain to be discovered since the partners for cyclins C, F and G as well as for Cdk3 have not yet been identified (33).

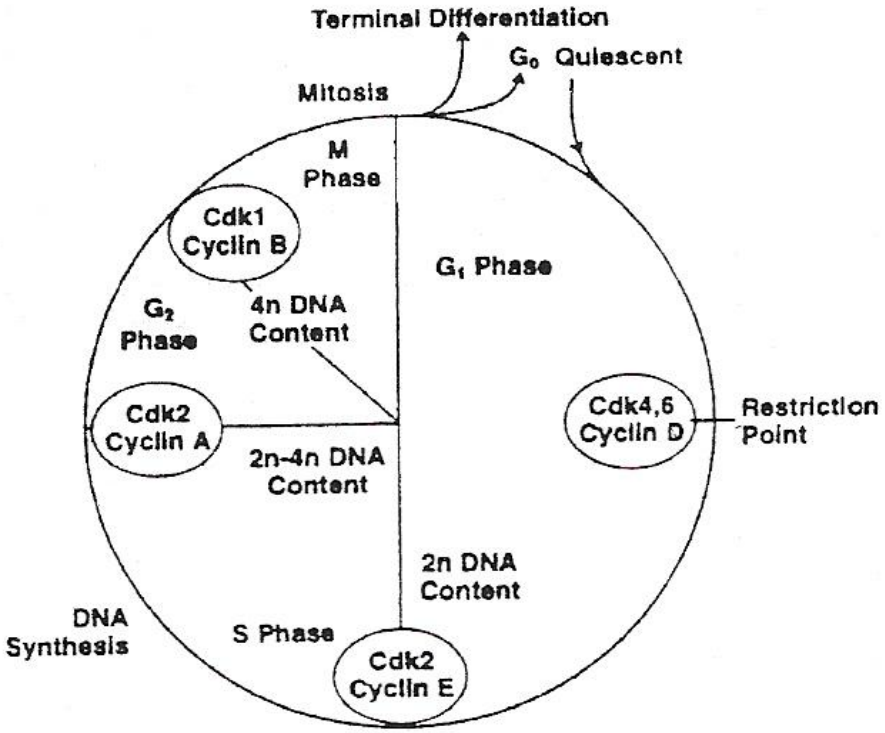

Figure 1.3: Schematic drawing of the cell cycle and various Cdk-cyclin complexes that regulate progression through the cell cycle. Reproduced from Veterinary Pathology, 1998, vol. 35, pp. 461-478 by copyright permission of Veterinary Pathology (35).

1.4.3 Cdk inhibitory proteins

Inhibitory components also play a role in the control of cell cycle transition. When an activating component is associated with an inhibitory component, the cell cycle transition is blocked (56). The cell cycle progression continues when the association is abolished, for example, through proteolytic destruction of the inhibitory component in response to appropriate signals (56). In some cases, the inhibitory component has served a positive role in a previous step in the cell cycle (56). Cdk inhibitory proteins are downstream targets for many of the different signal transduction cascades that regulate cell proliferation (39).

In the G_1- and S-phases of the cell cycle, the most important inhibitors are the p16 and p21 families (35). In G_1, the retinoblastoma protein (pRb) sequesters transcription factors (notably members of the E_2F/DP family) that are involved in regulating genes

required for S-phase progression (33,35). Hypophosphorylated pRb binds the E_2F transcription factor, making it unavailable for transcription (35). Cdk4 or Cdk6 complexed to cyclin D phosphorylates pRb, which causes the release and activation of the E_2F/DP transcription factors (33,35). The p16 family members prevent the phosphorylation and inactivation of pRb by binding Cdk4 and Cdk6 (33,35). p53 acts as a transcription factor that causes expression of several responder genes, among them the p21 Cdk inhibitor (51). p21 (also referred to as CIP1, WAF1, CAP20 or SDI1) inhibits a number of different Cdk/cyclin complexes (35). For example, p21 bind cyclins, thereby preventing the Cdk from phosphorylating pRb and inducing its dissociation from E_2F (35). Because p21 acts so widely on a variety of cyclin:Cdk complexes, a p53-initiated block can apparently occur in both the G_1- and G_2/M-phases of the cell cycle (51). Alternatively p53 may activate the apoptotic apparatus (51). p15 target exclusively Cdk4 and Cdk6 and prevent their binding to cyclins and p27 inhibit Cdk2/cyclin E (33).

1.5 Regulation of the cell cycle

1.5.1 Cell cycle control by phosphorylation/dephosphorylation

Much of the cell cycle regulation is determined by phosphorylation/dephosphorylation of certain proteins (35,52). Multiple phosphorylation and dephosphorylation events occur on both Cdk and cyclin subunits (33) and various target proteins are phosphorylated by cyclin/Cdk complexes during distinct phases of the cell cycle (51). Furthermore, phosphorylation can control the activity of kinases both negatively and positively, depending on the phosphorylation sites (33).

At the G_2/M transition, the total amount of intracellular protein-bound phosphate increases dramatically, indicating that phosphorylation constitutes a major mechanism for bringing about the profound structural reorganizations that accompany entry of cells into mitosis (33). In mammalian cells, Cdc25 phosphatases are encoded by a multigene family consisting of Cdc25A, Cdc25B and Cdc25C that control distinct aspects of cell cycle progression (53). Cdc25A is vital for entry into S-phase while Cdc25B is essential for pre-initiating G_2/M transition and S-phase progression and

Cdc25C controls entry into mitosis by dephosphorylating the protein kinase Cdk1 (53,57).

There is ample evidence that phosphorylation controls spindle assembly and microtubule dynamics as well (33). A number of cellular factors regulate the dynamic instability of microtubules, including the structural microtubule-associated proteins (MAPs), which in turn are regulated by phosphorylation (47). Phosphorylation of MAPs influences their microtubule-stabilizing capacity (47). Microtubule-affinity-regulating kinases (MARKs) phosphorylate the tubulin-binding domain of MAPs and thereby cause their detachment from microtubules (47).

At anaphase onset proteins in the spindle pole are dephosphorylated and the Cdk1/cyclin B complex is degraded (48).

1.5.2 The maturation- or mitosis-promoting factor

Mitosis is initiated by the maturation- or mitosis-promoting factor (MPF) (33,38,55,58). The MPF is a protein kinase that comprises a catalytic sub-unit, called Cdk1, and a regulatory sub-unit called cyclin B (33,38,39,55,59). Once the Cdk1 kinase is activated it brings about the various events of M-phase (59). Both Cdk1 and cyclin B have also been identified at the level of the centrosome (60,61), suggesting a role for these proteins in the regulation of mitotic spindle formation (62). Cdk1 kinase activity is responsible for chromosome condensation, the cytoplasmic reorganization to convert the interphase microtubule array to the mitotic spindle and nuclear envelope breakdown (41,45,59). It is possible that the cell is kept in an M-phase state by high Cdk1 kinase activity (59). Cdk1 is subject to multiple levels of regulation including periodic association with the B-type cyclins, reversible phosphorylation, and intracellular compartmentalization (33,34,59,62,63).

Throughout interphase, Cdk1/cyclin B1 complexes shuttle between the nucleus and the cytoplasm (34,63). The apparent cytoplasmic localization of Cdk1/cyclin B1 complexes is due to a nuclear export signal (NES) in cyclin B1, which facilitates rapid export of Cdk1/cyclin B1 complexes from the nucleus (34,63). Phosphorylation of the NES in late prophase is proposed to block the nuclear export of cyclin B1 by

interfering with the binding of the nuclear export receptor CRM1 leading to the nuclear accumulation of Cdk1/cyclin B1 complexes (34,63). The accumulation of active Cdk1/cyclin B1 complexes in the nucleus is required for the entry into mitosis (63).

Cdk1 has phosphorylation sites that are both inhibitory and stimulatory (35). Phosphorylation occurs on three regulatory sites, i.e., threonine 14, tyrosine 15, and threonine 161 (34,63). Cdk1 is retained in an inactive state throughout the S- and G_2-phases of the cell cycle by phosphorylation at tyrosine 15 and threonine 14, which are located within the active site of the kinase (34,35,39,53,59,63). Wee1 kinase phosphorylates Cdk1 on tyrosine 15 to inhibit Cdk1 activity. Wee1 distribution is altered cyclic between nuclear and cytoplasmic compartments to regulate Cdk1 activity (62). Wee1 is localized subcellularly during the cell cycle and is found in the nucleus in interphase (55). Upon entry of the Cdk1-cyclin B complex into the nucleus, Wee1 kinase phosphorylates Cdk1 on tyrosine 15, thereby protecting the nucleus from premature exposure to an active mitotic kinase (33,34,35,55,64). At mitosis Wee1 enters the cytoplasm (55). Baldin *et al*. reported the localization of Wee1 during late telophase and cytokinesis in association with microtubular structures and they hypothesized that the inhibitory activity of Wee1 on cyclin-dependent kinase might also be involved in the regulation of microtubule stability (62). Phosphorylation of Cdk1 at tyrosine 15 and threonine 14 to prevent kinase activity can also be performed by Mik1, and Myt1 protein kinases (34,35,53,63). p53 induce the formation of p21, which is also a potent Cdk1 inhibitor (65,66).

Cdc25, a protein tyrosine phosphatase opposes the action of Wee1 (39,55,64,67,68). In late G_2, when the cell is ready to divide, Cdc25C dephosphorylates Cdk1 at tyrosine 15 and threonine 14, thereby activating the Cdk1/cyclin B1 complex (33,34,35,63,66,67,68). Once a small amount of Cdk1 became activated by Cdc25C, an auto-amplification loop would be initiated whereby activated Cdk1 promotes the activation of Cdc25C which in turn triggers further activation of Cdk1 (39,63). This pathway coupled to the one that downregulates the Cdk1 inhibitory kinases provides a mechanism for the rapid amplification of Cdk1 activity observed as cells enter into mitosis (63). Although it is unclear how the interactions between Cdk1 and Cdc25 are initiated, one requirement may be the dephosphorylation of Cdc25C on serine 216 and

subsequent loss of 14-3-3σ protein binding (63). 14-3-3σ proteins is a class of phospho-serine binding proteins involved in a variety of signalling pathways and through interacting with Cdc25C, 14-3-3σ regulates entry into the cell cycle (39,64,69). Throughout interphase, but not in mitosis, Cdc25C is phosphorylated on serine-216 and bound to 14-3-3σ proteins (57,64) to prevent dephosphorylation of Cdk1 that is critical for G_2/M progression (53). During mitosis serine 216 is dephosphorylated and Cdc25C disassociates from 14-3-3σ proteins (64). Loss of 14-3-3σ binding allows Cdc25C to move into the nucleus more efficiently and in turn enhances the accessibility of Cdc25C to nuclear pools of Cdk1/cyclin B1 (63).

Wee1 and Cdc25C are themselves regulated by phosphorylation, thereby forming an activation cascade (33,35,65). Cdk1 is one of the kinases that may phosphorylate Wee1 and Cdc25C, forming positive and negative feedback loops (33,35). The coordinate regulation of Cdc25 and Wee1 determines the timing of entry into mitosis (39,59). Phosphorylation of Cdk1 on threonine 161 by Cdk-activating kinase (CAK), a complex containing Cdk7 and cyclin H, is also necessary for Cdk1 kinase activity (33,35,39). At the onset of anaphase in the normal course of events, B-type cyclins are destroyed, MPF kinase loses activity, and the many changes required for a return to interphase are initiated (33,39,46,54,59,61).

1.5.3 The anaphase-promoting complex/cyclosome

The anaphase-promoting complex/cyclosome (APC/C) is a large multi-subunit protein complex that regulates progression from metaphase to anaphase and exit from M-phase into G1 (38,56,70,71,72). The APC/C is an E3 ubiquitin ligase that targets substrate proteins for rapid degradation by the proteasome (38). Ubiquitin-mediated degradation of proteins is a primary mechanism by which a change in cell cycle state is achieved (56). Ubiquitin chains attach covalently to lysine residues in a target protein, leading to its recognition and degradation by the proteasome (56). The high specificity of ubiquitin-mediated proteolysis allows for a single protein within a larger complex to be modified and destroyed (56). Furthermore, ubiquitin-mediated proteolysis is both rapid and irreversible and therefore change in cell cycle state can occur in a unidirectional switch-like fashion (56).

The APC/C is active under conditions of both high and low Cdk activity (56) and contributes to the proteolysis of mitotic cyclins, securins (Pds1/Cut2), Ase1, geminin, Cdc20, Cdc5, and polo-like kinase 1 (Plk1) (71). The substrate specificity of the APC/C changes at late M-phase from anaphase inhibitors to mitotic cyclins (71). The APC is activated in mitosis and G_1 by Cdc20 and Cadherin 1 (Cdh1), and inhibited by the mitotic arrest deficiency protein (Mad), Mad2 (72). Mad 2 is a specific inhibitor of Cdc20 (72).

The two activators, Cdc20 and Cdh1, display differential sensitivity to Cdk activity (56). APC^{Cdc20} functions in the presence of high Cdk activity and require Cdk function for activation (56). Cdc20 levels fluctuate in a cell cycle-dependent manner, through transcriptional and posttranslational mechanisms, thus restricting APC^{Cdc20} activity by limiting the amount of Cdc20 available to bind to the APC/C (56). Cdc20 is undetectable in G_1, accumulates from late S-phase, peaks at the G_2/M and is rapidly degraded as cells exit from M-phase by an APC^{Cdh1}-dependent mechanism (56,71). Therefore, APC^{Cdc20} is activated as cells approach metaphase (56). Cdh1 undergoes inhibitory phosphorylation by Cdks that prevents APC/C binding, thus restricting APC^{Cdh1} activity to points in the cell cycle when Cdk activity is low (56). Binding of Cdh1 occurs during late M/early G1-phase (38). Therefore, APC^{Cdh1} is activated during exit from mitosis and persists until the G_1/S transition (56). Unlike B-type cyclins, G_1 cyclins are immune to the action of the APC/C and therefore can accumulate when APC^{Cdh1} activity is high (56).

Despite striking differences between the timing of cyclin A and B proteolysis, they both appear to be degraded as a result of polyubiquitination by the Cdc20-dependent form of the APC/C (73). Cyclin A is stable in S- and G_2-phases, but as cells enter mitosis, the APC/C is activated and targets the cyclin A for degradation (73). Cyclin A is degraded by APC/C^{Cdc20} at the time of nuclear envelope breakdown (38) and is almost completely degraded before the metaphase to anaphase transition (73).

Phosphorylation of core APC/C subunits occurs upon entry into mitosis and is required for optimal APC/C activity (56). These phosphorylation events are thought to be mediated by Cdk1/cyclin B and Polo protein kinases and have been shown to enhance the Cdc20-APC/C interaction (56). The APC/C is required to reduce B-type

cyclin levels as cells pass through anaphase and telophase, but the APC/C also restrains the accumulation of B-type cyclins during G1, and its inactivation is required for timely S-phase entry (56). Cyclin B degradation is started by APC/C^{Cdc20} during metaphase and is finally finished by APC/C^{Cdh1} after anaphase (38). Destruction of both cyclin B and securin by the APC is necessary to induce the segregation of chromatids to opposite poles (74).

E2-C is an ubiquitin-conjugating enzyme expressed in late G_2/M-phase (71). Ubiquitin is a 76-residue highly conserved protein that becomes linked to lysine residues in other intracellular proteins (38). Proteins of which a chain of ubiquitin molecules is added are usually degraded in a proteasome (38). Polyubiquitination and degradation of E2-C occurs as cells exit from M-phase (71). Mammalian E2-C is also a substrate of the APC/C-dependent proteolysis machinery, and its periodic expression may autoregulate APC/C activity and its substrate specificity (71).

1.5.4 Cell cycle checkpoints

Cell cycle checkpoints have been defined as “biochemical pathways that ensure dependence of one process upon another process that is biochemically unrelated” (35). Therefore, cell cycle checkpoints regulate progression between distinct steps within the cell cycle to guarantee high fidelity during ‘critical events’ like segregation of chromosomes (the spindle/mitotic checkpoint), DNA replication (the DNA replication checkpoint), and DNA damage-induced cell cycle arrest and apoptosis (the DNA damage checkpoint) (38). To ensure faithful replication and transmission of the genome and to promote survival, checkpoints fulfil at least four tasks: they rapidly induce cell-cycle delay, help activate DNA repair, maintain the cell-cycle arrest until repair is complete, and then actively re-initiate cell-cycle progression (75).

The cell cycle control system can halt the cycle at specific checkpoints to ensure that the next step in the cycle does not begin before the previous one has finished (32,36,52,54). This allows time for DNA replication and repair before the cell enters mitosis and for alignment of chromosomes on the spindle before the cell initiates anaphase (54). When these periodic events are incomplete, the checkpoint

systems block further transitions in the cell cycle (54). When DNA damage is irreparable, checkpoints eliminate such potentially hazardous cells by permanent cell-cycle arrest or cell death (75). A checkpoint should consist of three functional units: a sensor, a signal-transduction cascade and an effector (54). The sensor monitors events in the cell cycle and if there is a defect or the process is not complete, generates a signal (54). The initial signal is then amplified in a signal-transduction cascade and eventually modifies the cell-cycle machinery such that the cell cycle is halted until the defect is rectified (54). When loss of a cell cycle checkpoint occurs, genetic errors arise much more frequently giving rise to genetic instability and the cells progress to a malignant phenotype (52,54). Mutation of the genes encoding proteins involved in checkpoints may be an important event in the genesis of cancer cells, allowing genetic changes to accumulate more readily, although the stages at which checkpoint controls are lost may differ for different tumor types (54). Elimination of checkpoints may result in cell death, infidelity in the distribution of chromosomes or other organelles, or increased susceptibility to environmental perturbations such as DNA damaging agents (36).

Cell cycle arrest is produced by a variety of factors that may be intrinsic or extrinsic and may affect several different checkpoints (35). An example of an intrinsic factor is cell size, although it is more important in yeast and plays a less important role in mammalian cells (35). An example of an extrinsic factor is cell nutrition that is important in all cells and determines whether and the rate at which a cell progresses through the cell cycle (35).

The checkpoint controlling entry into S-phase prevents the cell from replicating damaged DNA (52). Cells arrest in G_1 to allow for repair before DNA replication (35). Loss of the G1-S checkpoint can lead to genomic instability, inappropriate survival of genetically damaged cells, and the evolution of cells to malignancy (52). G_1 arrest is p53 dependent (35). p53 recognizes and binds several types of DNA damage including single-stranded DNA, insertion/deletion mismatches, and free DNA ends (35). Cells with DNA damage rapidly increase p53 protein levels by a posttranscriptional mechanism (52). Following DNA damage, p53 stimulates the transcription of p21 (35). The p21 protein then inhibits G_1 Cdks (35). Likely targets for the G1-S checkpoint are Cdks containing the cyclins expressed early in the cell

cycle, such as cyclins D, E, and A (35). Another function of p53, is the p53-dependent stimulation of apoptosis following severe DNA damage (35).

The G_2/M transition is prevented by DNA damage and by incompletely replicated DNA (52). This checkpoint prevents chromosome segregation if the chromosome is not intact (52). Arrest in G_2 allows repair before chromosome separation in mitosis, but the role of p53 arrest in G_2 arrest is controversial (35). Arrest of the cell cycle at the G_2 checkpoint, induced by DNA damage, requires inhibitory phosphorylation of the kinase Cdk1 in human cells (76). Throughout interphase, human Myt1 localizes to the endoplasmic reticulum and Golgi complex (34). The overproduction of either kinase-active or kinase-inactive forms of Myt1 disrupts the intracellular trafficking of Cdk1/cyclin B1 and as a consequence cells delay in the G_2-phase of the cell cycle (34). Cdc25 is also a target of the DNA damage checkpoint in human cells (57,76). In response to DNA damage, Chk1 phosphorylates and inhibits Cdc25C, thus preventing activation of the Cdk1/cyclin B complex and mitotic entry (57,77).

Improper functioning of the mitotic spindle at metaphase can arrest cell cycle progression (52). A spindle checkpoint exists to ensure that chromosome assembly, orientation and segregation occurs with optimal fidelity (49,78).

1.5.4.1 The spindle assembly checkpoint

The spindle checkpoint regulates the metaphase to anaphase transition and the exit from mitosis, when cells progress form anaphase to the G_1 stage of the subsequent cell cycle (49). The spindle checkpoint is most clearly manifested when cells are treated with anti-microtubule drugs (78). Microtubule inhibitors like taxol, colchicines, nocodazole, or vinca alkaloids interfere with the assembly and degradation of the mitotic spindle apparatus and therefore affect mitotic segregation of chromosomes at the transition from metaphase to anaphase (38,78). Exposure to these compounds activates the spindle checkpoint and results in a cellular delay/inhibition of the onset of anaphase and/or in induction of apoptosis (38,78). Inducing the spindle checkpoint, for example by treating yeast cells with a microtubule-depolymerizing drug such as nocodazole, causes them to arrest the cell cycle prior to anaphase (49).

The spindle-assembly checkpoint is constituted by a signal transduction cascade that inhibits the onset of anaphase until a bipolar spindle is present and all the chromosomes are attached to the spindle and orientated properly at the metaphase plate (38,42,44,48,50,54,73,79). Progression in mitosis remains blocked even in the case where just a single chromosomal connection is missing (38). Thus, the signal for checkpoint-dependent arrest originates at the kinetochores and is broadcast to the rest of the cell (38,78).

The spindle assembly checkpoint operates at least in part by preventing cyclin B destruction (54) and thereby preventing activation of MPF (34,39,59,63,65). The spindle-assembly checkpoint also functions by preventing the APC from ubiquitinylating proteins whose destruction is required for anaphase onset and exit from mitosis (78,80). Ubiquitination by the APC/C and subsequent degradation of the anaphase inhibitor is required for liberation of a protease that degrades the cohesions holding the sister chromatids together, thereby initiating the metaphase-to-anaphase transition (81). Premature activation of the APC/C may cause unequal chromosome segregation (73). Gorbsky *et al.* proposed that kinetochores lacking stable attachments to the spindle microtubules serve as catalytic staging areas for the assembly of inhibitor complexes (78). These inhibitor complexes then leave the kinetochores and block activity of the APC/C throughout the cell (78). Microtubule occupancy at kinetochores or physical tension induced by microtubule capture turns off the capability of the kinetochore to produce the APC/C inhibitor (78). The APC/C becomes active again, inducing sister chromosome separation and segregation by securing protein proteolysis and inducing cytokinesis and exit from mitosis by cyclin B proteolysis (50,78).

Kinetochores in vertebrate cells contain multiple binding sites, and tension is generated at kinetochores after attachment to the plus ends of spindle microtubules (82). Checkpoint component Mad2 localizes selectively to unattached kinetochores (80,81,82,83). Mad2 is sensitive to microtubule interactions mediated by the kinetochore motor centromere protein-E (CENP-E) (80). Depletion of CENP-E from kinetochores in mammalian cells disrupts chromosome alignment, and cells become arrested in mitosis with high levels of Mad2 at unattached kinetochores (80). Mad2 disappears from kinetochores by late metaphase, when chromosomes are

properly attached to the spindle (80,81,82,83). Immunofluorescence and digital imaging techniques showed that decreasing tension at kinetochores, without detaching them from the spindle, was not sufficient to induce Mad2 binding to kinetochores, whereas unattached kinetochores consistently bound Mad2 (82). Mad1 and Mad2 are thought to be centrally involved in sensing chromosome positions and spindle attachment and transducing the signal to the cell cycle machinery (84). Antibody electroporation experiments by Li *et al.* indicated that the human homolog of Mad2 (hsMad2) is an essential component of the mitotic checkpoint in HeLa (human cervical carcinoma) cells (83). In prometaphase, when most, but not all of the kinetochores are attached to the spindle, hsMad2 is colocalized with the kinetochores (83). However, at metaphase and anaphase, hsMad2 staining was absent from the chromosomes, which could be due to either the loss of hsMad2 antigen from the kinetochore or epitope masking (83). These observations suggest that hsMad2 may monitor the completeness of the spindle-kinetochore attachment and may activate the mitotic checkpoint when this process is incomplete (83). Indeed, Li *et al.* observed persistent kinetochore localization of hsMad2 in HeLa cells arrested in mitosis by nocodazole treatment in which spindle-kinetochore interaction was inhibited (83). Therefore, they suggested that defects in the mitotic checkpoint might contribute to the sensitivity of certain tumors to mitotic spindle inhibitors (83). Wang *et al*. demonstrated an association between reduced expression of Mad2 protein and loss of mitotic checkpoint in nasopharyngeal carcinoma cells (84). Furthermore, removal of vertebrate Mad2 using Mad2 antibodies or disrupting one or both Mad2 alleles in mice led to inappropriate chromosome segregation (56).

A mitotic checkpoint complex (MCC) consisting of Mad2, BubR1 (budding uninhibited benzimidazole receptor 1), Bub3 (budding uninhibited benzimidazole) and Cdc20 in mammalian cells was shown to inhibit the APC/C (80). However, the association of this complex with the APC/C is regulated during the cell cycle is less clear (81). Although many reports showed that recombinant Mad2 can directly inhibit APC/C, Sudakin *et al.* determined that the inhibitory activity was over three orders of magnitude (> 3000-fold) weaker than the MCC (80). They believe that MCC inhibits APC/C by directly binding to it rather than via catalytic inactivation (80). Furthermore, although MCC is present during interphase, it was found that only APC/C from mitotic cells was sensitive to MCC inhibition (80). APC/C must undergo

mitotic modifications in order for it to be recognized by the MCC including phosphorylation of specific APC/C subunits and its association with Cdc20 (80). In the presence of unattached kinetochores, signals initiated at kinetochores modify the APC/C or APC-bound MCC to enhance their interactions and thus prolong its inhibition (80). The signal from the kinetochore can either be Mad2 as proposed or a kinase cascade that is initiated at the kinetochore by BubR1, Bub1, or other kinases (80). After chromosomes align, the signal from kinetochores decays along with the modifications (80). The MCC then dissociates and APC/C becomes active to drive cells out of mitosis (80). Sudakin *et al.* believe that MCC may not inhibit APC/C during interphase because it either lacks the appropriate phosphorylations or the APC/C is bound to a different substrate specificity factor, Cdh1 (80). A model for MCC function and regulation is represented in Figure 1.4 (80).

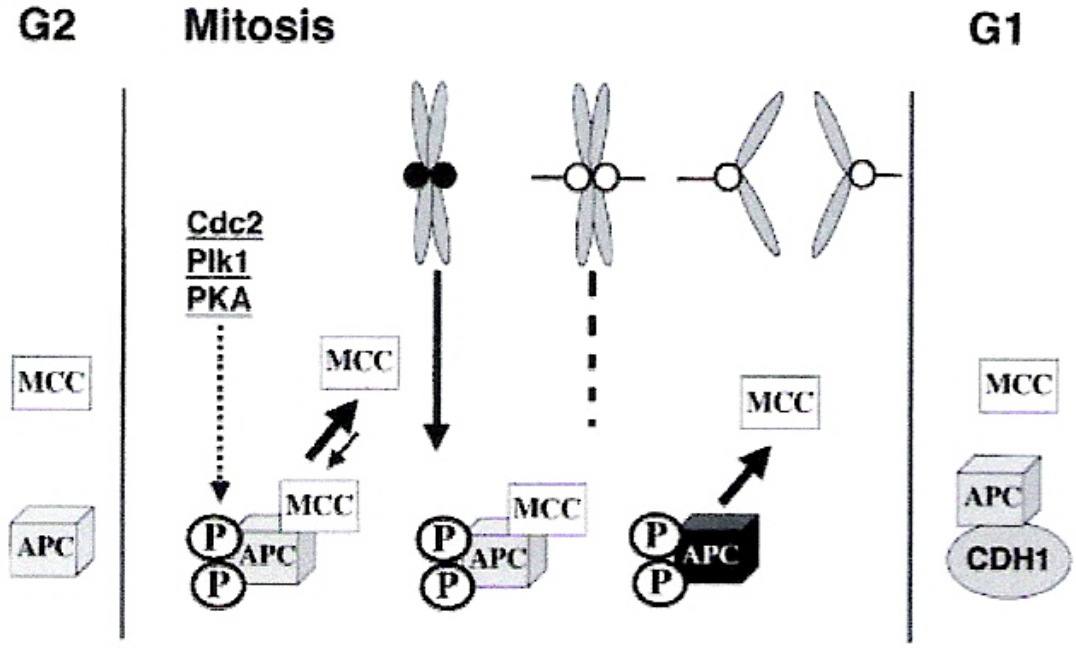

Figure 1.4: Model for MCC function and regulation. Reproduced from The Journal of Cell Biology, 2001, vol. 154(5), pp. 925-936 by copyright permission of The Rockefeller University Press (80).

The spindle assembly checkpoint delays the degradation of cyclin B1, and presumably that of securin, until the metaphase to anaphase transition (73). Purified Mad2 causes a metaphase arrest in cycling *Xenopus laevis* egg extracts and prevents cyclin B proteolysis by blocking its ubiquitination, indicating that Mad2 functions as an inhibitor of the cyclosome (85). Thus, Mad2 links the mitotic checkpoint pathway to

the cyclin B destruction machinery that is critical in controlling the metaphase to anaphase transition (85). Evidence suggests that Mad2 forms a complex with Mad1 and transmit its signal by associating with Cdc20 (84). Mad1 is needed for Mad2 localization to unattached kintochores, for the Mad2-Cdc20 interaction does not occur in the absence of Mad1 (56). Mad1 and Cdc20 bind to a similar region of Mad2, and this region undergoes a similar conformation change upon associaton with either Mad1 or Cdc20 (56). Mad2 is in a 'seatbelt' configuration that must unfold to release Mad1 (56). Mad1 binding to Mad2 and subsequent release from Mad1 induce a conformational change in Mad2 that enables it to bind to unattached kinetochores and Cdc20, culminating in the inactivation of APC^{Cdc20} (56). Mad2 forms a ternary complex with Cdc20 and Cdc27, a component of the APC/C, to inhibit APC/C^{Cdc20} dependent ubiquitination and degradation, thereby causing a cell cycle arrest in metaphase (56,81,83,85,86,87,88). Inhibition of APC/C^{Cdc20} prevents sister-chromatid separation by blocking degradation of securing (49,56,81). Securins are inhibitors of chromosome segregation during anaphase and the presence of securins leads to the sequestration of separins (for example Esp1), the initiators of anaphase (38). Once activated, the mitotic checkpoint arrests the cell cycle prior to the metaphase-anaphase transition with unsegregated chromosomes and high levels of cyclin B (85). Mad2 dissociates with the cyclosome/APC upon checkpoint release (85). Inhibition of the spindle assembly checkpoint accelerates the degradation of cyclin B1 (73).

It has been shown that kinetochore-induced pre-anaphase arrest requires Mad2 for establishment and Bub2 for maintenance in *Saccharomyces cerevisiae* (89). Protein kinase Bub1 is localized at the kinetochore and activated by the spindle checkpoint (38). In response to spindle disruption, Bub1 bind directly to the APC/C activator Cdc20 and encodes proteins that bind to the kinetochore and are required for a normal mitotic delay (50,78,90). Together with another kinase (Mps1), Bub1 leads to phosphorylation of Mad1 in a Bub3- and Mad2-dependent manner, subsequently resulting in activation of Mad2 and inhibition of APC/C^{Cdc20} through formation of a ternary $Mad2/APC/C^{Cdc20}$ complex (the so-called Bub/Mad pathway) (38,81,88,91). Bub2 protein is required continuously for maintenance of the spindle assembly checkpoint-mediated block even when its function is manipulated well after establishment of pro-metaphase arrest (89).

Chung *et al.* demonstrated that the ratio between Mad1 and Mad2 is critical for maintaining a pool of Mad1-free Mad2 that is necessary for the spindle checkpoint (88). They proposed that Mad2 may become activated and dissociated from Mad1 at kinetochores and is replenished by the pool of Mad1-free Mad2 (88). The pool of Mad1-free Mad2 protein ensures that Mad1 quickly binds new Mad2 when active Mad2 or Mad2-Cdc20 complex has dissociated, thus maintaining the checkpoint signal (88). The checkpoint is abolished when Mad1 and Mad2 fail to bind kinetochores (88). Once the checkpoint is satisfied, one can imagine that attachment of the spindle to the kinetochore somehow displaces or modifies the Mad1/Mad2 complex and prevents the loading of Mad 2 onto the APC/C (81). Free APC/C^{Cdc20} is now able to ubiquitinate its substrates, which in turn enables cells to proceed through the metaphase to anaphase transition (81). Phosphorylation of Mad2 *in vivo* peaks just after all the requirements for the spindle checkpoint has been met (81). Only the pool of unphosphorylated Mad2 is capable of associating with APC/C^{Cdc20}, perhaps due to changes in conformation, or just the correct localization (81). One or more Mad2-specific kinase(s) continuously phosphorylate Mad2 to displace it from APC/C^{Cdc20}, but as long as there is a single unattached kinetochore this Mad2 is dephosphorylated by one or more phosphatases to allow continuous loading onto Mad1 and APC/C^{Cdc20} (81). A phosphorylation-dephosphorylation cycle may be required to allow the transfer of Mad2 from Mad1 to the APC/C^{Cdc20} complex (81). As soon as the last kinetochore attaches to microtubules, the last Mad1/Mad2 complex is displaced from the kinetochore and Mad2 can no longer be loaded onto APC/C^{Cdc20} (81). APC/C^{Cdc20} becomes active by Mad2 phosphorylation and subsequent release from the complex, and metaphase to anaphase transition can now take place (81).

Another component of the spindle assembly checkpoint is p38 (92). This kinase is activated by disruption of the spindle and activated p38 will arrest the cell cycle in M-phase (92).

Regulation of the spindle checkpoint is represented in Figure 1.5 (38).

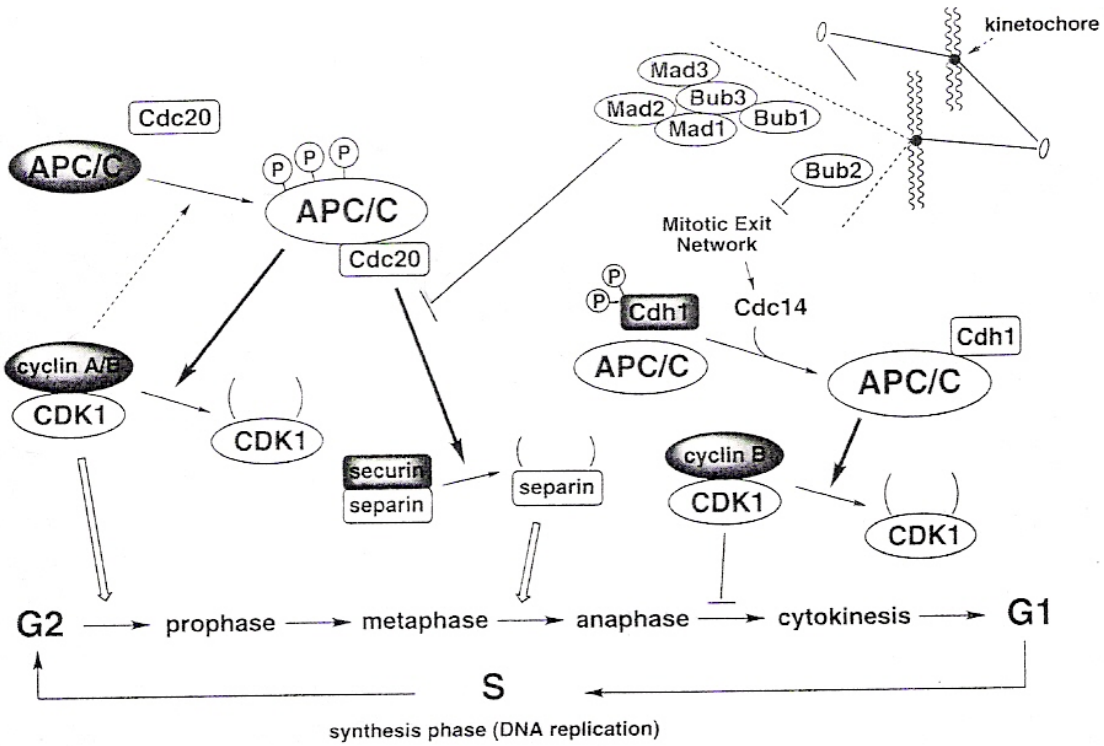

Figure 1.5: APC/C-dependent regulation of cell cycle progression and function of the spindle checkpoint in animal cells. Reproduced from ChemBioChem, 2002, vol. 3, pp. 506-516 by copyright permission of Wiley-VCH Verlag & Co. (38).

1.6 Anti-tumor activity of 2ME

2ME is a major metabolite of 17ß-estradiol in human serum (53,93) and it is formed in large amounts in liver and in estrogen target cells (21,24). Physiological concentrations of 2ME range from 3.768 to 10.3 pg/ml in serum, as reviewed by Schumacher and Neuhaus (94). 2ME is lipophilic and may accumulate within cells (95). 2ME suppresses proliferation of many cancer cell lines and inhibits the growth of solid tumors *in vivo* (8,11,28,96,97,98). Furthermore, 2ME seems to target rapidly dividing cancerous cells and have only minimal effects on normal cells. Maran *et al.* demonstrated that 2ME is highly cytotoxic to osteosarcoma cells, but not to primary cultures of normal human osteoblasts (99). 2ME's effect on cells appears to be pleiotropic (100) and include antiproliferative as well as antiangiogenic effects (8,18,28,29,96,98,101,102,103,104,105,106).

1.6.1 Antiproliferative activity

In normal cells oncoproteins carry a signal from the cell surface to the nucleus with the end result being transcription and initiation of the cell cycle (35). In transformed cells, these signal transduction pathways are always "turned on" or their inhibitory mechanisms are "turned off" (35). Failure to arrest proliferation of cells when genome integrity has been compromised or when the cell is not yet ready to divide may result in the formation of cancer cells (35). The slower the cell cycle, the more time there is for DNA repair and therefore decreased carcinogenesis (10).

2ME shows potent antiproliferative activity at low concentrations, against a large variety of cell lines (96,107). Qadan *et al.* found that 2ME is a powerful growth inhibitor of various prostate cancer cells (108). 2ME is also an effective agent inhibiting cellular proliferation in mesenchymal cells (109) and had a strong antiproliferative effect on human glioblastoma cells (95). Cushman *et al.* reported that 2ME was toxic to dividing cells of 55 different tumor cell lines (102). Furthermore, Mueck *et al.* found that 2ME enhanced the antipoliferative property of certain therapeutic compounds, such as the anti-hormonal substances tamoxifen and letrozole as well as various cytostatic substances (13). Various cell lines inhibited by 2ME and their inhibitory concentrations are listed in Table 1.2, taken from an article published by Pribluda *et al.* (164).

In vivo studies also confirm the antiproliferative activities of 2ME. After 2 weeks of treatment with 100 mg/kg/day of 2ME, the tumor growth of MethA (3-methyl-cholanthrene-induced) sarcoma and B16 melanoma cells was inhibited by 66 % and 88 %, respectively (18,28). In experiments by Qadan *et al.* primary prostate tumors from 2ME (75 mg/kg)-treated mice were significantly smaller (38 % reduction of wet weight) compared to placebo-treated mice (108).

In contrast to the above-mentioned, Fotsis *et al.* found no effects on normal, non-dividing quiescent cells, *in vitro* (28).

Table 1.2: Cell lines inhibited by 2-methoxyestradiol. Reproduced from Cancer and Metastasis Reviews, vol. 19, 2000, pp. 173-179, 2-Methoxyestradiol: an endogenous antiangiogenic and antiproliferative drug candidate, Pribluda VS, Gubish ER, LaVallee TM, Treston A, Swartz GM, Green SJ, table 1, copyright (2000) Kluwer Academic Publishers with kind permission of Springer Science and Business Media (164).

Cell type	Inhibitory concentration (μM)
Human tumor	
Lung (HOP-62)	0.7[a]
Lung (H460)	5.0[b]
Lung (A549)	5.0[b]
Colon (HCT-116)	0.47[a]
CNS (SF-539)	0.32[a]
CNS (SH-SY5Y)	1.3[a,b]
Melanoma (UACC-62)	0.36[a]
Ovarian (OVCAR-3)	0.21[a]
Renal (SN12-C)	0.95[a]
Prostates (DU-145)	1.8[a]
Breast (MDA-MB-435)	0.08–0.61[a,b]
Breast (MDA231)	1.03[a]
Breast (MCF-7)	0.45[a,b]
Lymphoblast (Jurkat)	0.3
Lymphoblast (TK6)	1–2[b]
Lymphoblast (WTK1)	1–2[b]
Human non-tumor	
Skin fibrobalst (HFK2)	2.0[a]
Human endothelial	
HUVEC	0.45[a,b]
Non-human tumor	
Lung (Lewis lung, Murine)	1.68[a,b]
Melanoma (B16BL6, Murine)	0.40[a,b]
Melanoma (B16F10, Murine)	0.30[a,b]
Endothelial (EOMA, Murine)	0.89[a,b]
Endothelial (H5V, Murine)	1.0
Non-human non-tumor	
Lung (V79, Hamster)	3.0
Ovarian (Granulosa, Porcine)	3.0
Smooth muscle (Aorta, Rabbit)	1.0
Adipocytes (Murine)	1.7
Non-human endothelial	
Brain capillary (Bovine)	0.19–0.49[a,b]
Pulmonary artery (Bovine)	0.5[b]

[a] IC50 measured by metabolic labeling or cell count.
[b] Cells assessed for apoptosis. In every instance, when evaluated, $2ME_2$ inhibition was accompanied by apoptosis.

1.6.2 Antiangiogenic activity

Solid tumor growth is dependent on new blood vessel formation, i.e. angiogenesis (110,111,112). A tumor triggers the surrounding tissue to form new blood vessels to converge upon the tumor (110). Angiogenesis has been shown to be a critical step in the proliferation of cancers that are larger than 1 mm^3 (18,112,113). Angiogenesis in the adult is largely controlled by the female reproductive cycles and pathological situations, such as wound healing and tumor growth (112). Antiangiogenic agents that specifically inhibit tumor-induced angiogenesis and not physiological angiogenesis would be of great importance in the development of anti-tumor drugs (110). A specific property of angiostatic therapy is that its effect is cytostatic and not cytotoxic (110) and is therefore expected to exhibit less systemic toxicity than chemotherapy (110). Furthermore, endogenous angiogenesis inhibitors are expected to have fewer side effects than exogenous ones, since they are a part of normal regulation of vascular growth (110).

Tumors are genetically unstable and the development of drug resistance and consequent treatment failure is therefore not uncommon (114). One way to overcome multidrug resistance is to rather target the genetically stable endothelial cells of the developing tumor. This would result in more specific and less toxic treatment (113,114,115). Although low concentrations of 2ME induce endothelial cell growth, pharmacological concentrations are potent antiangiogenic agents (116). The antiangiogenic activity of 2ME was discovered in 1994 by Folkman *et al.* (31) and several preclinical as well as clinical trials confirmed the potential of 2ME in the treatment of several disorders associated with aberrant angiogenesis (28,31). The antiangiogenic activities of 2ME vary with cell type and the regulatory microenvironment (18,93,107).

For some murine tumor models, administration of oral 2ME reduces the rate of tumor growth without signs of toxicity, with a concomitant reduction in tumor vascularization (18,28). 2ME reduced tumor vasculature in mice injected subcutaneously with MethA sarcoma and B16 melanoma cells and treated orally with 2ME (18,28,101). Xenograft experiments also found that 2ME targets both the tumor and the tumor vasculature (18). Oral administration of 2ME was effective at reducing

the rate of xenograft tumor growth and tumor vascularization in mice in the absence of significant toxicity (18,28). In a human neuroblastoma xenograft model in mice, 2ME was found to reduce tumor growth significantly after 14 days of treatment and showed clear antiangiogenic effects (18,110).

Thus, sufficient data exist to establish that 2ME effectively inhibits tumor growth as well as angiogenesis, but it is still difficult to isolate the exact mechanism(s) of action (18).

1.7 2ME - mechanisms of action

From all the *in vivo* and *in vitro* studies 2ME shows considerable promise as a therapeutic alternative in various solid tumors (18). Evidence suggests that 2ME has a broad spectrum of activity (96). According to Kumar *et al.* it is the only compound that has a dual advantage both as an anti-angiogenic and pro-apoptotic agent with an ultimate result of inhibition of tumor cell growth (53,117). In cancer cell cultures, 2ME produce cytotoxic effects that are associated with inhibition of DNA synthesis and mitosis, uneven chromosome distribution, faulty spindle formation, and an increase in the number of abnormal metaphases (29,30,98). However, the mechanisms of action of 2ME are complex and still remain to be fully elucidated (96,118).

Studies of the mechanisms of 2ME in cancer-derived cell lines provided conflicting evidence (119). Several possible mechanisms have been suggested (18), including the induction of p53 and apoptosis (18,28,98,101,110,120,121,122,123,124,125), inhibition of the proangiogenic transcription factor hypoxia-inducible factor 1α (HIF-1α) (96,118,126), c-Jun NH_2-terminal kinase (JNK) signalling (96,118), the generation of reactive oxygen species (ROS) (96,118), nitric oxide synthase (98,103), stress-activated protein kinases (98,104), proliferating cell nuclear antigen (PCNA) (98,127), inhibition of superoxide dismutase enzymatic activity (18,120,128), up-regulation of death receptor 5 (DR5) (120), interaction with tubulin (28,31,101, 110,120,129,130) and the impairment and imbalance of cell cycle kinases (28, 101,110). Although some of these proposed mechanisms are clearly sufficient to explain the activity of 2ME in certain cases, there is no evidence for a common mechanism of action operative in all of the cells sensitive to 2ME (120). Therefore,

the available evidence suggests that multiple mechanisms are involved that may be dependent on cell type (94,118).

1.7.1 Involvement of the estrogen receptor

Estrogens are retained in target cells by intranuclear estrogen receptors (ERs) that have a high affinity and specificity for estrogens (20). Once bound by estrogens, the ER undergoes a conformational change, allowing the receptor to bind with high affinity to chromatin and to modulate transcription of target genes (20). There are two types of estrogen-receptors, α and ß (7), but the biological significance of the existence of these two subtypes is still unclear at this moment (20). Perhaps the existence of two ER subtypes provides, at least in part, an explanation for the selective actions of estrogens in different target tissues (20). The α-receptor has a higher affinity for estrogen than the ß-receptor (7). *In vitro* α- and ß-receptors form heterodimers with each other and the ß-receptor decreases sensitivity of the α form to estradiol, thereby acting as a physiologic regulator of the proliferative effects of the α-receptor (7). The degree of variability in the expression of α- and ß-receptors in normal breast tissue is unknown, but the relative expression of the α- to expression of the ß-receptor is higher in invasive tumors than in normal breast tissue (7).

2ME has 500- and 3200-fold lower affinity than that of estradiol for estrogen receptors α and ß, respectively (18,24,120,131). 2ME inhibits proliferation and induces apoptosis in ER-negative HeLa cells and the estrogen-independent human breast cancer lines MDA-MB-435 and MDA-MB-231 were also found to be sensitive to 2ME treatment (18). Similarly, Maran *et al.* found that in osteosarcoma cells, 2ME was equally effective in killing cells expressing both low and high levels of endogenous estrogen receptors and that the high-affinity estrogen receptor ligand, ICI-182,780, did not reduce or potentiate the cytotoxic effects of 2ME (99). Multiple other studies also indicated that the effects of 2ME on target cells are independent of the presence of estrogen receptors and are not influenced by estrogen receptor antagonists or agonists (18,29,120). Therefore, it was suggested that the mechanism of antitumor activity of 2ME is not mediated through the estrogen receptor (18,101,102,109,120,132).

Although multiple studies found 2ME activity is independent of the ER, the findings of Liu *et al.* should also be mentioned. They compared the effects of 2ME on the growth of two ER-negative human breast cancer cell lines (MDA-MB-231 and MDA-MB-435) and two ER-positive human breast cancer cell lines (MCF-7 and T-47D) (133). They found that 2ME exerted a concentration-dependent antiproliferative action in the ER-negative cells and the presence or absence of exogenous estradiol in the culture medium did not affect the potency and efficacy of 2ME's antiproliferative action (133). When the ER-positive cells were cultured in a medium supplemented with 10 nM exogenous estradiol, 2ME at 750 nM to 2 μM concentrations exerted a similar antiproliferative effect (133). However, when the ER-positive cell lines were cultured in the absence of exogenous estradiol, 2ME at relatively low concentrations (10-750 nM) had a moderately mitogenic effect, with its apparent efficacy 75-80 % of that of estradiol (133). The mitogenic effect was inhibited in a concentration-dependent manner by ICI-182,780, a pure ER antagonist and was not due to its metabolic conversion to 2-hydroxyestradiol (133). While 2ME has a consistent antiproliferative effect in the ER-negative human breast cancer cells, it has both mitogenic and antiproliferative actions in the ER-positive human breast cancer cells (133). Therefore, Liu *et al.* suggested that while the antiproliferative effect of 2ME is independent of the ER status, the mitogenic action of 2ME in the ER-positive cancer cells is mediated by the ER and is largely attributable to the residual intrinsic estrogenic activity of 2ME (133).

1.7.2 Effects on the cell cycle

Tumors are genetically unstable (114) and chromosomal instability is consistently associated with the loss of function of a mitotic checkpoint (90). In tumors, cyclins are overproduced and inappropriate cell divisions are stimulated (35,134). Thus, the activation of cell-cycle checkpoints by exogenous agents might be used to improve the selectivity of chemotherapy by exploiting the differences between normal and transformed cells (90). Indeed, many drugs affect the cell cycle, often at specific points, as best illustrated by the numerous cancer chemotherapeutics (35). 2ME may exert its antiproliferative activity by selectively altering the expression of several kinases involved in cell cycle control (28,29,31,53,127). Whereas many drugs or toxins arrest cells in particular phases of the cell cycle, the simultaneous measurement

of cyclins may help localize more precisely at what point within a given phase the drug or toxin acts (35). Alternative methods for assessing stage of arrest include the determination of levels of cyclin expression and Cdk phosphorylation state by western blotting or immunoprecipitation (35). However, the effect of 2ME on cell-cycle distribution is dissimilar for different cancer cells (108). For example, in various pancreatic cancer cell lines, 2ME treatment results in an accumulation in the S-phase (97), whereas in some prostate cancer cell lines the accumulation occurs in the G_2/M-phase (108). These results suggest that 2ME utilizes diverse mechanisms to inhibit cell proliferation in different cells (108).

A clear increase in the mitotic figures has been demonstrated in cells treated with 2ME during metaphase (6,11,18). 2ME arrests cultures of the Jurkat T-cell line in G_2/M-phase in a reversible manner (11). Treated Jurkat cells had increased Cdk1 activity (11). The activity of Cdk1 immunoprecipitated from 2ME-treated cells was approximately 3-fold higher than in exponentially growing cells (11). The activity of Cdk kinase is expected to be elevated with an accumulation of cyclin B in cells arrested in mitosis (11). Given that degradation of cyclin B is a prerequisite for progression from metaphase to anaphase, the accumulation of cyclin B in 2ME-treated cells indicates a cell cycle block before the onset of anaphase (11). In many cell types, the duration of the mitotic arrest is not indefinite (79). Apoptosis may be the fate of cells that cannot correct their spindle defects (44,79).

Kumar *et al.* investigated the effects of 3 μM 2ME (24h) on the expression of G_2/M-specific proteins in prostate cancer cells. Western blot analysis indicated no significant changes in steady-state levels of Cdk1, cyclin B1 or Cdc25B. Wee1 kinase was not detected either in treated or untreated cells (53). However, expression of Cdc25C showed a clear shift in the mobility of the bands following treatment with 2ME (53). This may be due to differential phosphorylation of Cdc25C (53). With antibody that specifically detects phosphorylated Cdc25C, no phosphorylated Cdc25C in control extracts, after treatment the phosphorylated band was detectable (53). Based on their observations, Kumar *et al.* speculated that 2ME treatment possibly leads to phosphorylation of Cdc25C, which in turn associates, with 14-3-3σ proteins (53). This could lead to hyper-phosphorylation of Cdk1, making it inactive and blocking cells in G_2/M (38,53). Furthermore, 14-3-3σ-dependent sequestration of

the Cdc25C phosphatase prevents dephosphorylation of Cdk1 and thus inhibits the formation of active Cdk1/cyclin B complexes that would be required for entry into mitosis (38).

1.7.3 Microtubule activity

In vivo protein regulators of microtubule dynamics play a key role in transforming the long, stable microtubules of interphase into the short, dynamic microtubules of the mitotic spindle (42). Inhibiting some of the proteins that regulate microtubule dynamics *in vivo* might be expected to result in mitotic arrest (42). Drugs that affect the polymerization of microtubules constitute one of the most important classes of chemotherapeutics, possibly because perturbation of microtubule dynamics in the spindle activates the checkpoint pathway that leads to a prolonged mitotic arrest, followed by cell death (42,44,79).

Anti-microtubule drugs have been isolated from a variety of natural and synthetic sources and include the clinically important drugs paclitaxel (taxol) and the vinca alkaloids (vinblastine and vincristine), as well as epothilone, discodermolide, nocodazole and colchicines (44). At low concentrations both taxol and the vinca alkaloids suppress polymer dynamics at the (+) ends of microtubules (44). However, at saturating concentrations, taxol, epothilone and discodermolide stabilize microtubules, but the other drugs destabilize them (44). The immediate biochemical target of these drugs (free tubulin or assembled microtubules) has been determined, but very little is known about the physiological response to microtubule disruption (44).

In 1994 Folkman *et al.* identified 2ME as the most potent endogenous inhibitor of mammalian tubulin polymerization yet discovered (31). The available evidence indicates that the antiangiogenic and antitumorigenic effects of 2ME result from microtubule disruption (31,96,98). In endothelial cells, 2ME causes selective disruption of microtubules as opposed to other cytoskeletal structures (18,135). Also, micromolar amounts (EC_{50} = 2 µM) caused disruption of the microtubular network in nonsynchronized Chinese hamster V79 cells (6,18) and multipolar and irregular spindles in synchronized MCF-7 cells (18). 2ME, in superstoichiometric

concentrations, inhibits the nucleation and propagation phases of tubulin assembly but does not affect the reaction extent (18,31). Similarly, in substoichiometric concentrations, 2ME completely inhibits polymerization (18). 2ME inhibits the rate, but not the degree, of polymerization and depolymerization of tubulin induced by other agents (18).

Colchicine is a well-known antimitotic agent that inhibits cell division by interfering with microtubule assembly (136,137). Drugs with this effect have been applied in cancer therapy and hence are of great therapeutic interest (136). D'Amato *et al.* reported that 2ME interacts with tubulin at the colchicine binding site, thereby inhibiting tubulin polymerization and spindle formation, resulting in cells arrested in metaphase (31). This was supported by several other studies (18,21,97,101,102). In contrast, by making use of the stearic and elecrostatic alignment (SEAL) method, Feher *et al*. concluded that it is unlikely that 2ME fits the colchicines binding site well (136). However, it has been established that 2ME is a weak competitive inhibitor of colchicines binding (50 % inhibition is achieved only with a 2ME concentration of 40 µM to displace 2 µM colchicines) (31). Therefore, the possibility that 2ME interacts only with a portion of the binding site to inhibit tubulin polymerization is not precluded (138).

However, Atalla *et al.* suggested that 2ME-induced mitotic block is not due to inhibition of microtubule formation, because they've found that at concentrations where the drug effectively blocks cells in mitosis, the tubulin filaments are not depolymerized and only at higher concentrations 2ME prevents microtubule assembly *in vitro* (11). Sorger *et al.* also noted that anti-microtubule drugs exert their antiproliferative effects on cells in culture (and are used in the clinic) at concentrations so low that they do not affect the overall architecture of the microtubule cytoskeleton (44). With low doses of microtubule-polymerization inhibitors and taxol, normal bipolar attachment of chromosomes occurs and the spindle appears normal (79). It is thought, however, that in the presence of drugs the number of microtubules attached per kinetochore is less than normal and that the attachment is less stable than in the absence of drugs and this can also activate the checkpoint in animal cells (79). In contrast to its spindle disrupting properties, 2ME

was found to inhibit aromatase activity, which is a characteristic observed with drugs that stabilize tubulin and not with agents that inhibit tubulin polymerization (18,139).

According to their results, Atalla *et al.* suggested that treatment with 2ME rather leads to interference with mitotic spindle dynamics (11). Cells arrested in metaphase by treatment with 2ME contain morphologically intact mitotic spindles, but their chromosomes remain in the equatorial plate indicating a functionally impaired mitotic apparatus (11). Atalla *et al.* also found that 2ME inhibited calmodulin *in vitro* and concluded that it is possible that 2ME exerts its anti-mitotic effects via inhibition of calmodulin-regulated tubulin dynamics (11).

Mabjeesh *et al.* showed that 2ME inhibited both tumor cell growth and tumor vascularization following disruption of the microtubule cytoskeleton (126). Vascular endothelial growth factor (VEGF) is a major mediator of angiogenesis. Induction of VEGF is a multistage process in which the α subunit of HIF-1α plays a key role (126). HIF-1α is overexpressed in more than 70 % of human cancers and their metastases compared to their adjacent normal tissue (126). Disruption of interphase microtubules is required for HIF-1α downregulation (126). Mechanistically, Mabjeesh *et al.* found that at concentrations where 2ME depolymerizes microtubules, 2ME downregulates HIF-1α at the posttranscriptional level and inhibits HIF-1-induced transcriptional activation of VEGF expression (126). Therefore, their data support the hypothesis that 2ME disrupts microtubules and its downstream effects on the HIF pathway lead to inhibition of angiogenesis, resulting in vascular shutdown and massive tumor obliteration (126).

1.7.3.1 Multipolar spindles

MTOCs nucleate microtubule assembly and also establish microtubule polarity. Microtubules nucleate on amorphous pericentriolar materials (PCMs) that surround the centrosomes and therefore, are regarded as the MTOCs (43). Alterations in centrosomal organization by colcemid, X-rays, docetaxel, heat shock, cytomegarovirus, fungicides, such as methyl 2-benzimidazolecarbamate, and dimethylarsinic acid, etc., have been demonstrated in association with the induction of multipolar spindles and multinucleation (43).

γ-tubulin is a centrosomal protein that plays a role in the nucleation of microtubules in MTOCs and is often used as a marker for investigating centrosome integrity (43). Immunofluorescence double staining to visualize γ-tubulin (distribution of centrosome) and the microtubule network reveal one-dot signals of γ-tubulin in control interphase cells (43). Bipolar spindles in control mitotic cells colocalize with two-dot signals of γ-tubulins (43). Various steroidal estrogens and their derivatives were investigated in terms of their inducibility of centrosome disintegrity and multipolar spindles in cultured V79 cells (43). 2ME was the most potent inducer of the centrosome disintegrity and multipolar spindles and caused a decrease in mitotic cells with normal two-dot signals of γ-tubulin in a concentration- and a time-dependent manner (43). 1-5 μM 2ME for 6 h caused only weak morphological changes (43). Interphase cells became round-shaped and the microtubules were somewhat shortened, but still organized, with no influence on centrosome integrity (43). However, when cells were incubated with 5 μM 2ME for 24 h, abnormal spindles, such as tripolar and multipolar spindles, were induced and were colocalized with multiple signals of γ-tubulin (43). Even mitotic cells with more than 5 γ-tubulin signals were observed (43). In contrast, interphase cells still exhibited organized microtubules (43).

Estrogens and their derivatives, which caused the centrosome disintegrity and multipolar spindles, induced the appearance of non-dividing multinucleated cells, which followed an increase in the mitotic index (43). The mitotic indices in cells incubated with 2ME increased up to 6 h, then decreased and small second peaks were observed at 24 h. Multinucleated cells appeared at 24-30 h of incubation (43). The multinucleated cells changed to non-dividing giant cells with multiple micronuclei, and then died (43,140).

Likewise, Seegers *et al.* (29) have shown that estradiol and its metabolites, 2-hydroxy-estradiol and 2ME, were cytotoxic at high micromolar concentrations and caused mitotic arrest due to abnormal and fragmented polar formations as well as disorientated microtubule arrangement in the dividing cells (29,43). These observations are very similar to the effects seen when cells are treated with taxol. When cells are treated with concentrations of taxol high enough to dramatically alter spindle morphology, mitotic arrest results. Cells eventually exit mitosis and nuclear

envelopes reassemble around subgenomic chromosome fragments, giving rise to a multinucleated phenotype (44). It is not clear why cells treated with taxol ever exit mitosis (44). Sorger *et al.* suggested that perhaps they incorrectly perceive that their spindles are fully assembled or alternatively, a process of 'adaptation' may occur in which cells override the checkpoint despite the persistence of damage (44). Perhaps this is also the case in cells treated with 2ME. In most cases the formation of multinucleated cells are followed by the appearance of apoptotic cells (44).

There seems to be a good correlation between the cytotoxic effects and the microtubule-disrupting activity of 2ME (43). Furthermore, it has been demonstrated that microtubule disrupting effects of estrogens were not different between estrogen receptor positive and negative cells (43). This observation confirms the fact that the activities of 2ME are independent of the estrogen receptor. All the available results show that tubulin and/or microtubules are the target in the disturbance of cell division by estrogens (43). The centrosome appears to be the primary target that leads to the formation of aberrant spindles and multinucleated cells. However, the mechanism by which estrogens caused mitotic phase-specific centrosome abnormality remains obscure and further study on the fate of mitotic cells that have an abnormality in centrosome integrity is warranted (43).

Destruction of B-type cyclins is essential for somatic cells to exit from mitosis (61). Gallant *et al.* showed that expression of a non-destructible cyclin B2 protein caused HeLa cells to arrest in mitosis. A high proportion of the cells presented with multiple mitotic spindles (61). Cells did not enter mitosis prematurely, but were arrested once they entered mitosis (61). The mitotically arrested cells displayed mitotic spindles and fully condensed chromosomes, but many of the transfected cells contained up to four spindle poles (61). Concomitantly, the chromosomes were not aligned in either a metaphase plate or an anaphase configuration, but arranged as if the cells had attempted to segregate their chromosomes in multiple directions (61). Although the nuclear division cycle was arrested it seemed as if the centrosome cycle continued (61). Therefore, mitotic arrest and multipolar spindle formation after 2ME treatment may be the result of overexpression of cyclin B.

1.7.3.2 Ran-GTP

Ran is an abundant GTP-binding protein that is required for the trafficking of proteins and ribonucleic acid (RNA) in and out of the nucleus (141). The GTP-bound form of Ran is concentrated in the vicinity of chromosomes and is necessary for the nucleation and organization of microtubule structures during M-phase (141). GTP hydrolysis by Ran may have some secondary role in the elongation of previously nucleated microtubules (141). A Ran-binding protein (RanBPM) associates with centrosomes and could affect polymerization properties (141). Inhibition of Ran BPM or Ran activity can prevent *in vitro* aster formation and Ran-GTP has also been implicated in the formation of multipolar spindles (141). Split centrioles retain their functional integrity and can organize polarized microtubule arrays and therefore, spindles with multiple poles form when centrioles are split under abnormal circumstances during mitosis, as observed during (for example) mitotic arrest induced by non-degradable cyclin B (142). It's possible that Ran-GTP might play a role in the antitumor activity of 2ME (141).

1.7.4 Apoptotic activity

Apoptosis, or programmed cell death, is a highly regulated intracellular process in the elimination of unwanted or damaged cells from multicellular organisms (58). Common morphological and biochemical features of apoptotic cells include chromatin condensation, blebbing of the plasma membrane, internucleosamal DNA fragmentation, proteolytic cleavage of vital cellular constituents, and the relocation of phosphatidylserine from the inner to the outer aspect of the plasma membrane (143). Many different cell types undergo apoptosis in response to various different extracellular and intracellular stimuli, such as DNA damage, withdrawal of growth factors, inappropriate growth signals and viral infection (58). Cells undergoing mitosis and cells undergoing apoptosis share a number of morphological and biochemical features, including rounded cell morphology, surface blebbing, reduction in cell volume, nuclear membrane breakdown, chromatin condensation, and phosphorylation and disassembly of lamins (58,144). Therefore, it is believed that cell cycle and apoptosis are intimately linked and that a coordination and balance between

these two processes are crucial for normal cell physiology (58). Deregulation of this process is implicated in various diseases including cancer (58).

The central executors of apoptosis are a caspase family of cytoplasmic aspartate-specific cysteine proteases (58,145). Caspases often function in cascades, in which an upstream caspase, called initiator caspase, such as caspase-2, -8, -9 and –10, is activated by its interaction with caspase adaptor(s) (58). Once activated, the initiator caspase processes and activates one or more downstream caspases referred to as effector caspases, such as caspase-3, -6, and –7 (58). The activated effector caspases then cleave various cellular proteins, leading to apoptotic cell death (58). The caspase signalling cascade can be induced by intrinsic or extrinsic apoptotic pathways (145). The intrinsic pathway involves the cell sensing stress that triggers mitochondria-dependent processes, resulting in cytochrome c release and activation of caspase-9 (145). The extrinsic pathway involves activation of death receptors (DRs) that bind to their ligands to initiate a signal transduction cascade that leads to the activation of caspase-8 before caspase-9 and caspase-3 (145). Caspase-3 is the key player and is activated in a variety of cell types during apoptosis (58). It is responsible for proteolytic cleavage events that result in the characteristic biochemical and morphological changes associated with apoptosis (58,145).

2ME has been shown to inhibit the growth of various tumor cells through the induction of apoptosis (18,53,120). Exposure to 2ME had a strong antiproliferative effect on human glioblastoma cells and caused an increase in the population of apoptotic cells, detected by flow cytometry, in some of the investigated cell lines (95). Furthermore, the antiangiogenic activity of 2ME is through a direct apoptotic effect on endothelial cells (18,53,112). 2ME affects the angiogenesis cascade at various steps. It blocks the tubule formation, as well as the invasion through the collagen matrix (9,18). It is suggested that inhibition of angiogenesis induces metabolic stress, resulting in chromafin differentiation and apoptosis (110). Such agonal differentiation may be the link between angiostatic therapy and tumor cell apoptosis (110).

Apoptosis has been hypothesized to be the result of abnormal cell cycle control (138,146). However, the relationship between the mechanisms that induce cell cycle delay and those that induce apoptosis have not yet been established (44). From

the observation that cells undergoing mitosis and cells undergoing apoptosis share a number of morphological and biochemical features, it has been suggested that some of the cell cycle components that drive cells into mitosis may also be responsible for triggering apoptosis (147,148,149). The overexpression of cyclins (138,150) and activation of cyclin-dependent kinases have been shown to correlate with the onset of apoptosis in many experimental systems (55,138,144,147,148,149). However, the physiological target(s) of these kinases during apoptosis have not been elucidated (138). Several studies have shown that cyclin B expression or Cdk1 kinase activity is upregulated in apoptotic cells induced by various death signals (such as Fas), γ-radiation, camptothecin, paclitaxel, ragmentin, tumor growth factor-beta (TGF-ß), or retinoic acid (RA) (58). Premature activation of Cdk1 also accompanies apoptosis (147,148,149). Inhibition of Cdk1 activity by transient overexpression of a dominant-negative Cdk1 construct or human Wee1 kinase inhibited Fas-mediated apoptosis (148). In several reports, the increase in Cdk1 kinase activity observed during apoptosis were reported to be associated with tyrosine 15 dephosphorylation of Cdk1 (149,150,151). Apoptosis induction through the upregulated expression of cyclin B1 and/or Cdk1 is most likely due to the activation of caspase-3 (53,58). However, whether caspase activity is directly regulated by cyclin-dependent kinase is not entirely clear (58). Although several studies suggest that the activity of Cdk1 is a critical modulator of apoptosis triggered by several stimuli, other reports have indicated that it may not be obligatory for all forms of cell death (147,148). This implies that Cdk1 is not a part of the apoptosis machinery, but rather an upstream regulator of this machinery under certain conditions (147).

DNA-damaging agents in the form of radiation and chemotherapeutic drugs are the mainstays of most current cancer treatment regimens (100). They work in part by inducing a cellular response that involves p53 (100), a nuclear-localized protein that binds to specific DNA sequences and functions as a transcription regulator (152). p53 causes dephosphorylation of Cdk1 at tyrosine 15 and negative regulation of Wee1 expression is observed after p53 activation (151). By the dephosphorylation of Cdk1 and downregulation of Wee1, p53 may act to override an important cellular checkpoint that protects against apoptosis (151). Inactivation of Cdk1 inhibits p53-dependent apoptosis after ionising radiation (148). Selective expression of different p53 tumor suppressor protein isoforms in the apoptotic state, suggests that the

phosphorylation events generating these forms of p53 may play a role in apoptosis (152). Cells sustaining DNA damage, caused by ionizing radiation (IR), increase their production of p53 protein via a posttranscriptional mechanism, which coincidentally activates the p53-dependent transcription of a variety of genes involved in either G_1/S cell-cycle arrest or apoptosis (100).

Although apoptotic cell death induced by 2ME was shown to be p53 mediated in some studies (18,121,132), Kumar *et al.* found that 2ME-induced apoptosis is not associated with any significant alterations in the expression of p53 or Bax (53). Several other reports also indicate that the induction of apoptosis by 2ME may be p53 independent (18,97,109,135). Therefore, 2ME can apparently induce either p53-dependent or p53-independent apoptosis in human cancer cell lines depending on the tissue and cell type (100).

It appears that apoptosis can occur either directly from a mitotic arrest or following aberrant mitotic exit into a G_1-like 'multinucleated state' (44). 2ME treatment resulted in G_2/M cell cycle arrest in gastric carcinoma cell lines (SC-M1 and NUGC-3) and appeared to induce apoptosis through the extrinsic apoptotic pathway (18). However, Djavaheri-Mergny *et al.* found that 2ME induced apoptosis through the mitochondria-dependent pathway in Ewing sarcoma cells (153). Therefore, both the intrinsic and extrinsic apoptotic pathways were initiated by 2ME, with the relative roles of each pathway varying with specific cell types (96,118).

In studies by Choi *et al*., TGF-ß1-induced apoptosis was preceded by a slight increase of the cell population in the G_2/M-phase and induced a transient increase in the expression of Cdk1, Cyclin A, cyclin B, and cyclin D1 at an early phase apoptosis (138). TGF-ß1-induced apoptosis was suppressed by the overexpression of B-cell leukaemia/lymphoma 2 (Bcl-2). The activation of Cdk1 kinase, but not the activation of Cdk2 was affected, suggesting that Cdk1 plays a more critical role in TGF-ß1-induced apoptosis (138). Choi *et al*. found that Cdk1 and Cdk2 kinase activity transiently induced by TGF-ß1 phosphorylates retinoblastoma protein (pRB) as a physiological target in rat hepatoma cells (138). pRB hyperphosphorylation may trigger abrupt cell cycle progression, leading to irreversible cell death (138).

Apoptosis is a common response to microtubule-depolymerizing drugs, seen in some mammalian cells (54). Activation of the spindle checkpoint may eventually result in the induction of apoptosis. However, the mechanistic relationship between activation of the spindle checkpoint and induction of apoptotic cell death still remains unclear (38). Apoptosis may be a direct result of the activation of proteins involved in the checkpoint; alternatively, apoptosis may also result from an arrest in metaphase or may be induced by proapoptotic structures accumulating in cells that undergo aberrant mitosis (exit from mitosis in the absence of anaphase or cytokinesis) (38). In p53-positive lung cancer cells, 2ME did not affect microtubule structure and had no effect on the cell cycle (108). In this case, the likely mechanism of growth inhibition is induction of p53-mediated apoptosis (108).

2ME treatment resulted in the up-regulation of DR5 protein expression in a variety of tumor and endothelial cells *in vitro* and *in vivo* (18,145). This rendered cells more sensitive to the cytotoxic activities of the DR5 ligand, TRAIL (tumor necrosis factor-related apoptosis-inducing ligand) (145). Blocking DR signalling resulted in severe impairment of the apoptotic response induced by 2ME (18,145).

Nuclear factor kappa beta (NFκB) also coordinates the control of apoptotic cell death (53). 2ME may induce apoptosis through inhibition of NFκB-mediated cell survival signalling pathway as seen in DAOY (medulloblastoma-derived) cells (53). Kumar *et al*. showed that the transcriptional activity of NFκB promoter is reduced by 78% with 2ME-induced apoptosis (53). Shimada *et al*. investigated the mechanisms by which 2ME induce apoptosis in the human prostate cancer cell line LNCaP (119). The results suggested that not only p53 induction through p38/JNK-dependent NFκB/AP-1 activation, but also JNK-dependent Bcl-2 phosphorylation are required for 2ME-induced apoptosis (119).

Bcl-2 protein is frequently expressed in breast cancer (4,154). Bcl-2 is a proto-oncogene that protects cells from different forms of apoptotic stimuli by preventing caspase activation (4,154). Bcl-2 expression is associated with low cell proliferation rate and inversely associated with expression of the mutated p53 expression, which, in turn, is associated with increased cell proliferation rate and generally poor outcome (154). In studies by Zhou *et al*., 2ME induced apoptosis in CNE2 cells which was

associated to Bcl-2 down-regulation (155). Bu *et al.* illustrated that 2ME effectively induces apoptosis in Bcl-2-expressing human prostate and breast carcinoma cells *in vitro* and in a rat prostate tumor model *in vivo* (4). In several cell lines derived from prostate, breast, liver and colorectal carcinomas, 2ME treatment led to an activation of JNK and phosphorylation of Bcl-2, which preceded the induction of apoptosis (4). Thus 2ME induces apoptosis by rapidly activating JNK kinase, which appears to be correlated with phosphorylation of Bcl-2 (4,96). However, members of the Bcl-2 family fall into two categories on the basis of their ability to either promote or suppress apoptosis (143).

A phase I clinical trial is under way at the National Cancer Insitute (Bethesda, MD) in which 2ME is being evaluated in patients with histologically confirmed solid tumors (18). One of the objectives of the study is to assess changes in apoptosis on biopsy specimens of endothelial cells or tumor cells (18).

1.7.5 Production of superoxides

ROS are generated by all aerobic organisms during the production of adenosine triphosphate (ATP) in the mitochondria (156). Superoxide (O_2^-) and hydroxyl ($OH^\cdot$) radicals are generated during the electron-transport steps of ATP production and may lead to the production of hydrogen peroxide (H_2O_2), from which further hydroxyl radicals are generated (156). Excessive amounts of ROS can start lethal chain reactions, which oxidize and disable structures that are required for cellular integrity and survival (156). DNA of neoplasm, especially adenocarcinoma, is more exposed to ROS than its non-tumorous counterpart and it is believed that cancer cells themselves produce ROS (157). In several human carcinoma cell lines, including breast carcinoma, large amounts of hydrogen peroxide were reportedly produced *in vitro* without exogenous stimulation (157). Furthermore, the antioxidant system of cancer cells was suppressed (157). According to Toyokuni *et al.*, persistent oxidative stress may partly explain the characteristics of cancer, such as activated proto-oncogenes and transcription factors, genomic instability, chemotherapy-resistance, invasion and metastasis (157).

ROS has been found to regulate translocation of NF-κB (158) as well as translocation of p53 and the p53-mediated apoptosis pathway (159). However, antioxidant defence systems exist to protect cells from the damaging effects of ROS. These defence systems include intracellular superoxide dismutases (SODs), which convert O_2^- into H_2O_2; enzymes that inactivate H_2O_2 or hydroxyl radicals; and enzymes that trap free radicals or transition metals (such as Fe^{2+}) that are reservoirs for electrons (156). There are two intracellular SODs: mitochondrial-associated manganese-dependent SOD (MnSOD) and cytoplasmic/nuclear copper/zinc-dependent SOD (CuZnSOD) (156). Tumor cells are always low in copper and zinc superoxide dismutase activity (157). If radical-scavenging cellular antioxidants cannot handle the amounts of ROS produced in the cells, apoptosis results (153).

Many tumor cells have a higher level of aerobic metabolism compared with normal cells, and would therefore have increased numbers of ROS (157,159), making tumor cells more dependent on SOD than normal cells (4,128,156). Furthermore, tumor cells have lower levels of SOD than normal cells (156). Therefore, drugs that target the enzymes that regulate the levels of reactive oxygen species, might have potential as antitumor agents (156). However, previous attempts to inhibit SODs have not proved to be clinically useful, because of unacceptable levels of damage to normal cells. This is due to the fact that ions that could successfully compete for binding to SODs were not specific enough to cancer cells (156).

Huang *et al*. (128) showed that a group of estrogen derivatives bind to, and inhibit the transcription and therefore activity of SOD enzymes (128). 2ME was found to be a more potent antioxidant than vitamin E (116). However, 2ME was also found to inhibit the activity of SOD enzymes (128). Inhibition of SOD causes accumulation of cellular O_2^- and leads to free-radical-mediated damage to mitochondrial membranes and the release of cytochrome *c* from mitochondria. Huang *et al*. reported that damage to mitochondria by the inhibition of SOD, induced apoptosis in a variety of human leukaemia cells *in vitro* (128,156). The authors reported that 2ME inhibited both CuZnSOD and MnSOD and were toxic to human leukaemia cells but not to normal lymphocytes (18). They found that O_2^- scavengers or antioxidants protect leukemia cells from the lethal effects of this compound (128,156).

In another study, Kachadourian *et al.* (160) found that when HL-60 human leukemia cells were incubated in a medium containing 2ME, cells showed 53 % decrease in aconitase activity (aconitases are very sensitive to superoxide-mediated inactivation) compared with that of controls (18,160). Paraquat (a superoxide-generating oxidation-reduction cycling agent) decreased aconitase activity in HL-60 cells by 67 % (18,160). In contradiction to the study by Huang *et al*., Kachadourian *et al.* showed that although 2ME supported the increased production of superoxides, it did not produce that effect by inhibiting SOD (18,160). According to Kachadourian *et al*. (160) it seemed likely that the catecholestrogens interfered with the SOD assay that Huang *et al*. (128) chose. They demonstrated using several SOD assays including pulse radiolysis, that 2ME does not inhibit SOD, but rather interferes with the SOD assay originally used (160). They demonstrated that 2ME does not inhibit SOD, but that it does impose an oxidative burden on HL-60 cells (160).

Hagen *et al.* found that 2ME inhibits mitochondrial respiration, that leads to ROS production and eventually results in apoptosis induction (161). Similarly, Lin *et al*. compared 2-methoxyestradiol-induced, docetaxel-induced, and paclitaxel-induced apoptosis in hepatoma cells and found that these antimicrotubule agents increased the formation of ROS (159). However, they concluded that the drug-induced apoptosis was independent of ROS formation, because antioxidant treatment did not block the drug-induced growth inhibition and apoptosis effects (159).

1.8 2ME as a therapeutic agent

An effective anticancer drug must selectively kill tumor cells. Designing safe, effective drugs with high sensitivity and specificity is a very difficult task. Most anticancer drugs have been discovered by chance, and the molecular alterations that provide selective tumor cell killing are unknown. Even understanding the detailed molecular mechanism by which a drug acts often provides little insight into why the treated tumor cell dies (162). Although its mechanism of action is still unclear, numerous studies have shown the potential of 2ME as an antitumor drug.

The advantages of 2ME as an antitumor drug include the following:

a) Therapy targeting both tumor cells and endothelial cells is more effective than therapy directed against tumor cells alone (110,113). *In vivo*, 2ME not only inhibits angiogenesis necessary for tumor formation, but also attacks tumor cells directly, making it a strong anti-tumor agent (53,94,118).

b) 2ME has differential sensitivity towards different cell lines and appears to be tumor specific, since very little or no toxicity has been observed in normal tissues or in *in vivo* experiments (28,53,120,121,125). For example, 2ME has been shown to induce apoptosis in transformed breast epithelial skin fibroblasts cells, but not in normal fibroblasts (53). 2ME also had no effect on either cell viability or apoptosis of normal bronchial cells (53). Therefore, many normal tissues may be relatively resistant to the toxic effects of 2ME (53). It is still unclear why 2ME kills cancer cells more efficiently than normal cells. Originally it was thought that cancerous cells are more susceptible to drugs that disturb the cell cycle because they replicate more quickly and more frequently than normal cells. However, there are many normal cell populations that replicate at least as quickly as cancerous cells and some slow-growing cancer cells are more sensitive to conventional anti-cancer treatments than fast-growing cells (163).

c) It is presently unclear what effect 2ME has on the highly proliferating pool of non-neoplastic cells in the pediatric age group (53). Under usual physiological conditions, plasma 2ME is in the picomolar range, but increases during pregnancy (53). In various pre-clinical studies it has been shown that the plasma levels of 2ME attained at efficacious doses are similar to the levels attained normally during the third trimester of pregnancy (164) indicating that therapeutically effective doses of 2ME would not be expected to be harmful even to a developing fetus at late stages of pregnancy (53). According to Kumar *et al*., based on these observations, even if 2ME is found to have an effect on non-neoplastic cells, it is unlikely to be a toxic effect (53). It should, however, also be mentioned that Sibonga *et al.* found some evidence that 2ME inhibit normal bone elongation in growing rats (165). They suggested that this

potential toxicity should be monitored in ongoing and future clinical trials (165).

d) 2ME is relatively non-toxic (53,120). Toxic effects commonly associated with conventional chemotherapy, such as hair loss, gastrointestinal disturbance, infection or inhibition of leukopoiesis, were not observed or reported in any of the *in vivo* experiments (28,101,102,105,108,110). Even daily doses of 100 mg/kg body weight was nontoxic to animals (100). There are numerous 2ME clinical trials under way in the United States (18,94). No serious toxicities have been reported, although hot flushes, fatigue, diarrhea, and reversible liver enzyme elevations have occurred (18). The only side effect that patients receiving 100 mg/day experienced was hot flushes (18). A phase I clinical trial of 2ME 200, 400, 600, 800, and 1000 mg/day in 15 patients with breast cancer showed significant reduction in bone pain and analgesic intake in some patients, with no significant adverse effects (18). Another phase I study of 2ME 200-1000 mg/day in combination with docetaxel 35 mg/m^2/week for 4-6 weeks performed in 15 patients with advanced refractory metastatic breast cancer showed no serious drug-related adverse effects (18). There was no grade 4 toxicity (18). Grade 3 fatigue occurred in five patients, diarrhea in four and hand-foot syndrome (palmar-plantar erythodysthesia) in one (18). Three patients had grade 3 aminotransferase elevations that returned to normal with continued treatment. Extensive metabolism to 2-methoxyestrone was observed (18). In a phase II multicenter, randomised, double-blind trial of two dosages (400 and 1200 mg/day) of 2ME in 33 patients, 2ME was very well tolerated and a small number of patients showed grades 2 and 3 liver function abnormalities, but liver function returned to normal rapidly after discontinuation of 2ME (18).

e) *In vitro* data indicate that 2ME may beneficially influence the cardiovascular system by positively modulating the production of vasoactive substances (116,135,166). Also, administration of 2ME would directly protect the cardiovascular system without the need for metabolism, thus rendering more consistent effects (116).

f) 2ME is active when administered orally (53). Several *in vivo* studies reported inhibition of growth and formation of transplanted or chemically induced tumors by oral administration of 2ME (21,28,101). The oral administration makes a clinical application technically easy for outpatient treatment (94). Oral administration of 2ME significantly enhanced the radiation effect on a subcutaneous tumor without any toxicity and suggesting that this strategy may be clinically useful as an adjuvant therapy (100).

g) 2ME does not have feminizing effects, and could therefore be used therapeutically in both women and men (116).

h) 2ME can also be used in combination with more conventional cancer treatments. Endocrine therapy is widely accepted for the treatment of hormone receptor-positive breast cancer (166). However, in many cases eventually resistance develops and the tumor regrows so that new endocrine treatment options are needed (166). Tamoxifen has been the most widely used endocrine drug for the management of all stages of breast cancer in women with estrogen-dependent tumors. However, tamoxifen treatment is associated with adverse effects such as an increased risk of uterine cancer, tromboembolism, hot flushes, sexual dysfunction and cataracts. Combination therapy may be one way to resolve this problem (166). *In vitro* studies by Seeger *et al.* indicated that a combination of tamoxifen with 2ME have an additive inhibitory effect on breast cancer cell lines (166). This combination may allow ameliorating of adverse events of tamoxifen by reducing its concentrations and probably also drug resistance (166). Furthermore, the mechanism of the anti-proliferative effect of these substances seems to be different and the combination may have some advantages in breast cancer treatment compared to the monosubstances (166). This should be tested in clinical trials (166).

1.9 Relevance and specific aims of the study

Numerous studies have shown the applications of 2ME in the inhibition of tumor growth. The mechanism of growth inhibition, however, is not yet fully understood. The available evidence suggests that multiple mechanisms are involved that may be

dependent on cell type (94). Unraveling the mechanisms of 2ME are crucial in the development of more effective medical therapy for tumors with better sensitivity, oral bioavailability, less long-term morbidity and new opportunities for drug and radiation combinations in order to circumvent some of the limitations of 2ME (53,96).

The purpose of this study was to investigate and compare the possible differential action(s) of 2ME in normal breast (MCF-12A) and tumorigenic breast (MCF-7) cell lines by

a) performing cell growth studies, to determine the effect of 2ME on cell numbers and metabolic activity of the cells;

b) studying the morphological changes induced by 2ME with haematoxylin and eosin cell staining and immunocytochemistry techniques;

c) investigating the effects of 2ME on the cell cycle and identifying and studying the regulatory components of the cell cycle affected by 2ME.

This study may contribute to a better understanding about the treatment of cancer, which is important in the development and/or improvement of novel chemotherapeutic agents.

Chapter 2

Materials and Methods

All studies were conducted in the laboratory of the Department of Physiology at the University of Pretoria.

2.1 Cell cultures

The effects of 2ME were investigated in the following cell lines:

a) MCF-7 – cell line derived from a pleural effusion of human breast adenocarcinoma.

b) MCF-12A – non-tumorigenic epithelial cell line produced by long-term culture of normal mammary tissue.

The MCF-7 cell line was supplied by Highveld Biological (Sandringham, South Africa) and the MCF-12A cell line was a gift from Professor Parker (Division of Medical Biochemistry, University of Cape Town, Cape Town, South Africa).

Only two cell lines were used for the scope of this study. Ideally, all tumorigenic and normal breast cell lines should be included for a comprehensive study. Furthermore, a primary breast cell culture would be more representative of normal *in vivo* cells than the immortalized non-tumorigenic MCF-12A cells. However, primary cultures were not used in this study, because of its finite life span and the high variation between cultures, which could result in inconsistent results. It is also very difficult to obtain biopsies of normal mammary tissue and to obtain the required cell type. In contrast to primary cultures, continuous cell lines won't die after a few rounds of subculturing and have a greater proliferation rate. Furthermore, they proliferate to form identical replicates and therefore can maintain consistency during experimental procedures. In order to evaluate the diagnostic and/or prognostic value of results, it has to be assumed that *in vitro* results would be representative of *in vivo* conditions.

2.2 General laboratory procedures

a) Materials

Dulbecco's Modified Eagle's Medium (DMEM) with glucose, sodium pyruvate and L-glutamine, Ham's F12 medium with L-glutamine, fetal calf serum (FCS), penicillin, streptomycin, fungizone and trypsin/versene were obtained from Highveld Biological (Sandringham, South Africa). Epidermal growth factor (EGF), cholera toxin, insulin, hydrocortisone, dimethyl sulphoxide (DMSO), 2ME and trypan blue were supplied by Sigma-Aldrich (St. Louis, United States of America). All other chemicals were from Merck (Darmstadt, Germany). Sterile cell culture flasks and plates were obtained through Laboratory Equipment Supplies (Germiston, South Africa) and 0.22-µm syringe filters from Aqualytic CC (Irene, South Africa).

b) Methods

2.2.1 General cell culture procedures

Cells were grown in 25 cm^2 or 75 cm^2 tissue culture flasks at 37 ^oC, 5 % CO_2 in a Forma Scientific water-jacketed incubator (Ohio, United States of America). The maintenance growth medium of the MCF-7 cells consisted of DMEM supplemented with 10 % heat-inactivated FCS (56 ^oC, 30 min), penicillin (100 µg/l), streptomycin (100 µg/l) and fungizone (250 µg/l). It has been shown that MCF-7 cells grow optimally when the growth medium is supplemented with 10 % heat-inactivated FCS (29). Growth medium for the MCF-12A cells consisted of a 1:1 mixture of DMEM and Ham's F12 medium, 20 ng/ml epidermal growth factor, 100 ng/ml cholera toxin, 10 µg/ml insulin and 500 ng/ml hydrocortisone, supplemented with 10 % heat-inactivated FCS (56 ^oC, 30 min), penicillin (100 µg/l), streptomycin (100 µg/l) and fungizone (250 µg/l).

A ten times concentrated stock solution of phosphate buffered saline (PBS) consisting of 80 g/l NaCl, 2 g/l KCl, 2 g/l KH_2PO_4 and 11.5 g/l $Na_2HPO_4.2H_2O$ was made and 50 ml aliquots stored at 4 ^oC. When needed, the PBS was diluted ten times, the pH

adjusted to 7.4 with 1M NaOH and the dilution autoclaved (20 min, 120 °C, 15 psi) before use.

At one to three day intervals the growth medium of the cells were replaced with fresh medium and the cells were trypsinized when confluent. When confluent, cells were washed with and incubated in PBS (37 °C, ± 20 min), then incubated in trypsin/versene for ± 10 min, 37 °C. The trypsin solution was removed and the cells detached from the surface of the tissue culture flask by gently tapping the flask against the hand. Cells were resuspended in fresh medium and divided into subcultures or used in experiments. When required, the cells were frozen in cryotubes in a –70 °C freezer. The freeze medium consists of 10 % growth media, 10 % DMSO and 80 % FCS. The cooling rate during the freezing process is estimated at ± 1 °C/min.

Aseptic techniques were applied throughout, with all work being carried out in a laminar flow cabinet from Labotec (Midrand, South Africa), all solutions being filter-sterilized (0.22 µm pore size) and all glassware and non-sterile equipment being sterilized by autoclaving (20 min, 120°C, 15 psi).

2.2.2 General methods for experiments

For experiments cells were seeded in sterile 96-well tissue culture plates or on heat-sterilized coverslips in 6-well culture plates. Cells were harvested by trypsinization as described above and an aliquot of the cells resuspended in media was counted by making use of a haemocytometer. 50 µl trypan blue was added to 50 µl of the cell suspension before counting the cells to determine cell viability. Dead cells take up the dye, are stained blue and they are not counted. Viable cells do not take up the dye, remain clear and are counted.

The number of cells per ml is determined by the following calculation:

Cells/ml = Average count per five squares in haemocytometer x dilution factor x 10^4

The cell suspension was diluted with medium to give the required cell number and was seeded into the appropriate tissue culture plates.

A stock solution of 2 x 10^{-3} M 2ME dissolved in DMSO was made. Prior to exposure of the cells, the stock solution was diluted with medium to the desired concentrations. The medium of all control cells was supplemented with an equal concentration of DMSO. The DMSO content of the final dilutions never exceeded 0.1 % (v/v).

2.3 Analytical experimental protocols

2.3.1 Cell growth studies

2.3.1.1 DNA staining – crystal violet

a) Materials

Gluteraldehyde, crystal violet and Triton X-100 were purchased from Merck (Darmstadt, Germany).

b) Methods

Cell numbers were determined spectrophotometrically employing crystal violet as a DNA dye, to obtain an indication of the effect of 2ME exposure on cell growth. Exponentially growing MCF-7 and MCF-12A cells were seeded at a cell density of 5 000 cells per well in 96-well tissue culture plates. Cells were incubated at 37 ^{o}C for 24 h to allow the cells to adhere to the microtiter plates before exposure to the test compound. Cells were exposed to concentrations ranging between 1x10^{-5} M and 1x10^{-9} M of 2ME and incubated for 72 h, before the assay was performed. A baseline reading (before exposure) was also conducted.

The medium was discarded and 100 µl of 1 % gluteraldehyde (in PBS) added to each well. After 15 min incubation at room temperature, the gluteraldehyde was discarded and 100 µl crystal violet (0.1 % in PBS) added and incubated for 30 min at room temperature. The microtiter plates were immersed in running tap water for 15 min and

left to dry. 200 µl 0.2 % Triton X-100 was added to each well and incubated at room temperature for 30 min. 100 µl of the solution was transferred to a clean microtiter plate and the absorbance read at 570 nm. An EL_X800 Universal Microplate Reader from Bio-Tek Instruments Inc. (Vermont, United States of America) was used to read the absorbance.

2.3.1.2 Metabolic activity – MTT assay

a) Materials

3-[4,5 dimethylthiazol-2-yl]-2,5-diphenyl tetrazolium bromide (MTT) and DMSO were supplied by Sigma-Aldrich (St. Louis, United States of America). All other chemicals were from Merck (Darmstadt, Germany).

b) Methods

Exponentially growing MCF-7 and MCF-12A cells were seeded at 5 000 cells per well in 96-well tissue culture plates. After a 24h incubation period (37 ^{o}C) to allow the cells to adhere to the microtiter plates, cells were exposed to concentrations between $1x10^{-5}$ M and $1x10^{-9}$ M 2ME and incubated for 72 h. 20 µl MTT (5 mg/ml in PBS) was added to each well containing 200 µl medium. The microtiter plates were incubated for 4h at 37 ^{o}C in a CO_2 incubator. The plates were centrifuged at 2000 revolutions per minute (rpm) for 10 min and the supernatant removed without disturbing the pellet. The pellets were washed with 150 µl PBS and again centrifuged at 2000 rpm for 10 min. After removal of the supernatant 100 µl DMSO was added to each well and plates were shaken for 1 h on a shaker before the absorbance was read at 570 nm (reference 630 nm), using an EL_X800 Universal Microplate Reader from Bio-Tek Instruments Inc. (Vermont, United States of America).

2.3.2 Morphology studies

2.3.2.1 Light microscopy - haematoxylin and eosin cell staining

a) Materials

Bouin's fixative was from Sigma-Aldrich (St. Louis, United States of America) and haematoxylin, eosin, ethanol, xylol and Entellan® fixative were purchased from Merck (Darmstadt, Germany).

b) Methods

Exponentially growing MCF-7 and MCF-12A cells were seeded at 300 000 cells per well in 6-well plates on heat-sterilized coverslips. After a 24 h incubation period (37 ^{o}C) to allow the cells to adhere, cells were exposed to $1x10^{-6}$ M or $1x10^{-8}$ M 2ME and incubated for 24 h or 48 h at 37 ^{o}C. The coverslips were transferred to staining dishes and fixed with Bouin's fixative for 30 min. The Bouin's was discarded and coverslips was left in 70 % ethanol for at least 20 min, before they were rinsed with tap water. After 20 min in Mayer's Hemalum, the coverslips were rinsed with water for 2 min and then with 70 % ethanol before they were subjected to 1 % eosin for 2 min. This was followed by rinsing twice for 5 min with 70 % ethanol, 96 % ethanol, 100 % ethanol and xylol, consecutively. The coverslips were mounted on microscope slides with resin and left to dry before evaluation with a Nikon Optiphot microscope (Nikon, Japan) (167).

2.3.2.2 Immunofluorescent ß-tubulin detection

a) Materials

Mouse monoclonal antibody against human ß-tubulin (Clone 2-28-33), biotin-conjugated anti-mouse Fab-specific IgG (immunoglobulin G) developed in goat, fluoroisothiocyanate (FITC)-conjugate diluent, ExtrAvidin®-FITC conjugate were purchased from Sigma-Aldrich (St. Louis, United States of America). All other chemicals were of analytical grade and supplied by Merck (Darmstadt, Germany).

b) Methods

To compare the effect of 2ME on spindle formation in MCF-7 and MCF-12A cells, indirect immunofluorescence was employed. 300 000 cells were seeded onto heat-sterilized glass cover slips in 6-well plates. After a 24h incubation period (37 ^{o}C) to allow the cells to adhere, cells were exposed to 1x10^{-6} M 2ME for a period of 24 h at 37 ^{o}C. The coverslips were transferred to staining dishes and the cells fixed in 10 % formalin (2 mM EGTA in PBS) for 10 min and permeabilized in ice-cold 97 % methanol (2 mM EGTA) at –20 ^{o}C for 10 min. Cells were subsequently washed in PBS (3 x 5 min) before incubation for 1 h with a mouse monoclonal antibody against human ß-tubulin (Clone 2-28-33; 1:1000). The cells were again washed 3 x 5 min with PBS and incubated for 1h with biotin-conjugated anti-mouse IgG (Fab-specific, developed in goat) in FITC-conjugate diluent as secondary antibody (1:15). After washing with PBS (3 x 5 min), cells were finally incubated with ExtrAvidin®-FITC conjugate (1:200 in FITC-conjugate diluent) for 1h. Following the final 3 x 5 min wash with PBS, the coverslips were mounted with a glycerol-based mounting fluid. The cells were examined with a Nikon Optiphot microscope equipped with an episcopic-fluorescence attachment and an excitation-emission filter with an average wavelength of 495 nm for FITC (Nikon, Japan).

2.3.2.3 Immunocytochemistry – detection of estrogen receptors

a) Materials

MDA-MB-231 cells were from the department of Urology, University of Pretoria, South Africa. Antibody against estrogen receptor developed in rabbit was from Zymed (San Francisco CA, United States of America). Goat anti-rabbit IgG peroxidase conjugate and 3,3’ diaminobenzidine (DAB) were supplied by Sigma-Aldrich (St. Louis, United States of America). All other chemicals were of analytical grade and supplied by Merck (Darmstadt, Germany).

b) Methods

For the detection of estrogen receptors, 300 000 MCF-7, MCF-12A and MDA-MB-

231 cells were seeded onto heat-sterilised glass cover slips in 6-well plates. After a 24 h incubation period (37 °C) to allow the cells to adhere, the coverslips were transferred to staining dishes and the cells fixed in 10 % formalin (2 mM EGTA in PBS) for 10 min. The cells were permeabilized in ice-cold 97 % methanol (2 mM EGTA) at –20 °C for 10 min and washed in PBS (3 x 5 min) before incubation for 1 h with antibody against estrogen receptor developed in rabbit (1:1000 in PBS). The cells were again washed 3 x 5 min with PBS and incubated for 1 h with goat anti-rabbit IgG peroxidase conjugate (1:200 in PBS). Following the final 3 x 5 min wash with PBS, antigen detection was achieved by adding DAB as substrate (60 mg in 200 ml PBS, containing 0.1 % hydrogen peroxide). The coverslips were then mounted with a glycerol-based mounting fluid. The cells were examined with a Nikon Optiphot microscope equipped with an episcopic-fluorescence attachment and an excitation-emission filter with an average wavelength of 495 nm for FITC.

2.3.3 Cell cycle studies

2.3.3.1 Cell cycle length determination

a) Materials

Hydroxyurea (HU) was purchased from Sigma-Aldrich (St. Louis, United States of America).

b) Methods

300 000 cells per well were seeded onto heat-sterilised glass coverslips in 6-well plates. After a 24 h incubation period (37 °C) to allow the cells to adhere, 2 mM HU was added to the sub-confluent cultures for 20 h. HU blocks cells in early S-phase (52,168). Although it has been reported that HU is toxic to some cells, preliminary studies indicated that HU was not toxic to either MCF-7 or MCF-12A cells. Cells were rinsed with PBS (3 x, 10 min, 37 °C) to wash out the HU and to allow the synchronized cells to continue through S-phase. This point was considered as time zero (0 h). Unsynchronized and synchronized slides served as controls at 0 h. Half of the remaining wells were exposed to $1x10^{-6}$ M 2ME. At 2 h intervals exposed

and control coverslips were fixed and stained with haematoxylin and eosin and their mitotic indices determined in order to investigate the effect of 2ME on the length of the cell cycle.

2.3.3.2 Cell cycle checkpoint regulatory molecules – checkpoint kinase assay

a) Materials

The CycLex® Checkpoint Kinase Assay/Drug Discovery Kit-1 was purchased from MBL Medical & Biological Laboratories (Nagoya, Japan). Wash buffer (10 x containing 2 % Tween®-20), kinase buffer, ATP (Adenosine triphosphate), horseradish peroxidase (HRP) conjugated anti-phospho-Cdc25C S216 (1F1) antibody, tetra-methylbenzidine substrate reagent (TMB) and stop solution (0.5 N H_2SO_4) were supplied with the kit. Tris-HCl, NP-40 (Nonidet P40), EDTA (ethylene diamine tetraacetic acid), EGTA (ethylene glycol-bis-(beta-aminoethyl ether)N,N,N',N'-tetra-acetate), PMSF (phenyl methyl sulfonyl fluoride), beta-glycerophosphate, Na_3VO_4, mercaptoethanol and the protease inhibitor cocktail were from Sigma-Aldrich (St. Louis, United States of America). NaCl and NaF were from Associated Chemical Enterprises (Southdale, South Africa).

b) Methods

MCF-7 and MCF-12A cells were grown in 75 cm^2 flasks until 80 % confluent. Cells were exposed to 2 mM HU for 20 h, to block the cells in early S-phase. The HU was washed out with PBS (3 x, 10 min, 37 ^oC) and half of the cells were exposed to $1x10^{-6}$ M 2ME. The cells were allowed to progress through the cell cycle until mitotic peak was reached. Cells were harvested and washed three times with PBS. 10^7 cells were suspended in 500 µl extraction buffer (20 mM Tris-HCl, pH 8.5, 250 mM NaCl, 0.2 % NP-40, 1 mM EDTA, 1 mM EGTA, 0.2 mM PMSF, 5 mM beta-glycerophosphate, 2 mM NaF, 2 mM Na_3VO_4, 5 mM mercaptoethanol, 0.8 % protease inhibitor cocktail) and lysed by three cycles of freezing and thawing. The extracts were centrifuged for 10 min at 10 000 x g and diluted 1:5 with Q-buffer (20 mM Tris-HCl, pH 8.5, 0.2 mM EDTA, 1 mM EGTA, 0.2 mM Na_3VO_4, 5 mM mercaptoethanol, 0.8 % protease inhibitor cocktail). After 15 min on ice, the diluted extracts were centrifuged for

30 min at 10 000 x g and the supernatant diluted 1:200 in kinase buffer. Protein content was confirmed with the Bradford method (169).

10 µl of these enzyme fractions and 90 µl kinase reaction buffer (50 µM ATP in kinase buffer) were added to the microtiter wells (coated with recombinant Cdc25C) provided with the kit. A positive control (10 m unit/well C-TAK positive control), inhibitor control (10 µM staurosporine to positive control), ATP minus control (no kinase reaction buffer) and no enzyme control were included. The plate was sealed and incubated 60 min, 30 °C. Wells were washed five times with wash buffer, 100 µl HRP-conjugated detection antibody 1F1 were added to each well, the plate was sealed and incubated for 60 min at room temperature. After washing five times with wash buffer, 100 µl substrate solution was added to each well and the plate incubated at room temperature for 15 min. 100 µl stop solution was added to each well and the absorbance measured at 450 nm using an EL_X800 Universal Microplate Reader (Bio-Tek Instruments Inc., Analytical Diagnostic Products, Weltevreden, South Africa).

2.3.3.3 Cell cycle checkpoint regulatory molecules – Cdc2 kinase assay

a) Materials

The MESACUP Cdc2 Kinase Assay Kit and HCK-gel suspension were purchased from MBL Medical & Biological Laboratories (Nagoya, Japan). Cdc2 reaction buffer, biotinylated MV peptide, POD (peroxidase) conjugated streptavidin, wash concentrate (10x PBS), substrate A (*o*-phenylenediamine), substrate B (H_2O_2), stop solution (20 % H_3PO_4) and phosphorylation stop reagent (PBS containing 50 mM EDTA) were supplied with the kit. ATP, Tris-HCl, EDTA, EGTA, Brij35, PMSF, beta-glycerophosphate, Na_3VO_4, 2-mercaptoethanol and the protease inhibitor cocktail were from Sigma-Aldrich (St. Louis, United States of America). NaCl was from Associated Chemical Enterprises (Southdale, South Africa), $MgCl_2$ from Merck (Darmstadt, Germany) and HEPES was from BDH Laboratory Supplies (Poole, England).

b) Methods

MCF-7 and MCF-12A cells were grown in 75 cm^2 flasks until 80 % confluent. Cells were exposed to 2 mM HU for 20 h, to block the cells in early S-phase. The HU was washed out with PBS (3 x, 10 min, 37 ^oC) and half of the cells were exposed to $1x10^{-6}$ M 2ME. The cells were allowed to progress through the cell cycle until mitotic peak was reached. Cells were harvested and washed (three times) with PBS. 2 x 10^7 cells were suspended in 1000 µl sample buffer (50 mM Tris-HCl, pH 7.5, 0.5 mM NaCl, 5 mM EDTA, 2 mM EGTA, 0.01 % Brij35, 1 mM PMSF, 25 mM beta-glycerophosphate, 1 mM Na_3VO_4, 50 mM mercaptoethanol, 0.08 % protease inhibitor cocktail) and lysed by sonication on ice. Cell extracts were centrifuged for 1h at 100 000 x g. Protein content was confirmed with the Bradford method (169). 20 µl of the HCK-gel was prepared by washing twice with sample buffer before it was incubated with 300 µl of the cell extract for 1 h on ice. After incubation, the HCK-gel were washed three times in sample buffer and twice with 2nd washing buffer (25 mM HEPES buffer, pH 7.5 and 10 mM $MgCl_2$), followed by centrifugation for 5 min at 1 500 x g. The phosphorylation reaction was set up on ice, by adding 5 µl of the gel pellet, 5 µl 10 x Cdc2 reaction buffer, 5 µl biotinylated MV peptide, 30 µl distilled water and the reaction was started by adding 5 µl 1 mM ATP and incubated for 30 min, 30 °C. The reaction was terminated with 200 µl phosphorylation stop solution and centrifuged for 20 s at 11 000 x g. 100 µl of the reaction mixture was transferred to the microwell strips coated with monoclonal antibody 4A4, provided with the kit. After 60 min incubation at 25 °C the wells were washed five times with wash solution and 100 µl POD conjugated streptavidin added to each well. After 30 min incubation at 25 °C the wells were washed five times with wash solution and 100 µl POD substrate solution added to each well. The microwell strips were incubated for 5 min at 25 °C before 100 µl stop solution was added to each well and the absorbance read at 450 nm in an EL_X800 Universal Microplate Reader (Bio-Tek Instruments Inc., Analytical Diagnostic Products, Weltevreden, South Africa).

2.4 Statistical analysis of data

Statistical analysis of the quantitative data was done by prof. F.E. Steffens from the Department of Statistics, University of Pretoria. Cell growth studies were repeated

thrice, with sample size (n) = 6 in each experiment and analysed by means of an analysis of variance (ANOVA). Cell cycle kinase assays were repeated twice, with n = 3 in each experiment and analysed with the Wilcoxon two-sample rank test (nonparametric test). A *P*-value of less than 0.05 was accepted as significant. Means of quantitative experiments are presented in bar charts, with T-bars referring to standard deviations (SD). All experiments included a set of appropriate controls.

Chapter 3

Results

3.1 Cell growth studies

3.1.1 DNA staining – crystal violet

2ME displays antiproliferative actions in various human breast cancer cells (13). Cell numbers were determined spectrophotometrically and expressed as a percentage of the control, in order to obtain an indication of the effect of 2ME exposure on cell proliferation in tumorigenic MCF-7 and non-tumorigenic MCF-12A cells. 5 000 cells were seeded per well in 96-well plates and exposed to five different concentrations of 2ME, ranging from 10^{-5} to 10^{-9} M, for 72 h. The concentration range chosen for the cell growth studies were similar to the concentration range Lippert *et al.* used for cell proliferation studies with endogenous estradiol metabolites (170). Crystal violet was employed as a DNA dye. Gillies *et al*. showed that when the absorbed dye is solubilized in Triton X-100, the optical density of the solution is linearly related to cell number and that the technique is applicable to study agents that affect cell proliferation (171). Kueng *et al*. showed that the procedure can be adapted for use in 96-well plates with high sensitivity and cost effectiveness (172).

From Figure 3.1 it is clear that 2ME reduced cell proliferation in both the non-tumorigenic MCF-12A and the tumorigenic MCF-7 cell line in a dose-dependent manner. ANOVA revealed a statistical significant difference (*P*-value < 0.05) in growth inhibition between the normal and tumorigenic cell line at all the concentrations, except for 10^{-5} M 2ME. In the MCF-12A cell line, cell proliferation was not reduced at 10^{-7} M and lower concentrations of 2ME. Cell growth was reduced by 83 % at 10^{-6} M and by 98 % at 10^{-5} M 2ME in this cell line. For the MCF-7 cells, cell proliferation was reduced at all the tested concentrations, with a 15 % reduction at 10^{-9} and 10^{-8} M, 23 % at 10^{-7} M, 91.5 % at 10^{-6} M and 98.5 % at 10^{-5} M 2ME.

Special concentration parameters, 50 % growth inhibitory concentration (GI_{50}), total growth inhibitory concentration (TGI) and 50 % lethal concentration (LC_{50}) were determined to compare the growth inhibition induced by 2ME between the two cell lines. The GI_{50} value is the concentration of the test drug that causes 50 % growth inhibition and measures the growth inhibitory power of the test agent. The GI_{50} is the concentration where

$100 \times (T - T_0)/(C-T_0) = 50$

T is the optical density of the test well after 72 h exposure to the test drug

T_0 is the optical density at time zero

C is the control optical density

The TGI is the concentration of the test drug that causes a cytostatic effect. It is the concentration where

$100 \times (T - T_0)/(C-T_0) = 0$

The LC_{50} signifies a cytotoxic effect and is the concentration of the test drug where

$100 \times (T - T_0)/T_0 = -50$

Figure 3.2 shows the growth inhibition graphs of the two cell lines, calculated by the formula $100 \times (T - T_0)/(C-T_0)$. Although it is clear from the graph that 2ME has a greater growth inhibitory effect on the tumorigenic MCF-7 cells than the non-tumorigenic MCF-12A cells, the GI_{50} for both cell lines are between 10^{-7} and 10^{-6} M 2ME. The TGI for the MCF-7 cell line is at 10^{-6} M, and lies between 10^{-6} and 10^{-5} M 2ME for the MCF-12A's.

Graphs for the cytotoxic effect of 2ME is represented in Figure 3.3. For both cell lines the LC_{50} value lies between 10^{-6} and 10^{-5} M 2ME.

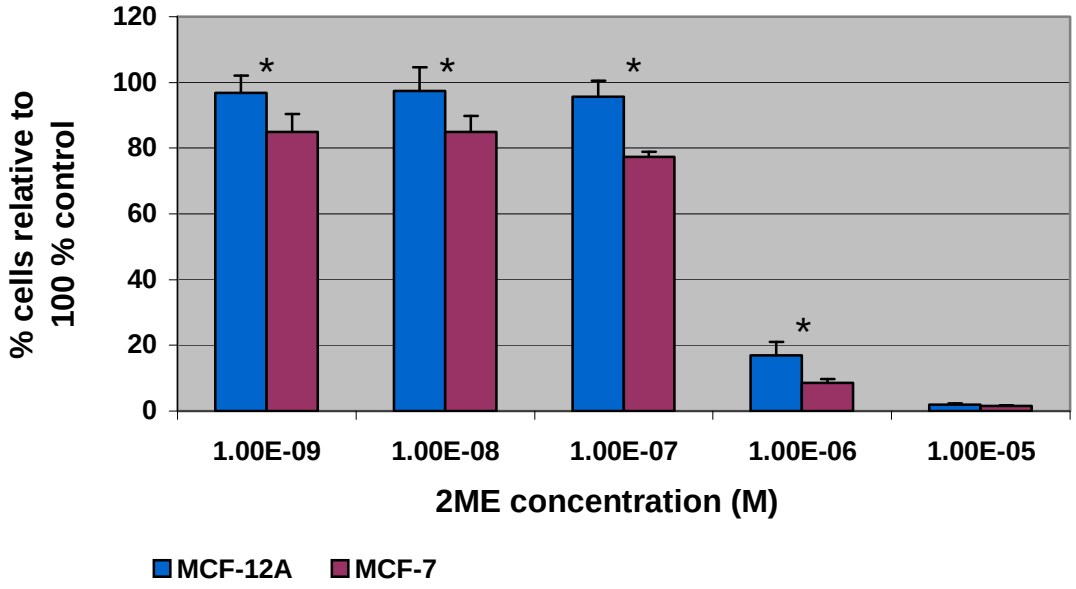

Figure 3.1: MCF-12A and MCF-7 cell numbers expressed as a percentage of cells relative to 100 % control, after exposure to different concentrations of 2ME (10^{-5}, 10^{-6}, 10^{-7}, 10^{-8}, 10^{-9} M) for 72h. * Indicates a *P*-value < 0.05 for growth inhibition between cell lines.

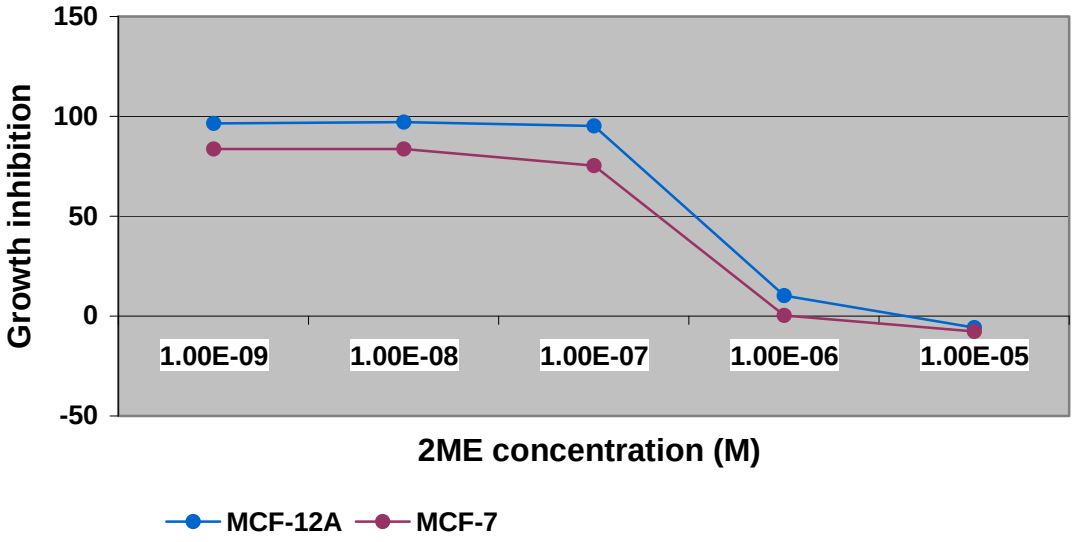

Figure 3.2: Growth inhibitory effect of 2ME on MCF-7 and MCF-12A cells. Growth inhibition = 100 x $(T - T_0)/(C-T_0)$.

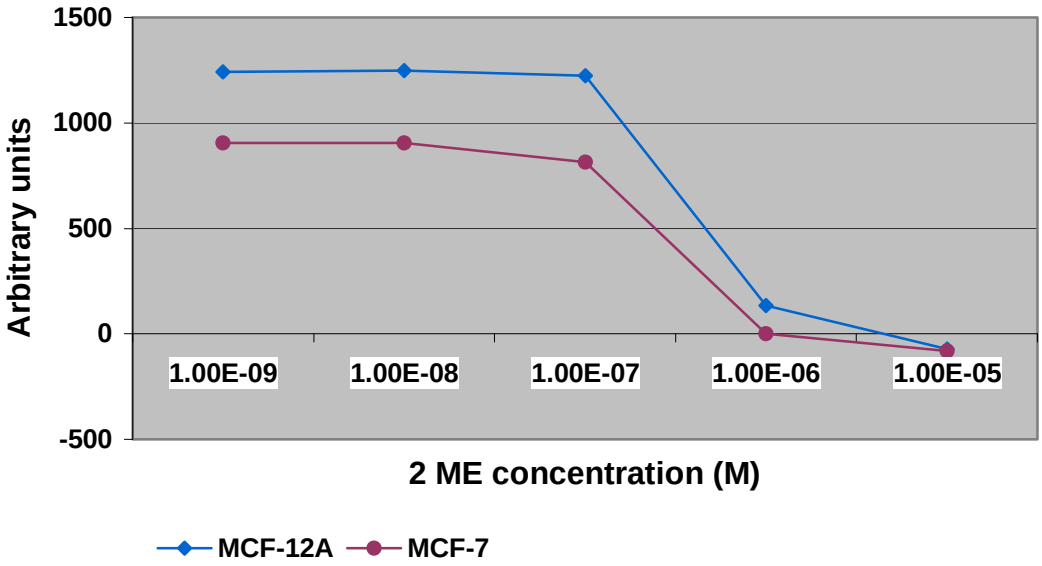

Figure 3.3: Cytotoxic effect of 2ME on MCF-12A and MCF-7 cells. $LC_{50} = 100 \times (T - T_0)/T_0 = -50$.

3.1.2 Metabolic activity - MTT assay

The MTT assay was used to determine cell survival and proliferation in MCF-7 and MCF-12A cells after exposure to 2ME. 5 000 cells per well were seeded in 96-well plates and exposed to five different concentrations of 2ME ranging from 10^{-5} to 10^{-9} M for 72 h. In order to be able to compare the two assays, concentrations and time of exposure to 2ME were exactly the same for the MTT assay and the assay employing crystal violet. MTT is a yellow soluble tetrazolium salt and is cleaved in active mitochondria by the mitochondrial dehydrogenase enzyme to form insoluble dark purple formazan crystals (173). Only viable cells with active mitochondria reduce significant amounts of MTT to formazan and therefore, the amount of formazan generated is directly proportional to the amount of viable, metabolically active cells (173).

From Figure 3.4 it is clear that cell growth is inhibited by 2ME in a dose-dependent manner in both cell lines. ANOVA revealed a statistical significant difference (*P*-value < 0.05) in growth inhibition between the normal and tumorigenic cell line at all the concentrations. In fact, in all cases the *P*-values were less than 0.001, except in the case of 10^{-5} M, that had a *P*-value of 0.034. In the MCF-12A cell line, cell proliferation was not reduced at 10^{-7} M and lower concentrations of 2ME. Cell growth was inhibited by 44 % at 10^{-6} M and by 95 % at 10^{-5} M 2ME in the MCF-12A cell line. Cell growth was inhibited by 11 % at 10^{-9} and 10^{-8} M, 20 % at 10^{-7} M, 84 % at 10^{-6} M and 96.5 % at 10^{-5} M 2ME in MCF-7 cells.

Special concentration parameters, GI_{50}, TGI and LC_{50} were determined as described in 3.1.1 for the cell number studies conducted with crystal violet in order to compare growth inhibition induced by 2ME between the two cell lines. Figure 3.5 illustrates that the GI_{50} is at 10^{-6} M 2ME for MCF-12A and between 10^{-6} and 10^{-7} M for MCF-7 cells. The TGI is between 10^{-5} and 10^{-6} M for MCF-12A cells and 10^{-6} M 2ME for the MCF-7 cell line. Graphs for the cytotoxic effect of 2ME is represented in Figure 3.6. For both cell lines the LC_{50} value lies between 10^{-6} and 10^{-5} M 2ME.

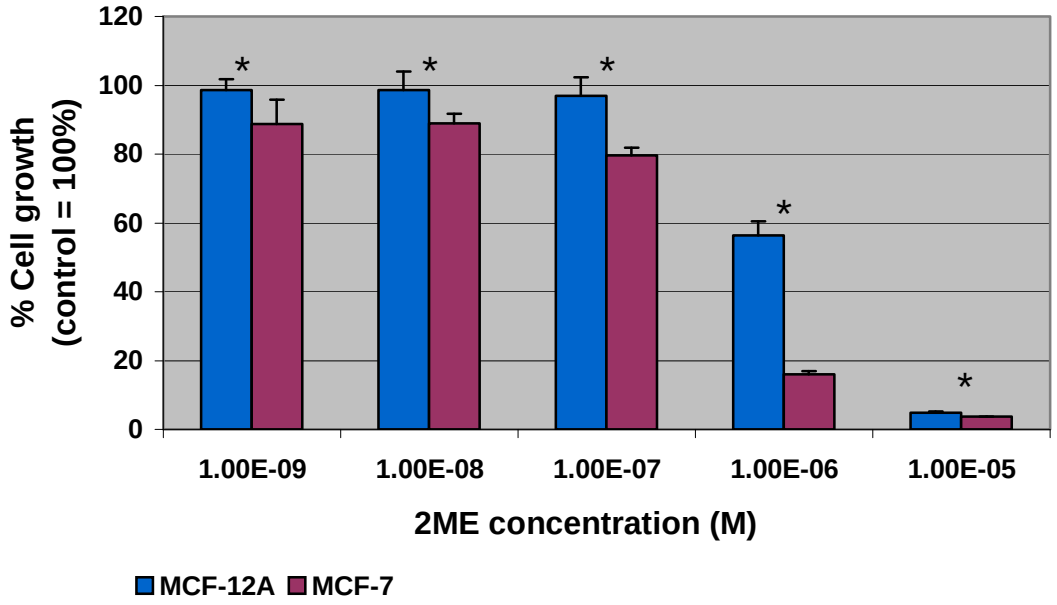

Figure 3.4: MCF-12A and MCF-7 cell growth expressed as a percentage of the control, after exposure to different concentrations of 2ME (10^{-5}, 10^{-6}, 10^{-7}, 10^{-8}, 10^{-9} M) for 72h. * Indicates a *P*-value < 0.05 for growth inhibition between cell lines.

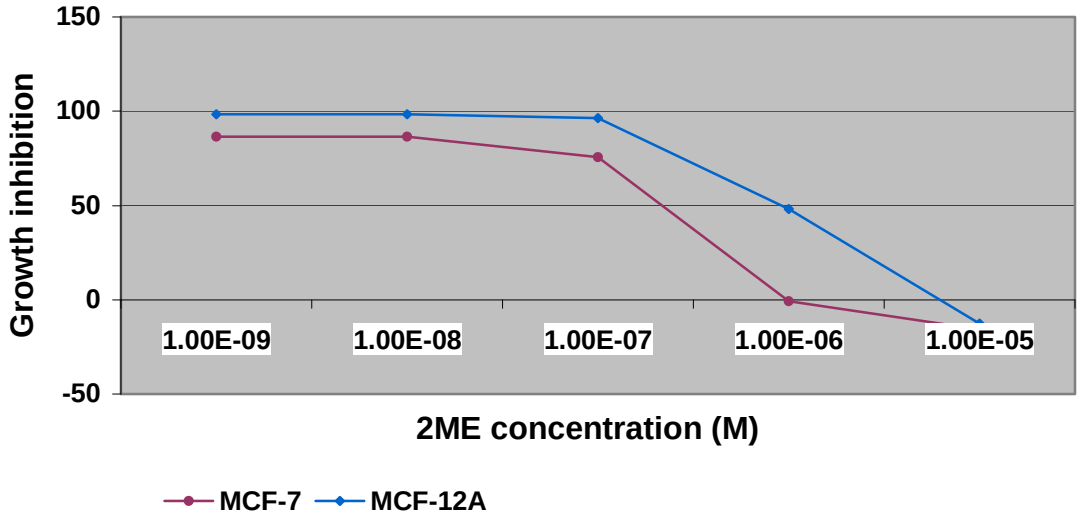

Figure 3.5: Growth inhibitory effect of 2ME on MCF-7 and MCF-12A cells. Growth inhibition = 100 x $(T - T_0)/(C-T_0)$.

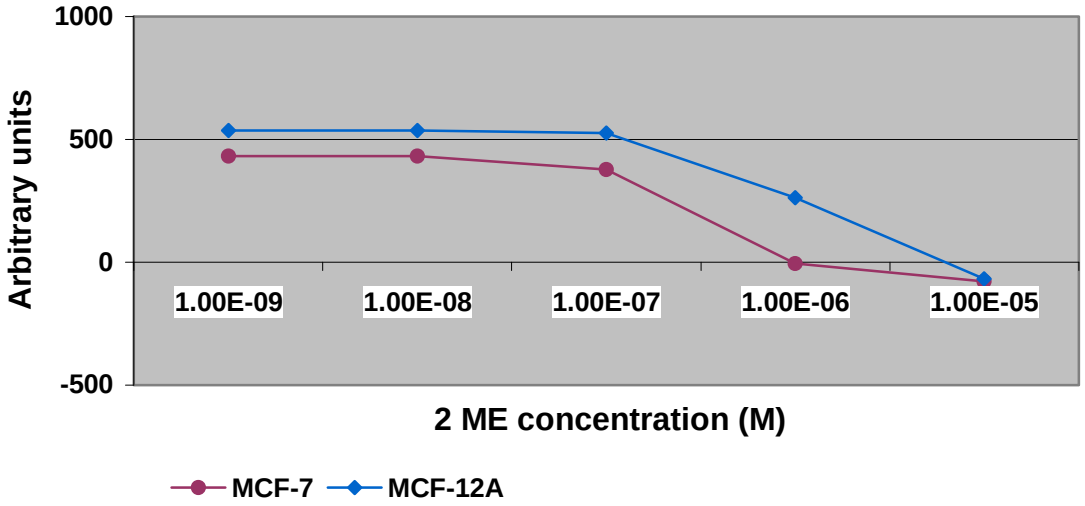

Figure 3.6: Cytotoxic effect of 2ME on MCF-12A and MCF-7 cells. $LC_{50} = 100 \times (T - T_0)/T_0 = -50$.

3.2 Morphology studies

3.2.1 Light microscopy - haematoxylin and eosin cell staining

In an attempt to obtain more insight into the anti-proliferative effect of 2ME observed in the cell growth studies, haematoxylin and eosin cell staining were used to compare the morphological characteristics of cytoplasm and nuclear components of MCF-12A and MCF-7 cells after exposure to 10^{-6} M or 10^{-8} M 2ME for 24 h and 48 h respectively. The two doses were chosen to investigate and compare the morphological effects of 2ME on the two cell lines at the concentration where the effect of 2ME on cell growth was most prominent (10^{-6} M) and at a lower concentration where the differential effect on cell growth was less prominent (10^{-8} M). 24 h and 48 h exposure times were chosen to investigate the morphological effects induced by 2ME that lead to the cytostatic and cytotoxic effects in the cell growth studies after 72 h.

Treated MCF-7's showed abnormal metaphase cells, membrane blebbing and apoptotic cells and the cell populations were less dense than in the control cells. These observations were not as prominent in the MCF-12A's. Of a thousand cells counted, 22 % of the treated MCF-7 cells were blocked in metaphase and 8.2 % showed membrane blebbing compared to only 1.4 % metaphase block and 0.1 % cells with membrane blebbing in treated MCF-12A's (Table 3.1). Treated MCF-7's also had a higher percentage of apoptotic cells than the MCF-12A's. Especially for the MCF-7 cell line the effects of 2ME were much more severe with higher concentrations of 2ME and with longer exposure periods. Consistent with the observation of a decline in cell density after 2ME treatment in this study, Kumar *et al.* reported a significant proportion of medulloblastoma-derived DAOY cells started to float after 24 h exposure and finally detached from the dishes (53). They also reported rounding of cells, condensation of cell content and induction of apoptosis after 2ME treatment (53).

Mitotic indices were calculated from the slides that were stained with haematoxylin and eosin. On each slide a thousand cells were counted and the mitotic indices were calculated and expressed as the percentage of cells in mitosis. Distinction was made

between normal mitotic cells and abnormal mitotic cells which included cells in metaphase block, cells with abnormal chromosome distribution and cells presenting with membrane blebbing (Figure 3.19). The treated MCF-7 cell line had the highest percentage of dividing cells, but most of these cells were abnormal and blocked in metaphase.

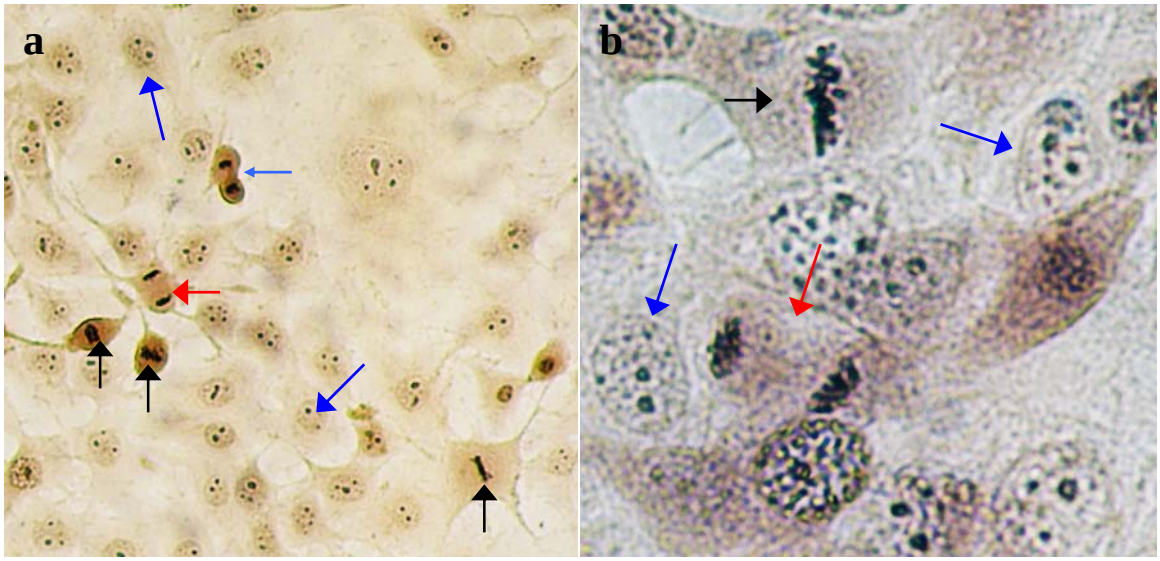

Figure 3.7: Haematoxylin and eosin staining of MCF-12A control cells exposed to 0.1 % DMSO (vehicle) for 24 h at 100X (a) and 400X (b) magnification. Cell population is dense and cells in various stages of mitosis are observed. Big blue arrows indicate interphase, black arrows metaphase, red arrows anaphase and the small blue arrow indicates telophase.

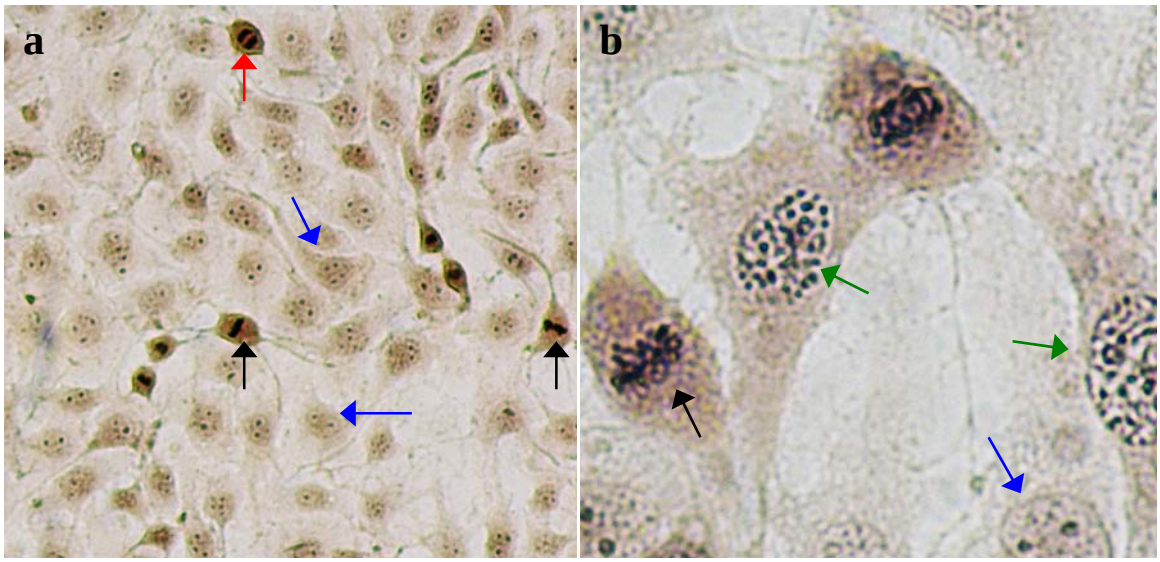

Figure 3.8: Haematoxylin and eosin staining of MCF-7 control cells exposed to 0.1 % DMSO (vehicle) for 24 h at 100X (a) and 400X (b) magnification. Cell population is dense and cells in various stages of mitosis are observed. Blue arrows indicate interphase, black arrows metaphase, the red arrow anaphase and the green arrows indicate prophase.

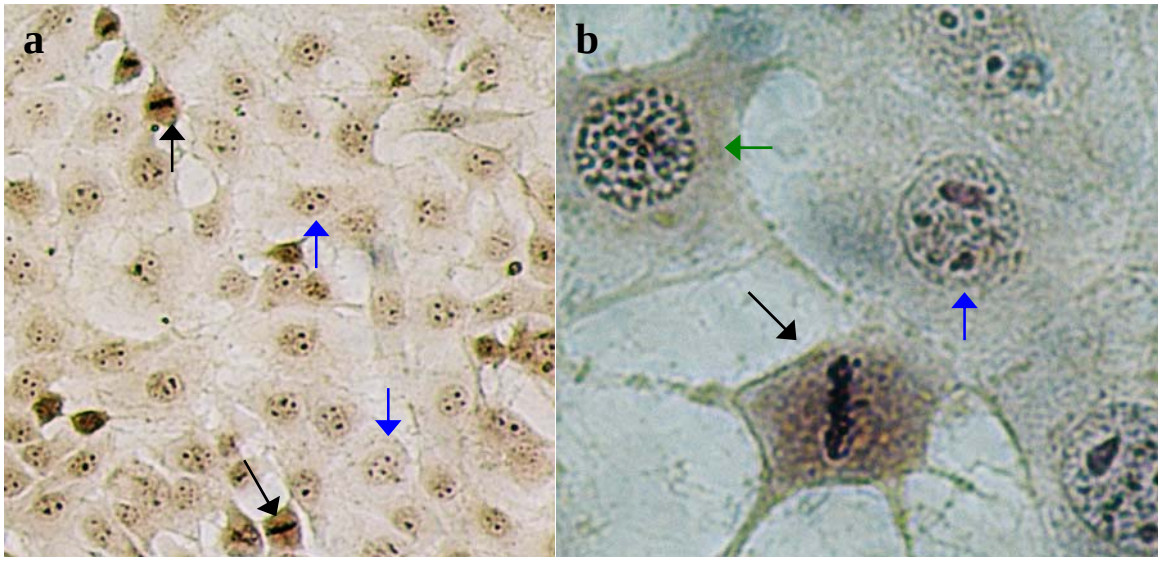

Figure 3.9: Haematoxylin and eosin staining of MCF-12A control cells exposed to 0.1 % DMSO (vehicle) for 48 h at 100X (a) and 400X (b) magnification. Cell population is dense and cells in various stages of mitosis are observed. Blue arrows indicate interphase, black arrows metaphase and the green arrow indicate prophase.

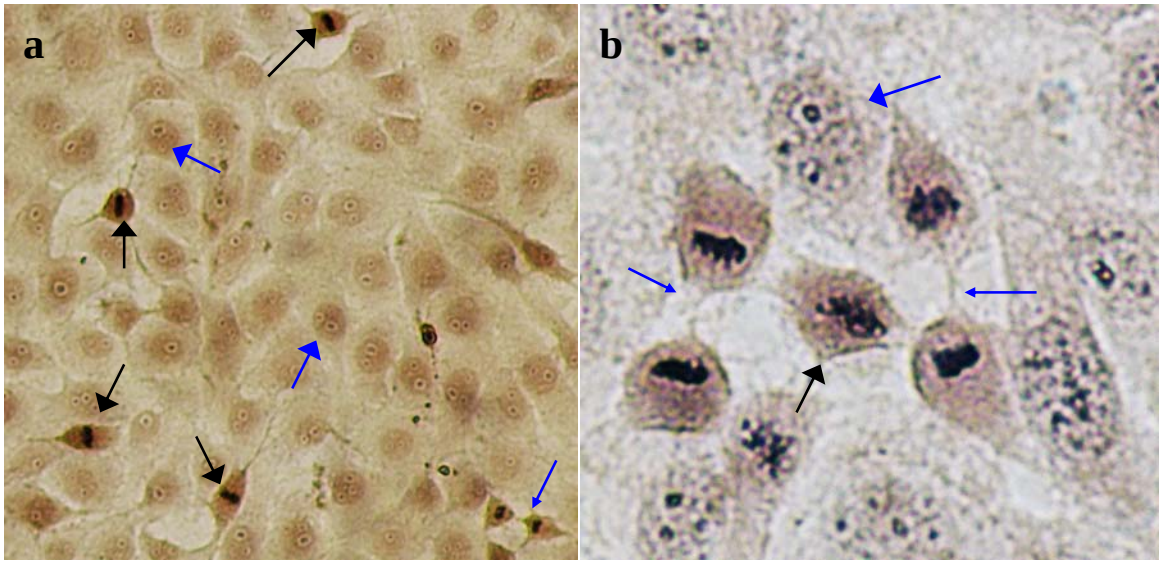

Figure 3.10: Haematoxylin and eosin staining of MCF-7 control cells exposed to 0.1 % DMSO (vehicle) for 48 h at 100X (a) and 400X (b) magnification. Cell population is dense and cells in various stages of mitosis are observed. Big blue arrows indicate interphase, black arrows metaphase and the small blue arrows indicate cytokinesis in late telophase.

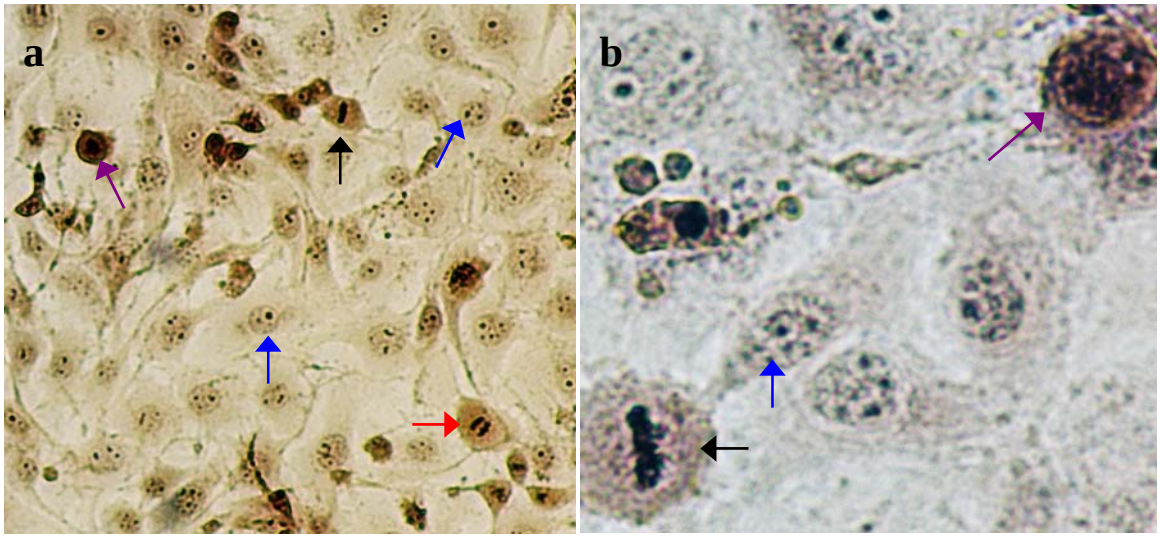

Figure 3.11: Haematoxylin and eosin staining of MCF-12A cells exposed to 10^{-6} M 2ME for 24 h at 100X (a) and 400X (b) magnification. Cell population is dense with still some normal mitotic cells (black arrows indicate normal metaphase and red arrow normal anaphase cells), but rounded cells with condensed contents are also observed (purple arrows). Blue arrows indicate interphase.

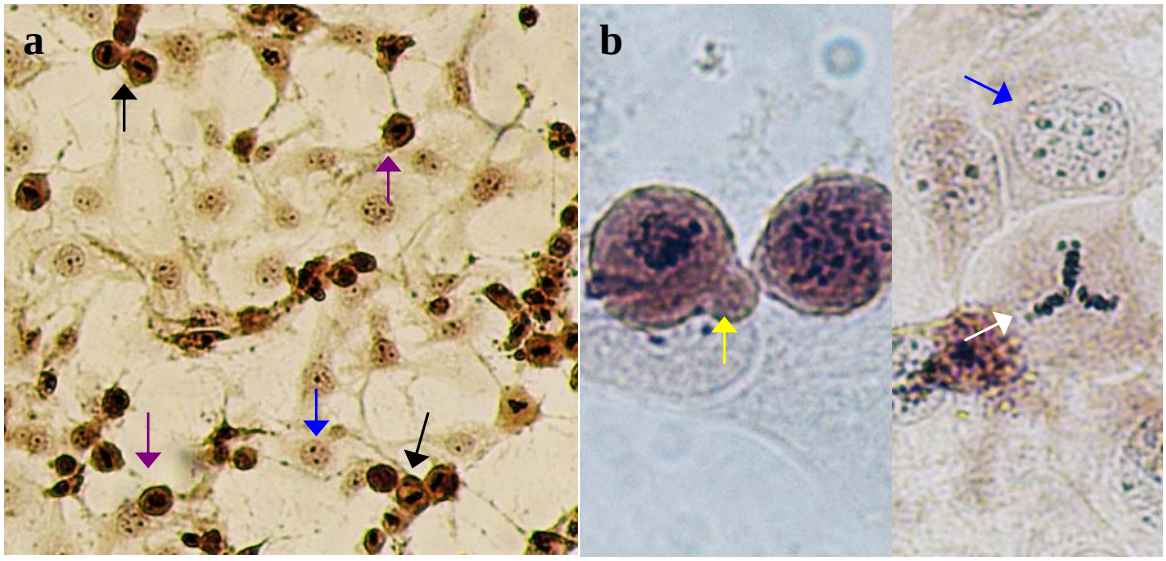

Figure 3.12: Haematoxylin and eosin staining of MCF-7 cells exposed to 10^{-6} M 2ME for 24 h at 100X (a) and 400X (b) magnification. Cell population is less dense and many rounded cells with condensed contents (purple arrows) and membrane blebbing (yellow arrow) are also observed. Many cells are blocked in metaphase (black arrows) and some triploid cells are also evident (white arrow). Blue arrows indicate interphase.

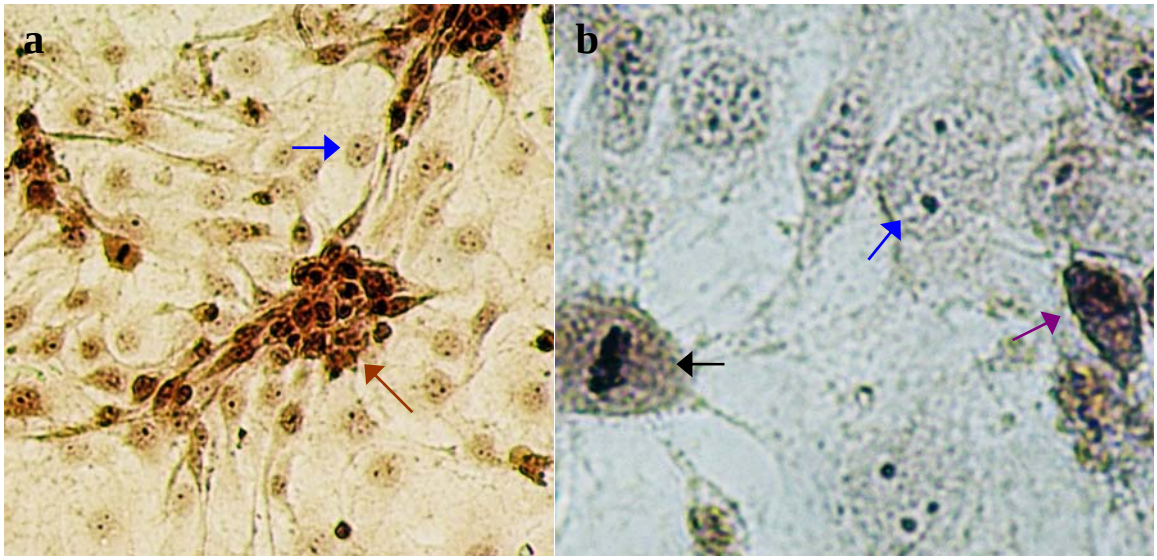

Figure 3.13: Haematoxylin and eosin staining of MCF-12A cells exposed to 10^{-6} M 2ME for 48 h at 100X (a) and 400X (b) magnification. Cell population is less dense and clusters of rounded cells are observed (brown arrow). Some normal dividing metaphase cells are observed (black arrow) and shrunken cells with condensed content are also noted (purple arrow). Blue arrows indicate interphase.

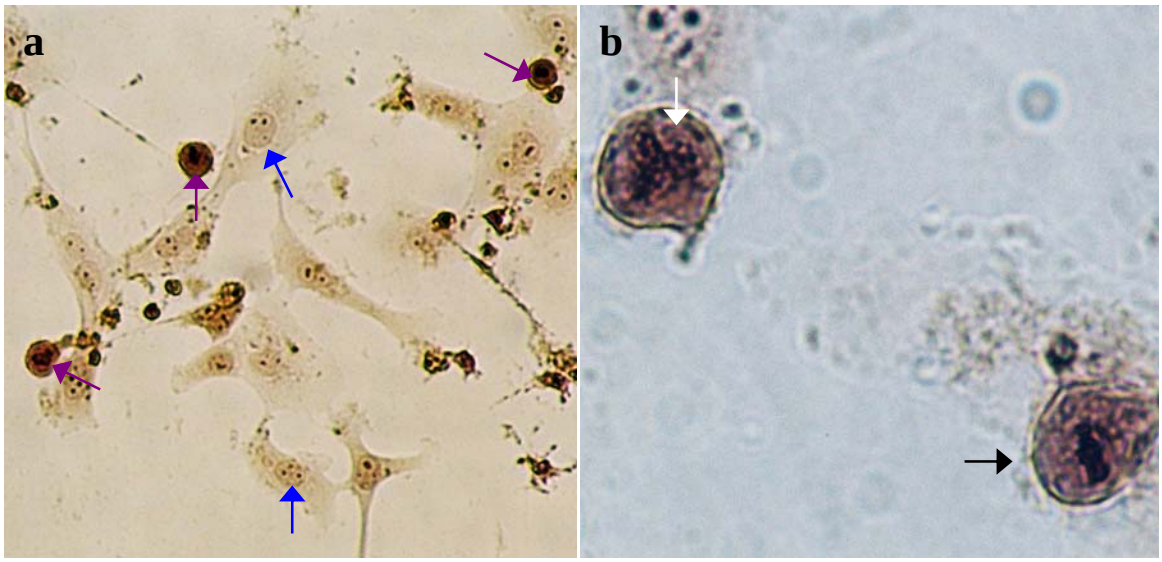

Figure 3.14: Haematoxylin and eosin staining of MCF-7 cells exposed to 10^{-6} M 2ME for 48 h at 100X (a) and 400X (b) magnification. Cell population is much less dense and many rounded cells with condensed contents are observed (purple arrows). Cells have irregular surfaces and triploid cells (white arrow) and cells blocked in metaphase are seen (black arrow). Blue arrows indicate interphase.

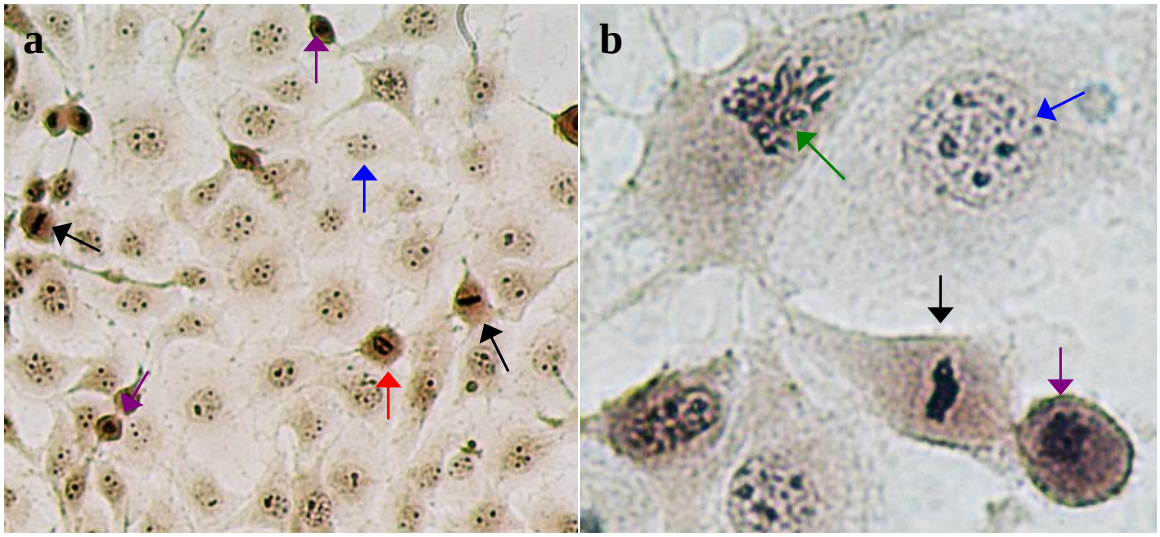

Figure 3.15: Haematoxylin and eosin staining of MCF-12A cells exposed to 10^{-8} M 2ME for 24 h at 100X (a) and 400X (b) magnification. Cell population is dense with many normal mitotic cells. Black arrows indicate normal metaphase, the red arrow normal anaphase and the green arrow indicate prophase. Some rounded cells with condensed contents are also observed (purple arrows). Blue arrows indicate interphase.

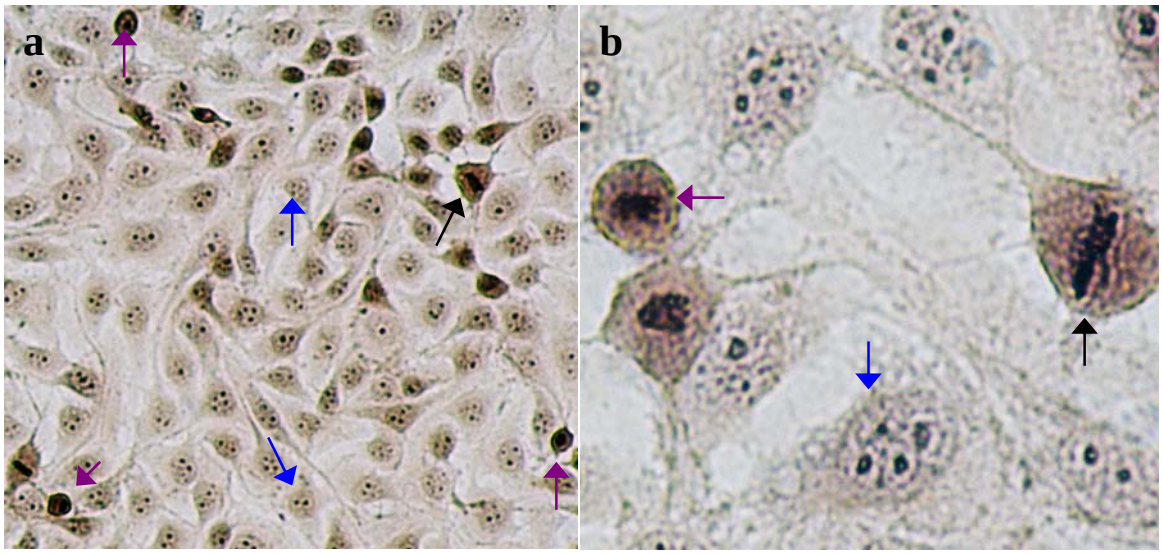

Figure 3.16: Haematoxylin and eosin staining of MCF-7 cells exposed to 10^{-8} M 2ME for 24 h at 100X (a) and 400X (b) magnification. Some normal metaphase cells (black arrows) are observed and rounded cells with condensed contents are also evident (purple arrows). Blue arrows indicate interphase.

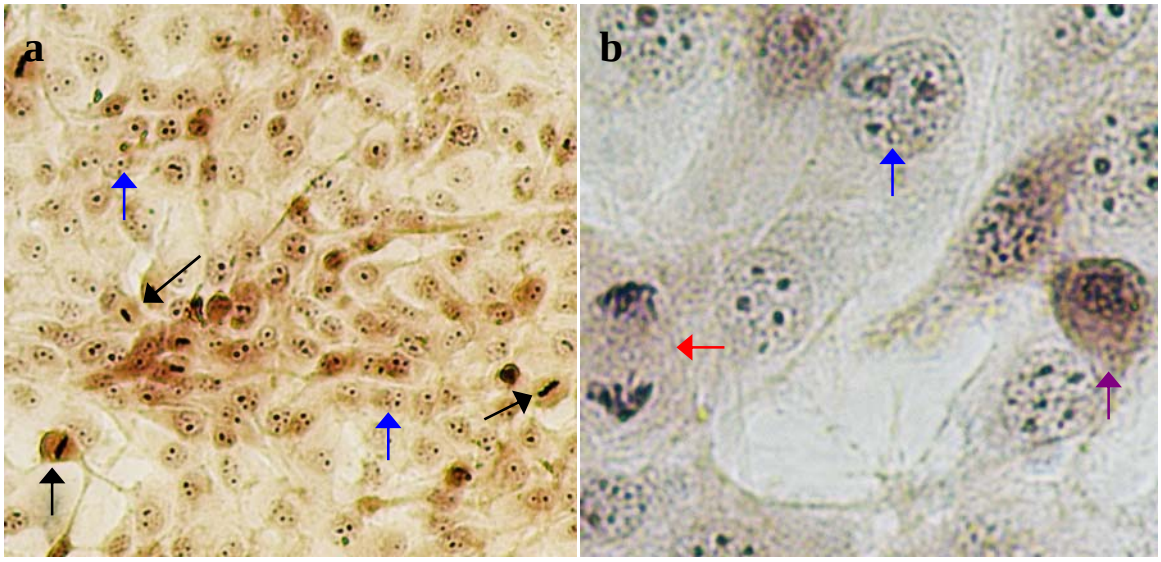

Figure 3.17: Haematoxylin and eosin staining of MCF-12A cells exposed to 10^{-8} M 2ME for 48 h at 100X (a) and 400X (b) magnification. Cell population is dense and normal mitotic cells are observed (Black arrows indicate normal metaphase cells and the red arrow normal anaphase). Few rounded cells with condensed contents (purple arrow) are observed. Blue arrows indicate interphase.

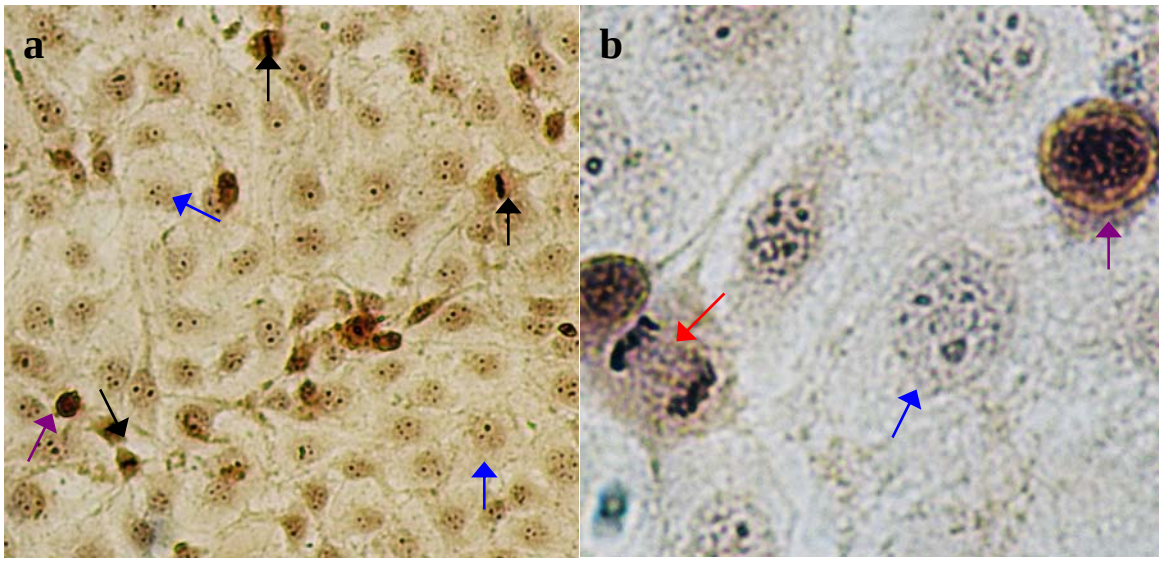

Figure 3.18: Haematoxylin and eosin staining of MCF-7 cells exposed to 10^{-8} M 2ME for 48 h at 100X (a) and 400X (b) magnification. Some normal mitotic cells (black arrows indicate metaphase and red arrow indicate anaphase) and rounded cells with condensed contents are observed (purple arrows). Blue arrows indicate interphase.

Table 3.1: Cells in prophase, metaphase, anaphase and telophase, cells blocked in metaphase, cells presenting with membrane blebbing and apoptotic cells expressed as percentage of a thousand cells counted after 24 h exposure to 2ME. Accurate values for 48 h exposure could not be obtained, because of low cell density and were excluded from the table.

	Prophase	Metaphase	Anaphase	Telophase	Metaphase block	Membrane blebbing	Apoptotic cells
MCF-7 cells							
DMSO control	3.7	1.6	0.5	0.8	0.2	0	0.6
2ME (10^{-8} M)	3.4	1.4	0.1	0.2	2.3	0.1	1.6
2ME(10^{-6} M)	1.1	0	0	0	22	8.2	9.3
MCF-12A cells							
DMSO control	2.6	1	0.3	0.3	0.2	0	0.1
2ME (10^{-8} M)	1.6	0.7	0.3	0.3	0.9	0	0.7
2ME(10^{-6} M)	2.3	0.4	0	0.1	1.4	0.1	3.7

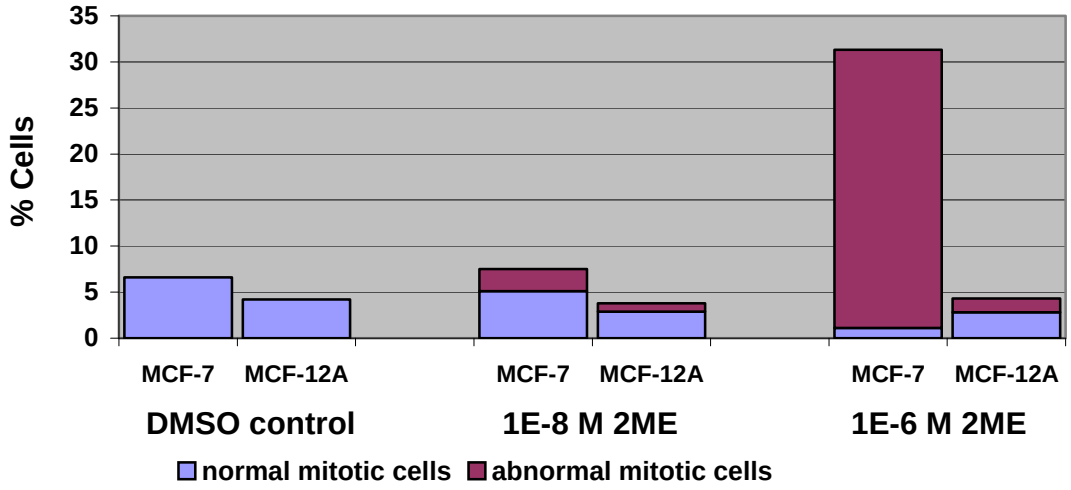

Figure 3.19: Mitotic indices for MCF-12A and MCF-7 cells after exposure to 2ME, expressed as the percentage of a thousand cells counted. Distinction was made between normal mitotic cells and abnormal mitotic cells, which included cells in metaphase block and cells presenting with membrane blebbing.

3.2.2 Immunofluorescent ß-tubulin detection

It was clear from the morphological studies that 2ME-treated cells, especially in the MCF-7 cell line, were blocked in metaphase and could not progress through the cell cycle. This observation was best illustrated after 24 h exposure to 10^{-6} M 2ME. Therefore, the effect of 2ME on spindle formation was investigated by making use of indirect immunofluorescence at the aforementioned exposure time and dose. MCF-12A and MCF-7 control cells that were not exposed to 2ME presented with normal spindles (Figure 3.20a and Figure 3.21a). The treated MCF-12A cell line also had normal spindles (Figure 3.20b), but the treated MCF-7 cells presented with multipolar spindles (Figure 3.21b).

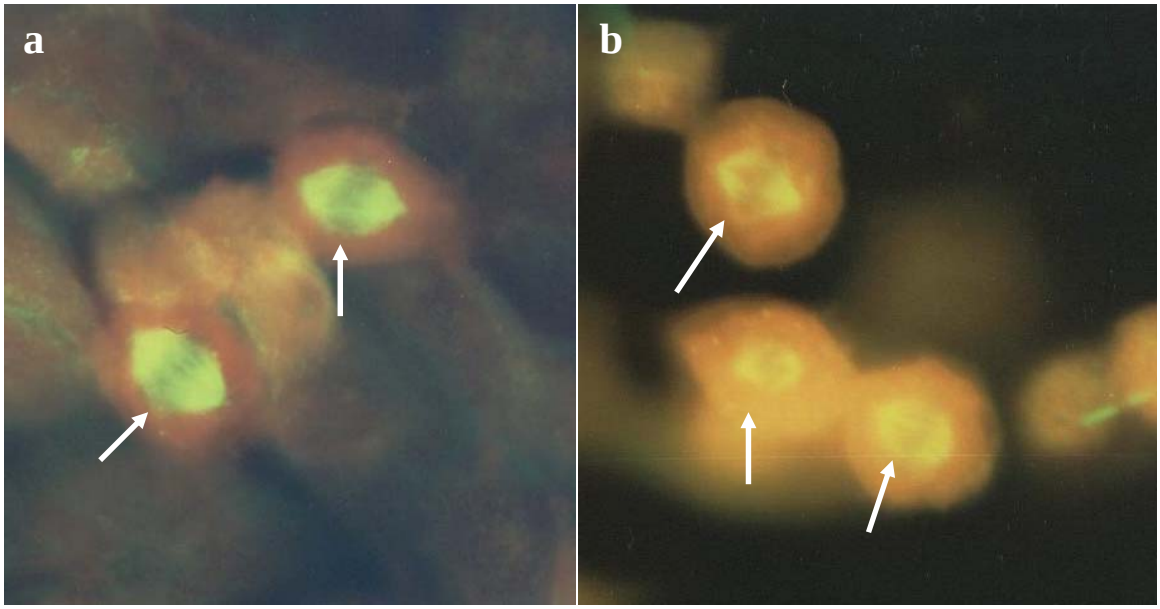

Figure 3.20: Detection of β-tubulin in non-tumorigenic MCF-12A cells (400X magnification). Control cells, exposed to 0.1 % DMSO (vehicle) (a) as well as cells exposed to 10^{-6} M 2ME (b) presented with normal spindle formation (white arrows).

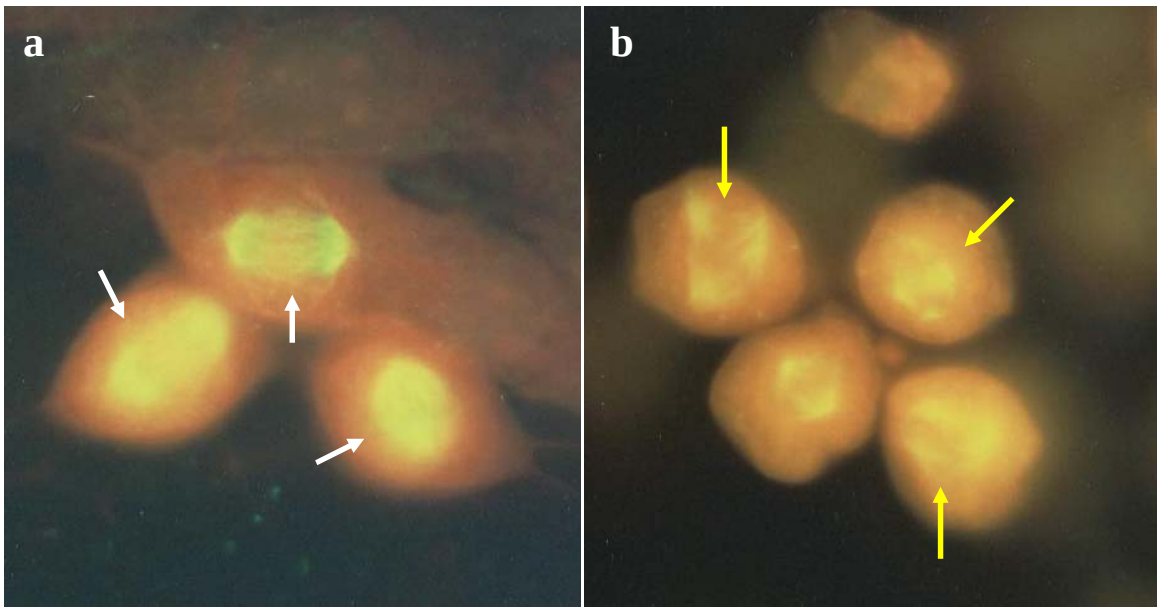

Figure 3.21: Detection of β-tubulin in tumorigenic MCF-7 cells (400X magnification). Control cells exposed to 0.1 % DMSO (vehicle) (a) presented with normal spindle formation (white arrows), but cells exposed to 10^{-6} M 2ME presented with multipolar spindles (yellow arrows), indicating abnormal spindle formation.

3.2.3 Immunocytochemistry – detection of estrogen receptors

The MCF-7 cell line is known to be ER-positive (13,29,114,133,174). However, some controversy exists about the ER-status of the MCF-12A cell line, for it has been reported as ER-positive (175) and as ER-negative (176) in the literature. Immunocytochemistry was used to determine the ER-status of the MCF-12A cell line. The MCF-7 cells were used as a positive control and the ER-negative MDA-MB-231 cell line (18,175), as a negative control. From the results it is clear that the MCF-12A cell line used in this study is ER-negative (Figure 3.22).

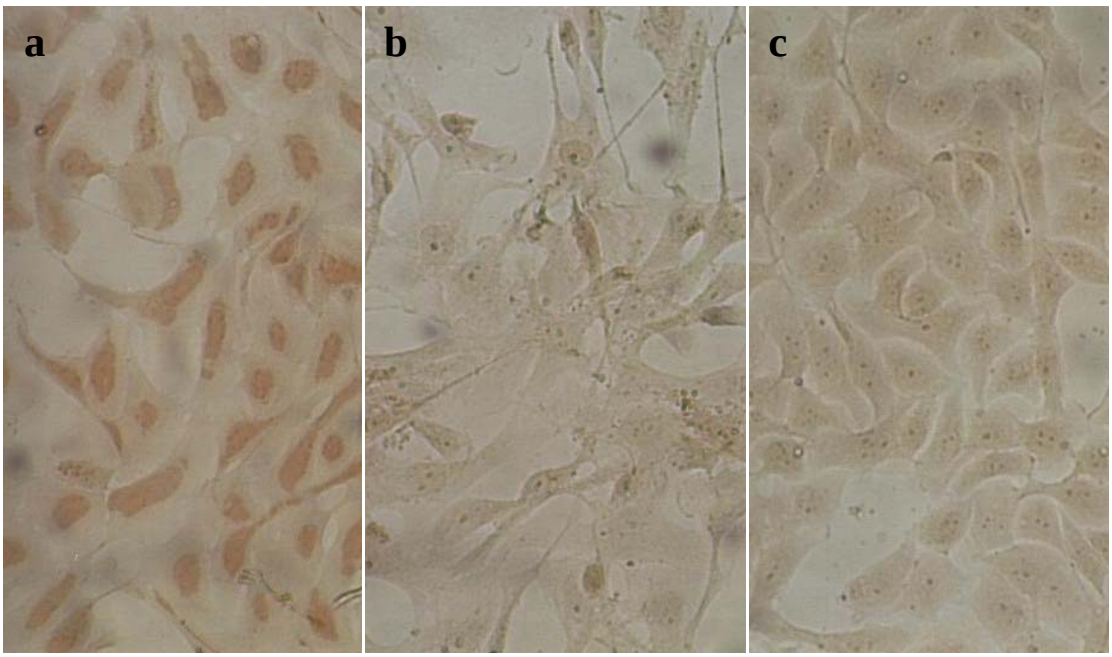

Figure 3.22: Detection of estrogen-receptor status in MCF-12A cells (c). MDA-MB-231 cells were used as negative control (a) and MCF-7 cells as positive control (b) (100X magnification).

3.3 Cell cycle studies

3.3.1 Cell cycle length determination

The effect of 2ME treatment on the length of the cell cycle and the mitotic peak in the MCF-12A and the MCF-7 cell line was determined by monitoring synchronized cells over a period of 24 h at 2 h intervals. The point where cells were released from the early S-phase block was considered as time zero (0 h) and unsynchronized and synchronized slides served as controls at 0 h. Mitotic indices were calculated as described in section 3.2.1 to determine the hour at which peak mitosis occurs.

The mitotic index of the synchronized cells was significantly less than in the unsynchronized cells at 0 h, as illustrated in Figure 3.23 and Figure 3.24. From these figures it can also be seen that 2ME treatment had no effect on the length of the cell cycle in either of the cell lines. In the MCF-12A cell line peak mitosis occurred at 20 h for both the exposed and the unexposed cells (Figure 3.23) and in the MCF-7 cell line peak mitosis was at 13 h (Figure 3.24). After peak mitosis was reached in the 2ME-treated MCF-7 cell line, the percentage of cells in mitosis remained high, indicating that the cells were blocked in mitosis (Figure 3.24).

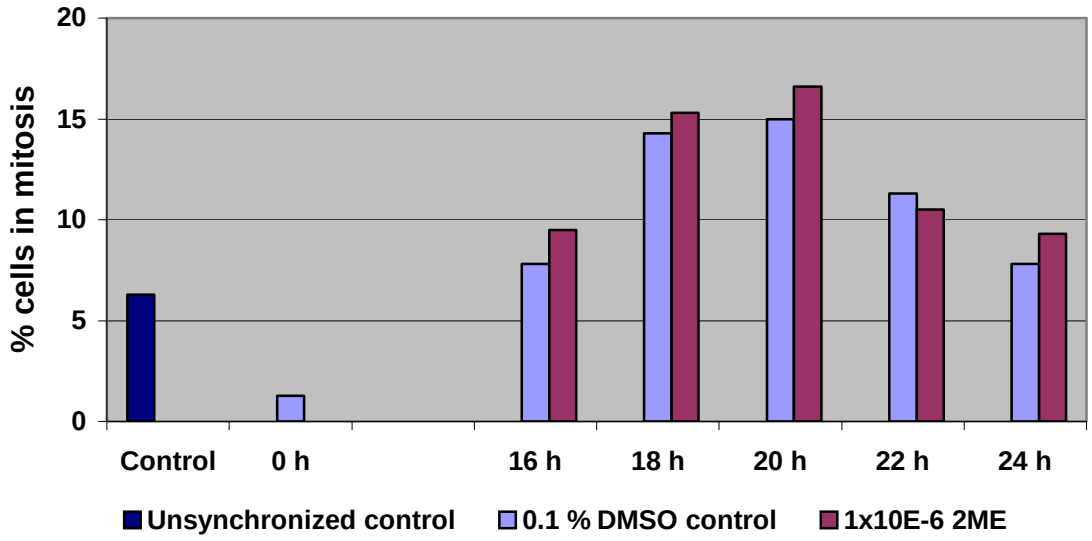

Figure 3.23: Percentage of synchronized MCF-12A cells in mitosis at 2h intervals. Peak amount of cells in mitosis occurred at 20h for exposed and unexposed cells.

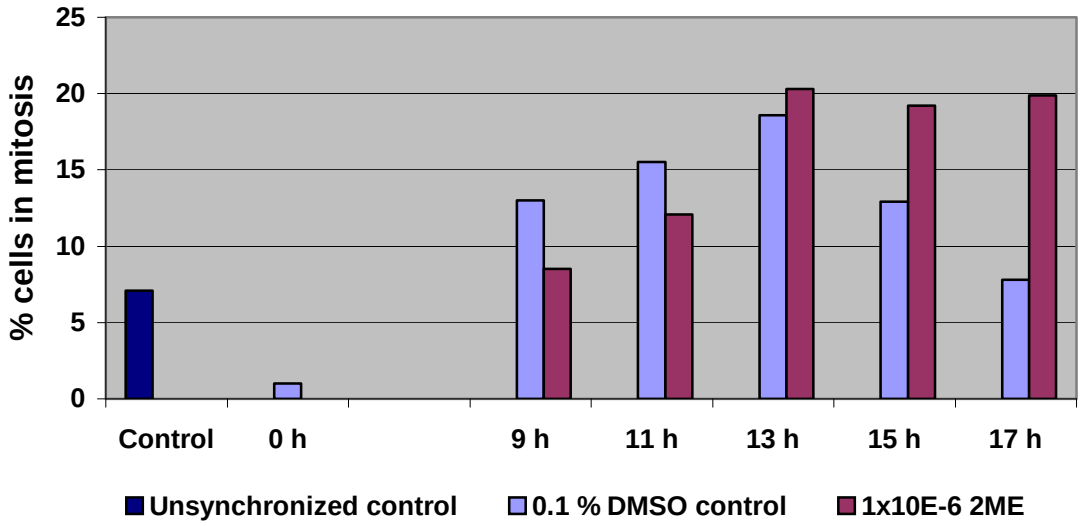

Figure 3.24: Percentage of synchronized MCF-7 cells in mitosis at 2h intervals. Peak amount of cells in mitosis occurred at 13 h for exposed and unexposed cells. Mitotic indices for exposed MCF-7 cells remained high.

3.3.2 Cell cycle checkpoint regulatory molecules – checkpoint kinase assay

The CycLex Checkpoint Kinase Assay was used to determine the effects of 2ME treatment on the activities of checkpoint kinases. A phospho-specific monoclonal antibody used in the assay kit recognizes the phospho-serine 216 residue in Cdc25C, which is phosphorylated by checkpoint kinases. No significant difference in the activity of kinases that phosphorylate Cdc25C between the control cells and cells exposed to 1 x 10^{-6} 2ME was detected in this assay (Figure 3.25).

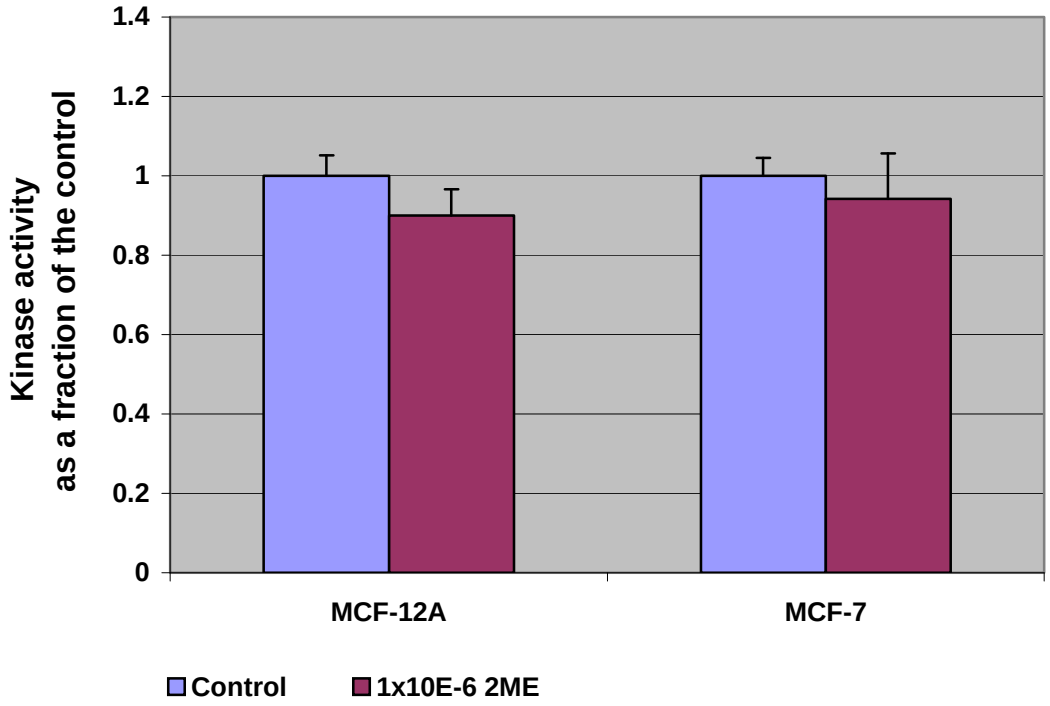

Figure 3.25: The effect of 2ME treatment on checkpoint kinase activity in MCF-12A and MCF-7 cells. The effect was not statistically significant.

3.3.3 Cell cycle checkpoint regulatory molecules – Cdc2 kinase assay

The effect of 2ME treatment on Cdc2 kinase activity was determined by making use of the MESACUP Cdc2 Kinase Assay Kit from MBL. The kit is based on enzyme-linked immunosorbent assay (ELISA) that utilizes a synthetic peptide as a substrate for Cdc2 kinase and a monoclonal antibody recognizing the phosphorylated form of the peptide substrate. The Wilcoxon two-sample rank test (nonparametric test) revealed that 2ME significantly enhanced Cdc2 kinase activity and to a significantly greater extent in the MCF-7 cells compared to the MCF-12A cells (Figure 3.26). A one-sided *P*-value of 0.025 was obtained, which means that the difference is significant at the 5 % level of significance.

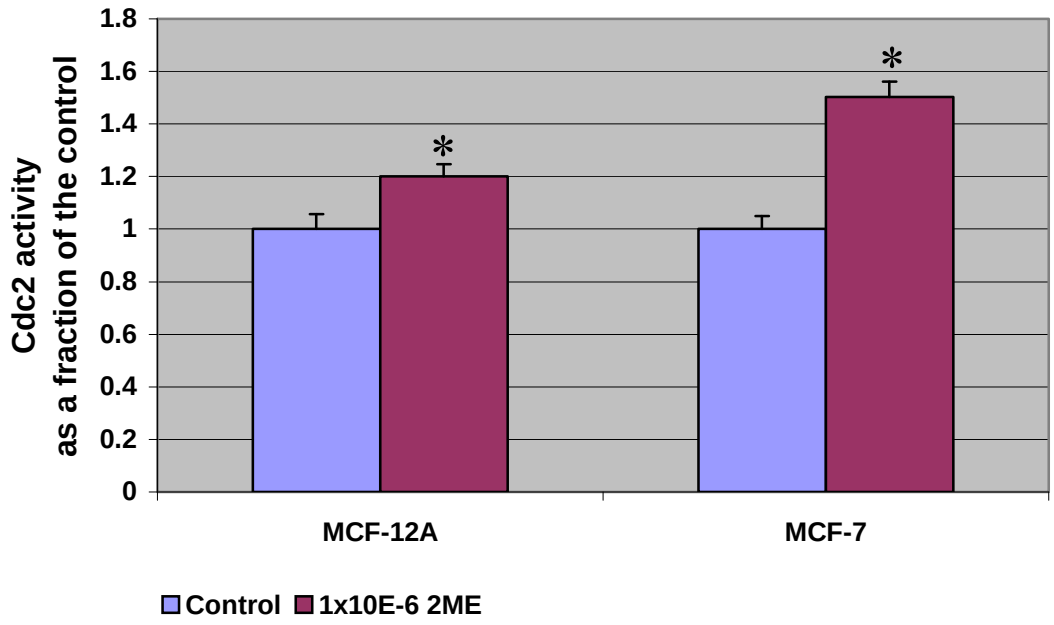

Figure 3.26: The effect of 2ME treatment on Cdc2 kinase activity in MCF-12A and MCF-7 cells. * $P < 0.05$

Chapter 4

Discussion and conclusions

"All substances are poisons; there is none which is not a poison.
The right dose differentiates a poison and a remedy."
Paracelsus (1493-1541)

The purpose of this study was to investigate and compare the possible differential action(s) of 2ME in non-tumorigenic MCF-12A and tumorigenic MCF-7 cell lines by investigating the effects of 2ME on cell growth, morphology and cell cycle regulatory components.

It is clear from the cell growth studies (employing crystal violet as DNA dye, as well as the MTT assay) that 2ME inhibits cell growth in both the tumorigenic MCF-7 and the non-tumorigenic MCF-12A cell line. Liu *et al.* reported that the crystal violet staining method was not only rather convenient and cost far less, but it also yielded highly reproducible results compared to the MTT assay (133). Furthermore, they found that the MTT assay had larger interassay variations than the crystal violet method and failed to produce reliable results when the cell density was too high (133). However, in this study the results from the MTT assay confirmed the results found with the crystal violet staining method. Both assays revealed a dose-dependent growth inhibition in the MCF-12A and MCF-7 cells after 2ME exposure. These results are consistent with the findings of Cushman *et al.*, who reported that 2ME was toxic to dividing cells of 55 different tumor cell lines (102). Several *in vivo* studies also confirmed the antiproliferative activities of 2ME (18,28).

It is evident from this study that exposure to 2ME inhibited cell growth from much lower concentrations and to a greater extend in the tumorigenic MCF-7 cell line than in the normal MCF-12A cell line. Cell growth was significantly reduced in the MCF-7 cells from as low as 10^{-9} M 2ME, whereas in the MCF-12A cells, growth was significantly inhibited only from 10^{-7} M 2ME. Although there was a greater reduction in cell numbers in the tumorigenic MCF-7 cells when compared to the non-

tumorigenic MCF-12A's in the crystal violet staining method, the GI_{50} was within the same concentration range for the two cell lines. This was also true for the TGI. However, with the MTT assay, 50 % growth inhibition and a cytostatic effect is only seen at a ten times higher concentrations in the normal cell line than in the tumorigenic cell line. At 10^{-6} M 2ME the MTT assay revealed that 2ME had a cytostatic effect on the MCF-7 cells, whereas at the same concentration it only had a 50 % growth inhibitory effect on the MCF-12A cells. This differential inhibition was not as substantial in the assay employing crystal violet, but could be explained by the fact that the crystal violet staining method only measures cell numbers (171,172), while the MTT assay measures the metabolic activity of viable cells (133,173). Thus, even though cell numbers were greatly reduced in both cell lines, the MCF-12A cells were metabolically more active than the tumorigenic MCF-7 cells. For both assays and cell lines a cytotoxic effect was seen in the range of 10^{-5} M 2ME exposure. The cell growth studies emphasize the importance of selecting the best concentration for therapeutic application, where 2ME has a maximum inhibitory effect on tumorigenic, but a minimal effect on normal cells. At 10^{-6} M 2ME showed the greatest selectivity for the tumorigenic MCF-7 cells, and therefore, this concentration was chosen for further investigation.

Since serum levels of 2ME achieved after treatment with a dosage of 1 mg were in the range of 100 to 600 nM (10^{-7} to 6 x 10^{-7} M) (13) and preliminary experiments with a new 2ME formulation demonstrated plasma concentrations up to 10 µM (10^{-5} M) (EntreMed, data on file) (13), concentrations used in this study were relevant to plasma concentrations of 2ME achieved in a clinical setting. Furthermore, the concentration that showed the greatest selectivity for the tumorigenic cell line in this study (10^{-6} M) would be pharmacologically achievable when administered to patients. This observation encourages further investigation.

Morphological studies were done to investigate possible differential effects of 2ME on morphological characteristics between the normal and tumorigenic cell line. The abnormal metaphase cells, membrane blebbing and apoptotic cells observed in the treated MCF-7 cells were not as prominent in the MCF-12A's, especially at 10^{-6} M. These morphological observations are consistent with the inhibition of cell growth seen after 2ME treatment. In the MCF-7 cells, the morphological effects of 2ME were

much more prominent at 10^{-6} M than at 10^{-8} M, consistent with the greater inhibition in cell growth at 10^{-6} M compared to 10^{-8} M. In the MCF-12A cells a similar relationship was seen between morphological effects and cell growth at 10^{-8} M. However, the metabolic activity and morphological observations did not reflect the reduction in cell numbers at 10^{-6} M in the MCF-12A cells. Although cell numbers were also greatly reduced, metabolically and morphologically the cells were less affected than the transformed cells. Therefore, the mechanism of growth inhibition in the normal cell line is still unclear. The possibility should be investigated that the normal cells would be able to recover and proliferate after 2ME treatment is ceased. The morphological studies support the hypothesis that differential mechanism of growth inhibition exists between the two cell lines.

Wang *et al.* demonstrated that an accumulation of cells with condensed chromosomes is characteristic of mitotic block (84), as was seen in the treated MCF-7 cells in this study. Similarly, Atalla *et al.* reported that Jurkat cells were blocked in metaphase after 2ME treatment (11). In contrast, however, Golebiewska *et al.* found that osteosarcoma cells exposed to 1 µM 2ME were arrested in G_1 (177). These diverse results also support the hypothesis that the action mechanisms of 2ME are dependent on cell type.

Although treated MCF-7 cells had the highest percentage of dividing cells, most of these cells were abnormal and blocked in metaphase. In other studies mitotic arrest was followed by the induction of apoptosis (159,177). This could explain the increase in apoptotic cells along with the increase in cells blocked in metaphase with condensed chromosomes in treated MCF-7 cells. In contrast, 2ME had only minimal effects on the non-tumorigenic MCF-12A cell line. These results suggest that 2ME might have a differential effect on spindle formation between the two cell lines.

Fluorescence microscopy confirmed that 2ME disrupted spindle formation and induced multipolar spindles in the MCF-7 cells. Likewise, Seegers *et al.* (29) have shown that estradiol and its metabolites, 2-hydroxy-estradiol and 2ME, were cytotoxic at high micromolar concentrations and caused mitotic arrest due to abnormal and fragmented polar formations as well as disorientated microtubule arrangement in the dividing cells (29,43). In contrast, in this study 2ME treatment did not disrupt spindle

formation in the MCF-12A cells. Therefore it is clear that 2ME has a differential effect on spindle formation between the tumorigenic and the normal breast cell line.

The MCF-7 cell line is known to be ER-positive (13,133,174) and here it was shown that the MCF-12A cell line used for this study is ER-negative. However, the differential mechanisms of growth inhibition and apoptosis induction between the two cell lines is very unlikely due to their differences in estrogen-receptor status, for it was proven that 2ME has a very low affinity for the estrogen receptor (18,24,120,131) and was shown to inhibit proliferation and induce apoptosis in estrogen-receptor negative as well as estrogen-receptor positive cancer cell lines (18).

From cell cycle length determination studies it can be seen that the MCF-12A cells have a much longer cell cycle than the MCF-7 cells. Originally it was thought that cancerous cells are more susceptible to drugs that disturb the cell cycle, because they replicate more quickly and more frequently than normal cells (163). However, there are many normal cell populations that replicate at least as rapidly as cancerous cells and some slow-growing cancer cells are more sensitive to conventional anti-cancer treatments than fast-growing cells (163). Therefore, although MCF-12A cells take longer to divide (and therefore longer before they are affected by disrupters of the cell cycle) than MCF-7 cells, this statement is not sufficient to explain the difference in growth inhibitory and morphological effects seen after 2ME treatment between the two cell lines.

In this study there was no significant alterations in the phosphorylation of Cdc25C after 2ME treatment, but Cdc2 activity was increased and to a greater extend in the MCF-7 cells compared to the MCF-12A's. In contrast, Kumar *et al.* reported phosphorylation of Cdc25C without any significant alterations in the expression of Wee1 kinase, cyclin B1 or Cdc2 after 2ME treatment in medulloblastoma cells (53). These contrasting results give further support to the hypothesis that the action mechanisms of 2ME are dependent on cell type.

Central to the regulation of mitosis in eukaryotes is the MPF, consisting of a Cdc2 and a cyclin B subunit (33,38,39,55,58,59,178). Activation of Cdc2 is necessary for the initiation of mitosis, whereas inactivation of Cdc2 is required for mitotic exit (178).

Cdc2 kinase activity is responsible for chromosome condensation, the cytoplasmic reorganization to convert the interphase microtubule array to the mitotic spindle (41) and nuclear envelope breakdown (41,45,59). Continued Cdc2 activity can maintain the cell in the mitotic state for a prolonged period until certain conditions are met for mitotic exit (178). Furthermore, Gallant *et al.* showed that expression of a non-destructable cyclin B2 protein caused HeLa cells to arrest in a pseudomitotic state characterized by condensed chromatin, a disassembled nuclear envelope, and, in a high proportion of cells, multiple mitotic spindles (61). Cdc2 is localized to spindle microtubules and kinetochores (178), and both Cdc2 and cyclin B have also been identified at the level of the centrosome (60,61), suggesting a role for these proteins in the regulation of mitotic spindle formation (62). Therefore, the increased Cdc2 activity in the treated MCF-7 cells is consistent with the morphological indicators of mitotic arrest and disrupted mitotic spindle formation observed in these cells. In contrast to the MCF-7 cells, Cdc2 kinase activity in the non-tumorigenic MCF-12A cell line was only slightly elevated. This is consistent with the normal spindle formation observed in these cells.

It is suggested that following 2ME treatment, signals initiated at kinetochores of disrupted spindles cause the MCC to bind to and inhibit the APC (89). The signal from the kinetochore can either be Mad2, that has been shown to localize selectively to unattached kinetochores, or a kinase cascade that is initiated at the kinetochore (80). Destruction of both cyclin B and securin by the APC is necessary to induce the segregation of chromatids to opposite poles (74). Thus, cyclin B would not be ubiquitinated and degraded when the APC is inhibited and Cdc2 kinase, which is a complex of cyclin B and Cdc2, will remain active (179,180). This will lead to activation of the spindle checkpoint and mitotic arrest (74). Prolonged mitotic arrest may result in apoptosis. Several studies also reported an increase in Cdc2 kinase activity observed during apoptosis (149,150,151). This is consistent with the increased amount of apoptotic cells observed after 2ME treatment in the tumorigenic MCF-7 cell line. In contrast to the MCF-7 cells, Cdc2 kinase activity in the non-tumorigenic MCF-12A cell line was only slightly elevated, and could explain why the increase in apoptotic cells was less pronounced in the treated normal cells.

A limiting factor in human cancer therapy is its toxicity to normal tissues (52). Thus, the ultimate cancer therapy would destroy cancer cells while sparing normal tissues (52). Although it is clear from this study that the tumorigenic MCF-7 cells are more susceptible to 2ME treatment than the normal MCF-12A cells, the basis for selectivity is not yet clear. To understand why tumorigenic breast cancer cells are more susceptible to 2ME treatment than the normal breast cells, knowledge on how tumor cells differ from normal cells are essential (162). Based on their studies, Chen *et al.* stated that normal cells and cancer cells may have markedly different requirements for certain proteins that perform otherwise similar biochemical functions in both cell types (181). Hartwell *et al.* also suggested that there are differences between cell cycle control in normal and cancer cells (52). Based on the results from the cell cycle kinase assays in this study, the differential effects of 2ME on the two cell lines may indeed be due to differences in cell cycle control and should be further investigated, *e.g.* the activity of Mad 1, Mad2, Bub1 and p38 involved in the spindle checkpoint. Ran-GTP has also been implicated in the formation of multipolar spindles and the effect of 2ME treatment on Ran-GTP activity should also be investigated.

In conclusion, 2ME showed potential for the treatment of breast cancer. Exposure to 2ME disrupted mitotic spindle formation and enhanced Cdc2 kinase activity that lead to persistence of the spindle checkpoint and thus prolonged metaphase arrest and resulted in the induction of apoptosis. The tumorigenic MCF-7 cells were especially sensitive to 2ME treatment compared to the normal MCF-12A cells. Therefore, selecting the concentration of 2ME that has maximum inhibitory effect on tumorigenic, but minimal effect on normal cells is crucial in its possible application as anti-tumor agent. Although, in general, 2ME seems to target tumorigenic cells, its action mechanisms are dependent on cell type and the basis for selectivity and mechanisms of action are not yet fully understood. Further research concerning the differential action mechanisms of 2ME is essential to create a better understanding regarding the treatment of cancer and may possibly contribute to the development and/or improvement of novel chemotherapeutic agents.

References

1 Parkin DM, Bray FI, Devesa SS. Cancer burden in the year 2000. The global picture. Eur J Cancer 2001;37:S4-66.

2 Russo J, Hu Y, Yang X, Russo IH. Developmental, cellular, and molecular basis of human breast cancer. J Natl Cancer Inst Monogr 2000;27:17-26.

3 Brody JG, Rudel RA. Environmental pollutants and breast cancer. Environ Health Perspect 2003;111(8):1007-19.

4 Bu S, Blaukat A, Fu X, Heldin N-E, Landström M. Mechanisms for 2-methoxyestradiol-induced apoptosis of prostate cancer cells. FEBS 2002;531:141-51.

5 Carrol KK. Obesity as a risk factor for certain types of cancer. Lipids 1998;33(11):1055-9.

6 Aizu-Yakota E, Susaki A, Sato Y. Natural estrogens induce modulation of microtubules in Chinese hamster V79 cells in culture. Cancer Res 1995;55:1863-8.

7 Clemons M, Goss P. Estrogen and the risk of breast cancer. N Engl J Med 2001;344:276-83.

8 Yager JD. Chapter 3: Endogenous estrogens as carcinogens through metabolic activation. J Natl Cancer Inst Monogr 2000;27:67-73.

9 James VHT, Reed MJ, Lai LC. Regulation of estrogen concentrations in human breast tissues. Ann NY Acad Sci 1990;595:227-35.

10 Pathak DR, Osuch JR, He J. Breast carcinoma etiology: current knowledge and new insights into the effects of reproductive and hormonal risk factors in black and white populations. Cancer 2000;88:1230-8.

11 Atalla H, Mäkelä TP, Adlercreutz H, Anderson LC. 2-Methoxyestradiol arrests cells in mitosis without depolymerising tubulin. Biochem Biophys Res Commun 1996;228:467-73.

12 Purdie DW. Consequences of long-term hormone replacement therapy. British Medical Bulletin 2000;56:809-23.

13 Mueck AO, Seeger H, Huober J. Chemotherapy of breast cancer-additive anticancerogenic effects by 2-methoxyestradiol? Life Sci 2004;75:1205-10.

14 MacMahon B. A biological framework for the risk factors for breast cancer. Adv Oncol 1994;10:3-9.

15 Davidson NE. Environmental estrogens and breast cancer risk. Curr Opin Oncol 1998;10:475-8.

16 McPherson K, Steel CM, Dixon JM. ABC of breast disease: breast cancer – epidemiology, risk factors and genetics. BMJ 2000;321:624-8.

17 Vorobiof DA, Sitas F, Vorobiof G. Breast cancer incidence in South Africa. J Clin Oncol 2001;19:125S-7.

18 Lakhani NJ, Sarkar MA, Venitz J, Figg WD. 2-Methoxyestradiol, a promising anticancer agent. Pharmacotherapy 2003;23(2):165-72.

19 Labat ML. Possible retroviral etiology of human breast cancer. Biomed & Pharmacother 1998;52:6-12.

20 Kuiper GGJM, Carlson B, Grandien K, Enmark E, Häggblad J, Nilsson S, *et al*. Comparison of the ligand binding specificity and transcript tissue distribution of estrogen receptors α and ß. Endocrinol 1997;138:863-70.

21 Zhu BT, Conney AH. Is 2-methoxyestradiol an endogenous estrogen matabolite that inhibits mammary carcinogenesis? Cancer Res 1998;58:2269-77.

22 Liehr JG, Ulubelen AA, Strobel HW. Cytochrome P-450 mediated redox cycling of estrogens. J Biol Chem 1986;261:16865-70.

23 Liehr JG, Roy D. Free radical generation by redox cyclin of estrogens. Free Radic Biol Med 1990;8:415-23.

24 Spicer LJ, Walega MA, Hammond JM. Metabolism of [^{3}H] 2-hydroxyestradiol by cultured porcine granulose cells: evidence for the presence of a catechol-*O*-methyltransferase pathway and a direct stimulatory effect of 2-methoxyestradiol on progesterone production. Biol Repr 1987;36:562-71.

25 Ball P, Knuppen R. Catecholoestrogens (2- and 4-hydroxy-oestrogens): chemistry, biogenesis, metabolism, occurrence and physiological significance. Acta Endocr Copenh 1980;93:1-127.

26 Fishman J. Biological action of catechol oestrogens. J Endocr 1981;89:59P-65.

27 Trendelenburg U. The metabolizing systems involved in the inactivation of catecholamines. Naunyn-Schmiedenberg's Arch Pharmacol 1986;332:201-7.

28 Fotsis T, Zhang Y, Pepper MS, Adlercreutz H, Montesano R, Nawroth PP, *et al*. The endogenous oestrogen metabolite 2-methoxyoestradiol inhibits angiogenesis and suppresses tumour growth. Nature 1994;368:237-9.

29 Seegers JC, Aveling M-L, Van Aswegen CH, Cross M, Koch F, Joubert WS. The cytotoxic effects of estradiol-17β, catecholestradiols and methoxyestradiols on dividing MCF-7 and HeLa cells. J Steroid Biochem 1989;32:797-809.

30 Lottering M-L, Haag M, Seegers JC. Effects of 17ß-estradiol metabolites of cell cycle evens in MCF-7 cells. Cancer Res 1992;52:5926-32.

31 D'Amato RJ, Lin CM, Flynn E, Folkman J, Hamel E. 2-Methoxyestradiol, an endogenous mammalian metabolite, inhibits tubulin polymerization by interacting at the colchicines site. Proc Natl Acad Sci USA 1994;91:3964-8.

32 Alberts B, Bray D, Johnson A, Lewis J, Raff M, Roberts K, *et al*. Cell cycle control and cell death. In: Essential cell biology. New York: Garland Publishing; 1998. p. 571-91.

33 Nigg EA. Cyclin-dependent protein kinases: key regulators of the eukaryotic cell cycle. BioEssays 1995;17(6):471-80.

34 Liu F, Rothblum-Oviatt C, Ryan CE, Piwnica-Worms H. Overproduction of human Myt1 kinase induces a G2 cell cycle delay by interfering with the intracellular trafficking of Cdc2-cyclin B1 complexes. Mol Cell Biol 1999;19:5113-23.

35 Schafer KA. The cell cycle: a review. Vet Pathol 1998;35:461-78.

36 Hartwell LH, Weinert TA. Checkpoints: controls that ensure the order of cell cycle events. Science 1989;246:629-34.

37 MacCarthy-Morrogh L, Townsend PA, Purohit A, Hejaz HAM, Potter BVL, Reed MJ, *et al*. Differential effects of estrone and estrone-3-O-sulfamate derivatives on mitotic arrest, apoptosis, and microtubule assembly in human breast cancer cells. Cancer Res 2000;60:5441-50.

38 Luch A. Cell cycle control and cell division: implications for chemically induced carcinogenesis. ChemBioChem 2002;3:506-16.

39 Hagan IM, Bridge AJ, Morphew M, Bartlett R. Cell cycle control and the mitotic spindle. Br J Cancer 1999;80:6-13.

40 Clark MS, Wall WJ. Nuclear division. In: Chromosomes: the complex code. London: Chapman & Hall; 1996. p. 94-132.

41 Walczak CE, Mitchison TJ. Kinesin-related proteins at mitotic spindle poles: function and regulation. Cell 1996;85:943-6.

42 Miyamoto DT, Perlman ZE, Mitchison TJ, Shirasu-Hiza M. Dynamics of the mitotic spidle – potential therapeutic targets. Prog Cell Cycle Res 2003;5:349-60.

43 Ochi T, Oda T. Structure-effect relationship in the induction of mitotic phase-specific abnormality of centrosome integrity and multipolar spindles by steroidal estrogens and their derivatives in cultured mammalian cells. J Steroid Biochem Molec Biol 2001;78:113-22.

44 Sorger PK, Dobles M, Tournebize R, Hyman AA. Coupling cell division and cell death to microtubule dynamics. Curr Opin Cell Biol 1997;9:807-14.

45 Hyman AA, Karsenti E. Morphogenetic properties of microtubules and mitotic spindle assembly. Cell 1996;84:401-10.

46 McIntosh JR. Spindle fiber action and chromosome movement. Ann Rev Cell Biol 1991;7:403-26.

47 Drewes G, Ebneth A, Mandelkow E-M. MAPs, MARKs and microtubule dynamics. TIBS 1998;23:307-11.

48 Rieder CL, Salmon ED. Motile kinetochores and polar ejection forces dictate chromosome position on the vertebrate mitotic spindle. J Cell Biol 1994;124:223-33.

49 Burke DJ. Complexity in the spindle checkpoint. Curr Opin Genet Dev 2000;10:26-31.

50 Canman JC, Sharma N, Straight A, Shannon KB, Fang G, Salmon ED. Anaphase onset does not require the microtubule-dependent depletion of kinetochore and centromere-binding proteins. J Cell Sci 2002;115:3787-95.

51 Lundberg AS, Weinberg RA. Control of cell cycle and apoptosis. Eur J Cancer 1999;35:531-9.

52 Hartwell LH, Kastan MB. Cell cycle control and cancer. Science 1994;266:1821-8.

53 Kumar AP, Garcia GE, Orsborn J, Levin VA, Slaga TJ. 2-Methoxyestradiol interferes with NFκB transcriptional activity in primitive neuroectodermal brain tumors: implications for management. Carcinogenesis 2003;24(2):209-16.

54 Wells WAE. The spindle-assembly checkpoint: aiming for a perfect mitosis, every time. Trends Cell Biol 1996;6:228-34.

55 Shi L, Chen G, He D, Bosc DG, Litchfield DW, Greenberg AH. Granzyme B induces apoptosis and cyclin A-associated cyclin-dependent kinase activity in all stages of the cell cycle. J Immunol 1996;157:2381-5.

56 Harper JW, Burton JL, Solomon MJ. The anaphase-promoting complex: it's not just for mitosis any more. Genes Dev 2002;16:2179-206.

57 Peng C-Y, Graves PR, Thoma RS, Wu Z, Shaw AS, Piwnica-Worms H. Mitotic and G2 checkpoint control: regulation of 14-3-3 protein binding by phosphorylation of Cdc25C on serine-216. Science 1997;277:1501-5.

58 Gu L, Zheng H, Murray SA, Ying H, Xiao Z-X J. Deregulation of Cdc2 kinase induces caspase-3 activation and apoptosis. Biochem Biophys Res Commun 2003;302:384-91.

59 Nurse P. Universal control mechanism regulating onset of M phase. Nature 1990;344:503-8.

60 Bailly E, Doree M, Nurse P, Bornens M. p34cdc2 is located in both nucleus and cytoplasm; part is centrosomally associated at G2/M and enters vesicles at anaphase. EMBO J 1989;8:3985-95.

61 Gallant P, Nigg EA. Cyclin B2 undergoes cell cycle-dependent nuclear translocation and, when expressed as a non-destructible mutant, causes mitotic arrest in HeLa cells. J Cell Biol 1992;117:213-24.

62 Baldin V, Ducommun B. Subcellular localisation of human wee1 kinase is regulated during the cell cycle. J Cell Sci 1995;108:2425-32.

63 Graves PR, Yu L, Schwarz JK, Gales J, Sausville EA, O'Connor PM, *et al*. The Chk1 protein kinase and the Cdc25C regulatory pathways are targets of the anticancer agent UCN-01. J Biol Chem 2000;275(8):5600-5.

64 Russell P. Checkpoints on the road to mitosis. TIBS 1998;23:399-402.

65 Mikhailov A, Cole RW, Rieder CL. DNA damage during mitosis in human cells delays the metaphase/anaphase transition via the spindle-assembly checkpoint. Curr Biol 2002;12:1797-806.

66 Matsuoka S, Huang M, Elledge SJ. Linkage of ATM to cell cycle regulation by the Chk2 protein kinase. Science 1998;282:1893-7.

67 Gautier J, Solomon MJ, Booher RN, Bazan JF, Kirschner MW. Cdc25 is a specific tyrosine phosphatase that directly activates $p34^{cdc2}$. Cell 1991;67:197-211.

68 Strausfeld U, Labbé JC, Fesquet D, Cavadore JC, Picard A, Sadhu K, *et al*. Dephosphorylation and activation of a $p34^{cdc2}$/cyclin B complex *in vitro* by human CDC25 protein. Nature 1991;351:242-5.

69 Yaffe MB, Rittinger K, Volinia S, Caron PR, Aitken A, Leffers H, *et al*. The structural basis for 14-3-3: phosphopeptide binding specificity. Cell 1997;91:961-71.

70 Passmore LA, McCormack EA, Au SWN, Paul A, Willison KR, Harper JW, *et al*. Doc1 mediates the activity of the anaphase-promoting complex by contributing to substrate recognition. EMBO J 2003;22:786-96.

71 Yamanaka A, Hatakeyama S, Kominami K, Kitagawa M, Matsumoto M, Nakayama K. Cell cycle-dependent expression of mammalian E2-C regulated by the anaphase-promoting complex/cyclosome. Mol Biol Cell 2000;11:2821-31.

72 Chen J, Fang G. MAD2B is an inhibitor of the anaphase-promoting complex. Genes Dev 2001;15:1765-70.

73 Geley S, Kramer E, Gieffers C, Gannon J, Peters J-M, Hunt T. Anaphase-promoting complex/cyclosome-dependent proteolysis of human cyclin A starts at the beginning of mitosis and is not subject to the spindle assembly checkpoint. J Cell Biol 2001;153:137-47.

74 Nasmyth K. Segregating sister genomes: the molecular biology of chromosome separation. Science 2002;297:559-65.

75 Bartek J, Lukas J. Mammalian G1- and S-phase checkpoints in response to DNA damage. Curr Opin Cell Biol 2001;13:738-47.

76 Furnari B, Rhind N, Russell P. Cdc25 mitotic inducer targeted by Chk1 DNA damage checkpoint kinase. Science 1997;277:1495-7.

77 Sanchez Y, Wong C, Thoma RS, Richman R, Wu Z, Piwnica-Worms H, *et al*. Conservation of the Chk1 checkpoint pathway in mammals: linkage of DNA damage to Cdk regulation through Cdc25. Science 1997;277:1497-501.

78 Gorbsky GJ, Kallio M, Daum JR, Topper LM. Protein dynamics at the kinetochore: cell cycle regulation of the metaphase to anaphase transition. FASEB J 1999;13:S231-4.

79 Rudner AD, Murray AW. The spindle assembly checkpoint. Curr Opin Cell Biol 1996;8:773-80.

80 Sudakin V, Chan GKT, Yen TJ. Checkpoint inhibition of the APC/C in HeLa cells is mediated by a complex of BUBR1, BUB3, CDC20, and MAD2. J Cell Biol 2001;154:925-36.

81 Wassmann K, Liberal V, Benezra R. Mad2 phosphorylation regulates its association with Mad1 and the APC/C. EMBO J 2003;22:797-806.

82 Waters JC, Chen R-H, Murray AW, Salmon ED. Localization of Mad2 to kinetochores depends on microtubule attachment, not tension. J Cell Biol 1998;141:1181-91.

83 Li Y, Benezra R. Identification of a human mitotic checkpoint gene: hsMAD2. Science 1996;274:246-8.

84 Wang X, Jin D-Y, Wong YC, Cheung ALM, Chun ACS, Lo AKF, *et al*. Correlation of defective mitotic checkpoint with aberrantly reduced expression of MAD2 protein in nasopharyngeal carcinoma cells. Carcinogenesis 2000;21:2293-7.

85 Li Y, Corbea C, Mahaffey D, Rechsteiner M, Benezra R. MAD2 associates with the cyclosome/anaphase-promoting complex and inhibits its activity. Proc Natl Acad Sci USA 1997;94:12431-6.

86 Kallio M, Weinstein J, Daum JR, Burke DJ, Gorbsky GJ. Mammalian p55CDC mediates association of the spindle checkpoint protein Mad2 with the cyclosome/anaphase-promoting complex, and is involved in regulating anaphase onset and late mitotic events. J Cell Biol 1998;141:1393-406.

87 Wassmann K, Benezra R. Mad2 transiently associates with an APC/p55Cdc complex during mitosis. Proc Natl Acad Sci USA 1998;95:11193-8.

88 Chung E, Chen R-H. Spindle checkpoint requires Mad1-bound and Mad1-free Mad2. Mol Biol Cell 2002;13:1501-11.

89 Krishnan R, Pangilinan F, Lee C, Spencer F. Saccharomyces cerevisiae BUB2 prevents mitotic exit in response to both spindle and kinetochore damage. Genetics 2000;156:489-500.

90 Cahill DP, Lengauer C, Yu J, Riggins GJ, Willson JKV, Markowitz SD, *et al*. Mutations of mitotic checkpoint genes in human cancers. Nature 1998;392:300-3.

91 Reimann JDR, Gardner BE, Margottin-Goguet F, Jackson PK. Emi1 regulates the anaphase-promoting complex by a different mechanism than Mad2 proteins. Genes Dev 2001;15:3278-85.

92 Takenaka K, Moriguchi T, Nishida E. Activation of the protein kinase p38 in the spindle assembly checkpoint and mitotic arrest. Science 1998;280:599-602.

93 Shang W, Konidari I, Schomberg DW. 2-Methoxyestradiol, an endogenous estradiol metabolite, differentially inhibits granulose and endothelial cell

mitosis: a potential follicular antiangiogenic regulator. Biol Repr 2001;65:622-7.

94 Schumacher G, Neuhaus P. The physiological estrogen metabolite 2-methoxyestradiol reduces tumor growth and induces apoptosis in human solid tumors. J Cancer Res Clin Oncol 2001;127:405-10.

95 Lis A, Ciesielski MJ, Barone TA, Scott BE, Fenstermaker RA, Plunkett RJ. 2-Methoxyestradiol inhibits proliferation of normal and neoplastic glial cells, and induces cell death, *in vitro*. Cancer Lett 2004;213:57-65.

96 Mooberry SL. New insights into 2-methoxyestradiol, a promising antiangiogenic and antitumor agent. Curr Opin Oncol 2003;15:425-30.

97 Schumacher G, Kataoka M, Roth JA, Mukhopadhyay T. Potent antitumor activity of 2-methoxyestradiol in human pancreatic cancer cell lines. Clin Cancer Res 1999;5(3):493-9.

98 Wang Z, Yang D, Mohanakrishnan AK, Fanwick PE, Nampoothiri P, Hamel E, *et al*. Synthesis of B-ring homologated estradiol analogues that modulate tubulin polymerization and microtubule stability. J Med Chem 2000;43:2419-29.

99 Maran A, Zhang M, Kennedy AM, Sibonga JD, Rickard DJ, Spelsberg TC, *et al*. 2-methoxyestradiol induces interferon gene expression and apoptosis in osteosarcoma cells. Bone 2002;30:393-8.

100 Huober JB, Nakamura S, Meyn R, Roth JA, Mukhopadhyay T. Oral administration of an estrogen metabolite-induced potentiation of radiation antitumor effects in presence of wild-type p53 in non-small-cell lung cancer. Int J Radiation Oncology Biol Phys 2000;48(4):1127-37.

101 Klauber N, Parangi S, Flynn E, Hamel E, D'Amato RJ. Inhibition of angiogenesis and breast cancer in mice by the microtubule inhibitors 2-methoxyestradiol and Taxol. Cancer Res 1997;57:81-6.

102 Cushman M, He H-M, Katzenellenbogen JA, Lin CM, Hamel E. Synthesis, antitubulin and antimitotic activity, and cytotoxicity of analogs of 2-methoxyestradiol, an endogenous mammalian metabolite of estradiol that inhibits tubulin polymerization by binding to the colchicines binding site. J Med Chem 1995;38:2041-9.

103 Tsukamoto A, Kaneko Y, Yoshida T, Han K, Ichinose M, Kimura S. 2-Methoxyestradiol, an endogenous metabolite of estrogen, enhances apoptosis and ß-galactosidase expression in vascular endothelial cells. Biochem Biophys Res Com 1998;248:9-12.

104 Yue CL, Wang X, Louden CS, Gupta S, Pillarisetti K, Gu J-L, *et al*. 2-Methoxyestradiol, an endogenous estrogen metabolite, induces apoptosis in endothelial cells and inhibits angiogenesis: possible role for stress-activated protein kinase signaling pathway and Fas expression. Mol Pharmacol 1997;51:951-62.

105 Josefsson E, Tarkowski A. Suppression of type II collagen-induced arthritis by the endogenous estrogen metabolite 2-methoxyestradiol. Arthritis Rheum 1997;40(1):154-63.

106 Reiser F, Way D, Bernas M, Witte M, Witte C. Inhibition of normal and experimental angiotumor endothelial cell proliferation and cell cycle progression by 2-methoxyestradiol. Proc Soc Exp Biol Med 1998;219(3):211-6.

107 Attalla H, Knuutila S, Mäkelä TP, Andersson LC, Adlercreutz H. Cytogenetic chromosomal preparations using 2-methoxyestradiol. Cancer Genet Cytogenet 1998;102:139-41.

108 Qadan LR, Perez-Stable CM, Anderson C, D'Ippolito G, Herron A, Howard GA, *et al*. 2-Methoxyestradiol induces G2/M arrest and apoptosis in prostate cancer. Biochem Biophys Res Commun 2001;285:1259.

109 Amant F, Lottering M-L, Joubert A, Thaver V, Vergote I, Lindeque BG. 2-Methoxyestradiol strongly inhibits human uterine sarcomatous cell growth. Gynecol Oncol 2003;91:299-308.

110 Wassberg E. Angiostatic treatment of neuroblastoma. Upsala J Med Sci 1999;104:1-24.

111 Miller TA, Bulman AL, Thompson CD, Garst ME, Macdonald TL. Synthesis and structure-activity profiles of A-homoestranes, the estratropones. J Med Chem 1997;40:3836-41.

112 Hanahan D, Folkman J. Patterns and emerging mechanisms of angiogenic switch during tumorigenesis. Cell 1996;86:353-64.

113 Folkman J. Angiogenesis in cancer, vascular, rheumatoid and other disease. Nat Med 1995;1:27-31.

114 Tinley TL, Leal RM, Randall-Hlubek DA, Cessac JW, Wilkens LR, Rao PN, *et al*. Novel 2-methoxyestradiol analogues with antitumor activity. Cancer Res 2003, 63:1538-49.

115 Kerbel RS. Inhibition of tumor angiogenesis as a strategy to circumvent acquired resistance to anti-cancer therapeutic agents. BioEssays 1991;13:31-6.

116 Dubey RK, Jackson EK. Cardiovascular protective effects of 17ß-estradiol metabolites. J Appl Physiol 2001;91:1868-83.

117 Hammers HJ, Saballus M, Sheikzadeh S, Schlenke P. Introduction of a novel proliferation assay for pharmacological studies allowing the combination of BrdU detection and phenotyping. J Immunol Methods 2002;264:89-93.

118 Mooberry SL. Mechanism of action of 2-methoxyestradiol: new developments. Drug Resistance Updates 2003;6:355-61.

119 Shimada K, Nakamura M, Ishida E, Kishi M, Konishi N. Roles of p38- and c-jun NH2-terminal kinase-mediated pathways in 2-methoxyestradiol-induced p53 induction and apoptosis. Carcinogenesis 2003;24:1067-75.

120 LaValee TM, Zhan XH, Herbstritt CJ, Kough EC, Green SJ, Pribluda VS. 2-Methoxyestradiol inhibits proliferation and induces apoptosis independently of estrogen receptors α and β. Cancer Res 2002;62:3691-7.

121 Mukhopadhyay T, Roth JA. Induction of apoptosis in human lung cancer cells after wild-type *p53* activation by methoxyestradiol. Oncogene 1997;14:379-84.

122 Mukhopadhyay T, Roth JA, Acosta SA, Maxwell SA. Two-dimentional gel analysis of apoptosis-specific p53 isoforms induced by 2-methoxyestradiol in human lung cancer cells. Apoptosis 1998;3:421-30.

123 Kataoka M, Schumacher G, Cristiano RJ, Atkinson EN, Roth JA, Mukhopadhyay T. An agent that increases tumor suppressor transgene delivery inhibits growth of metastatic lung cancer *in vivo*. Cancer Res 1998;58:4761-5.

124 Mukhopadhyay T, Roth JA. Superinduction of wild-type p53 protein after 2-methoxyestradiol treatment of Ad5p53-transduced cells induces tumor cell apoptosis. Oncogene 1998;17:241-6.

125 Seegers JC, Lottering M-L, Grobler CJS, van Papendorp DH, Habbersett RC, Shou Y, *et al*. The mammalian metabolite, 2-methoxyestradiol, affects P53 levels and apoptosis induction in transformed cells but not in normal cells. J Steroid Biochem Molec Biol 1997;62(4):253-67.

126 Mabjeesh NJ, Escuin D, LaVallee TM, Pribluda VS, Swartz GM, Johnson MS, *et al*. 2ME2 inhibits tumor growth and angiogenesis by disrupting microtubules and dysregulating HIF. Cancer Cell 2003;3:363-75.

127 Lottering M-L, de Kock M, Viljoen TC, Grobler CJS, Seegers JC. 17ß-Estradiol metabolites affect some regulators of the MCF-7 cell cycle. Cancer Lett 1996;110:181-6.

128 Huang P, Feng L, Oldham EA, Keating MJ, Plunkett W. Superoxide dismutase as a target for the selective killing of cancer cells. Nature 2000;407:390-5.

129 Hamel E, Lin CM, Flynn E, D'Amato RJ. Interactions of 2-methoxyestradiol, an endogenous mammalian metabolite, with unpolymerized tubulin and with tubulin polymers. Biochemistry 1996;35:1304-10.

130 Attalla H, Westberg JA, Andersson LC, Adlercreutz H, Mäkelä TP. 2-Methoxyestradiol-induced phosphorylation of Bcl-2: uncoupling from JNK/SAPK activation. Biochem Biophys Res Com 1998;247:616-9.

131 Martucci CP, Fishman J. Impact of continuously administered catechol estrogens on uterine growth and luteinizing hormone secretion. Endocrinol 1979;105:1288-92.

132 Carothers AM, Huges SA, Ortega D, Bertagnolli MM. 2-Methoxyestradiol induces p53-associated apoptosis of colorectal cancer cells. Cancer Lett 2002;187:77-86.

133 Liu Z-J, Zhu BT. Concentration-dependent mitogenic and antiproliferative actions of 2-methoxyestradiol in estrogen receptor-positive human breast cancer cells. J Steroid Biochem Molec Biol 2004;88:265-75.

134 Marx J. How cells cycle toward cancer. Science 1994;263:319-21.

135 Zacharia LC, Jackson EK, Gillespie DG, Dubey RK. Increased 2-methoxyestradiol production in human coronary versus aortic vascular cells. Hypertension 2001;37:658-62.

136 Feher M, Schmidt JM. Multiple flexible alignment with SEAL: a study of molecules acting on the colchicines binding site. J Chem Inf Comput Sci 2000;40:495-502.

137 Engelborghs Y. General features of the recognition by tubulin of colchicines and related compounds. Eur Biophys J 1998;27:437-45.

138 Choi KS, Eom YW, Kang Y, Ha MJ, Rhee H, Yoon J-W, *et al*. Cdc2 and Cdk2 kinase activated by transforming growth factor-ß1 trigger apoptosis through the phosphorylation of retinoblastoma protein in FaO hepatoma cells. J Biol Chem 1999;274:31775-83.

139 Purohit A, Singh A, Ghilchik MW, Reed MJ. Inhibition of tumor necrosis factor α-stimulated aromatase activity by microtubule-stabilizing agents, paclitaxel and 2-methoxyestradiol. Biochem Biophys Res Commun 1999;261:214-7.

140 Ochi T, Nakajima F, Nasui M. Distribution of γ-tubulin in multipolar spindles and multinucleated cells induced by dimethylarsinic acid, a methylated derivative of inorganic arsenics in Chinese hamster V79 cells. Toxicology 1999;136:79-88.

141 Kahana JA, Cleveland DW. Beyond nuclear transport: Ran-GTP as a determinant of spindle assembly. J Cell Biol 1999;146:1205-9.

142 Fiore BD, Ciciarello M, Mangiacasale R, Palena A, Tassin A-M, Cundari E, *et al*. Mammalian RanBP1 regulates centrosome cohesion during mitosis. J Cell Sci 2003;116:3399-411.

143 Newton K, Strasser A. The Bcl-2 family and call death regulation. Curr Opin Genet Dev 1998;8:68-75.

144 Meikrantz W, Gisselbrecht S, Tam SW, Schlegel R. Activation of cyclin A-dependent protein kinases during apoptosis. Proc Natl Acad Sci USA 1994;91:3754-8.

145 LaValee TM, Zhan XH, Johnson MS, Herbstritt CJ, Swartz G, Williams MS, *et al*. 2-Methoxyestradiol up-regulates death receptor 5 and induces apoptosis through activation of the extrinsic pathway. Cancer Res 2003;63:468-75.

146 Meikrantz W, Schlegel R. Suppression of apoptosis by dominant negative mutants of cyclin-dependent protein kinases. J Biol Chem 1996;271:10205-9.

147 Martin SJ, McGahon AJ, Nishioka WK, LaFace D, Guo X, Th'ng J, *et al*. $p34^{cdc2}$ and apoptosis. Science 1995;269:106-7.

148 Yao S-L, McKenna KA, Sharkis SJ, Bedi A. Requirement of p34cdc2 kinase for apoptosis mediated by the Fas/APO-1 receptor and interleukin 1ß-converting enzyme-related proteases. Cancer Res 1996;56:4551-5.

149 Shi L, Nishioka WK, Th'ng J, Bradbury EM, Litchfield DW, Greenberg AH. Premature p34cdc2 activation required for apoptosis. Science 1994;263:1143-5.

150 Fotedar R, Flatt J, Gupta S, Margolis RL, Fitzgerald P, Messier H, *et al*. Activation-induced T-cell death is cell cycle dependent and regulated by cyclin B. Mol Cell Biol 1995;15:932-42.

151 Leach SD, Scatena CD, Keefer CJ, Goodman HA, Song SY, Yang L, *et al*. Negative regulation of Wee1 expression and Cdc2 phosphorylation during p53-mediated growth arrest and apoptosis. Cancer Res 1998;58:3231-6.

152 Maxwell SA, Roth JA, Mukhopadhyay T. Analysis of phosphorylated isoforms of the p53 tumor suppressor protein in human lung carcinoma cells undergoing apoptosis. Electrophoresis 1996;17:1772-5.

153 Djavaheri-Mergny M, Wietzerbin J, Besancon F. 2-Methoxyestradiol induces apoptosis in Ewing sarcoma cells through mitochondrial hydrogen peroxide production. Oncogene 2003;22:2558-67.

154 Joensuu H, Pylkkänen L, Toikkanen S. Bcl-2 protein expression and long-term survival in breast cancer. Am J Pathol 1994;145:1191-8.

155 Zhou N, Zhu X, Zhou J, Li M, Zhang X, Huang P, *et al*. 2-Methoxyestradiol induces cell cycle arrest and apoptosis of nasopharyngeal carcinoma cells. Acta Pharmacol Sin 2004;25:1515-20.

156 Cleveland JL, Kastan MB. Cancer. A radical approach to treatment. Nature 2000;407:309-11.

157 Toyokuni S, Okamoto K, Yodoi J, Hiai H. Persistent oxidative stress in cancer. FEBS 1995;358:1-3.

158 Kheradmand F, Werner E, Tremble P, Symons M, Werb Z. Role of Rac1 and oxygen radicals in collagenase-1 expression induced by cell shape change. Science 1998;280:898-902.

159 Lin H-L, Liu T-Y, Chau G-Y, Lui W-Y, Chi C-W. Comparison of 2-methoxyestradiol-induced, docetaxel-induced, and paclitaxel-induced apoptosis in hepatoma cells and its correlation with reactive oxygen species. Cancer 2000;89:983-94.

160 Kachadourian R, Liochev SI, Cabelli DE, Patel MN, Fridovich I, Day BJ. 2-Methoxyestradiol does not inhibit superoxide dismutase. Arch Biochem Biophys 2001;392:349-53.

161 Hagen T, D'Amico G, Quintero M, Palacios-Callender M, Hollis V, Lam F, *et al*. Inhibition of mitochondrial respiration by the anticancer agent 2-methoxyestradiol. Biochem Biophys Res Commun 2004;322:923-9.

162 Hartwell LH, Szankasi P, Roberts CJ, Murray AW, Friend SH. Integrating genetic approaches into the discovery of anticancer drugs. Science 1997;278:1064-73.

163 Waldman T, Zhang Y, Dillehay L, Yu J, Kinzler K, Vogelstein B, *et al*. Cell-cycle arrest versus cell death in cancer therapy. Nat Med 1997;3:1034-6.

164 Pribluda VS, Gubish ER, LaVallee TM, Treston A, Swartz GM, Green SJ. 2-Methoxyestradiol: an endogenous antiangiogenic and antiproliferative drug candidate. Cancer Metastasis Rev 2000;19:173-9.

165 Sibonga JD, Sommer U, Turner RT. Evidence that 2-methoxyestradiol suppresses proliferation and accelerates apoptosis in normal rat growth plate chondrocytes. J Cancer Clin Oncol 2002;128:477-83.

166 Seeger H, Gückel B, Wallwiener D, Mueck AO, Huober J. Effect of tamoxifen and 2-methoxyestradiol alone and in combination on human breast cancer cell proliferation. J Steroid Biochem Molec Biol 2003;84:255-7.

167 Ausubel FM, Brent R, Kingston RE, Moore DD, Seidman JG, Smith JA, *et al*., editors. Counterstaining and mounting of autoradiographed *in situ* hybridisation slides: hematoxylin/eosin staining. In: Current protocols in molecular biology. Vol 2. New York: John Wiley & Sons; 1996. p. 14.5.2-3.

168 Schutze N, Vollmer G, Knuppen R. Catecholestrogens are agonists of estrogen receptor dependent gene expression in MCF-7 cells. J Steroid Biochem Molec Biol 1993;46:781-9.

169 Bradford MM. A rapid and sensitive method for the quantitation of microgram quantities of protein utilizing the principle of protein dye binding. Anal Biochem 1976;72:248-54.

170 Lippert C, Seeger H, Mueck AO. The effect of endogenous estradiol metabolites on the proliferation of human breast cancer cells. Life Sci 2003;72:877-83.

171 Gillies RJ, Didier N, Denton M. Determination of cell number in monolayer cultures. Anal Biochem 1986;159:109-13.

172 Kueng W, Silber E, Eppenberger U. Quantification of cells cultured on 96-well plates. Anal Biochem 1989;182:16-9.

173 Korting HC, Schindler S, Hartinger A, Kerscher M, Angerpointner T, Maibach HI. MTT-assay and neutral red release (NRR)-assay: relative role in the prediction of the irritancy potential of surfactants. Life Sci 1994;55:533-40.

174 Guppy M, Leedman P, Zu XL, Russell V. Contribution by different fuels and metabolic pathways to the total ATP turnover of proliferating MCF-7 breast cancer cells. Biochem J 2002;364:309-15.

175 Eisen SF, Brown HA. Selective estrogen receptor (ER) modulators differentially regulate phospholipase D catalytic Activity in ER-negative breast cancer cells. Mol Pharmacol 2002;62:911-20.

176 Thompson HGR, Harris JW, Brody JP. Post-translationally modified S12 absent in transformed breast epithelial cells, is not associated with the 26S proteasome and is induced by proteasome inhibitor. Int J Cancer 2004; 111:338-47.

177 Golebiewska J, Rozwadowski P, Spodnik JH, Knap N, Wakabayashi T, Wozniak M. Dual effect of 2-methoxyestradiol on cell cycle events in human osteosarcoma 143B cells. Acta Biochim Pol 2002;49:59-65.

178 Andreassen PR, Margolis RL. Microtubule dependency of $p34^{cdc2}$ inactivation and mitotic exit in mammalian cells. J Cell Biol 1994;127:789-802.

179 Panzer A, Joubert AM, Bianchi PC, Hamel E, Seegers JC. The effects of chelidonine on tubulin polymerisation, cell cycle progression and selected signal transmission pathways. Eur J Cell Biol 2001;80:111-8.

180 Glotzer M. Mitosis: don't get mad, get even. Curr Biol 1996;6:1592-4.

181 Chen Y-NP, Sharma SK, Ramsey TM, Jiang L, Martin MS, Baker K, *et al*. Selective killing of transformed cells by cyclin/cyclin-dependent kinase 2 antagonists. Proc Natl Acad Sci USA 1999;96:4325-9.